

# Easy-to-use diagnostic assays for thrombotic thrombocytopenic purpura

**Quintijn BONNEZ**

Supervisor: Prof. Dr. Karen Vanhoorelbeke

Mentor: *Charlotte Dekimpe*

Thesis presented in  
fulfillment of the requirements  
for the degree of Master of Science  
in Biochemistry & Biotechnology

Academic year 2019-2020

---

© Copyright by KU Leuven

Without written permission of the promotors and the authors it is forbidden to reproduce or adapt in any form or by any means any part of this publication. Requests for obtaining the right to reproduce or utilize parts of this publication should be addressed to KU Leuven, Faculteit Wetenschappen, Geel Huis, Kasteelpark Arenberg 11 bus 2100, 3001 Leuven (Heverlee), Telephone +32 16 32 14 01.

A written permission of the promotor is also required to use the methods, products, schematics and programs described in this work for industrial or commercial use, and for submitting this publication in scientific contests



# Acknowledgement

At first, I want to thank my promotor prof. dr. Karen Vanhoorelbeke for the opportunities I received to perform my master's thesis in the Laboratory for Thrombosis Research. As a bachelor student at KU Leuven Campus Kulak Kortrijk, we got to know her as an inspiring professor who excites students scientifically and is available for questions and help. Therefore, I am extremely grateful that I was not only able to perform my bachelor and master's thesis under her supervision, but also can start a PhD project in the near future.

Especially, I would also like thank my mentor Charlotte Dekimpe for guiding me during this academic year and assisting me with this master's thesis. Thanks to your help and advice, I have learned a lot on the practical lab work, but also on the writing parts. Over the whole year, you definitely had a strong influence on how I have grown into the scientist I am today. Your energetic enthusiasm is infectious to never give up, but you also managed to keep me with both feet on the ground when the lab work wasn't going fast enough as I hoped for.

I want to acknowledge our laboratory technicians Aline and Inge. Despite their busy schedules, they were always available to answer a lot of my questions and lead me through the lab whenever I forgot where to find all the products. Also, thanks to all colleagues researchers, there was a lovely atmosphere in the Laboratory for Thrombosis Research, which made me feel welcome from the very first moment. In particular, everyone's good morning greetings seems to be a small gesture but actually, they were an great pleasure to start off every day. Additionally, I like to thank the other master's thesis students, Astrid and Rebecca. Together, we shared a lot of time, jokes and laughter, but importantly we kept supporting each other.

Moreover, I want to especially thank Emiel, Elias, Mattijs, Bert and Jonas, but also all the roommates and biology and biochemistry friends, that I have met at KU Leuven Campus Kulak Kortrijk. It has been five turbulent, but wonderful years and I am glad that I have shared those years with each one of you. Together, we had some memorable nights out, the hardest 'days after' and our own most hilarious and valuable stories to never forget. Although everyone declared me crazy for waking up that early, the many hours of daily commuting between Leuven and Kortrijk and the late night arrivals at home, you all kept motivating me during this whole project, while respecting and supporting my objectives in sciences.

Lastly, I certainly have to thank my parents, brother, sister and all other family members, without your unconditional support, none of these would ever have been possible. Although lacking any background in biochemistry, you all remained very interested and proudly followed all the achievements over the years. In my opinion, your support was the biggest of all, so therefore: Thank you very, very much!

# Summary

Thrombotic thrombocytopenic purpura (TTP) is a life-threatening microangiopathic orphan disease, caused by a deficiency in ADAMTS13. ADAMTS13 plays a key role in the maintenance of the haemostatic balance by processing von Willebrand factor (VWF) multimers. As a clinical emergency, the rapid and appropriate diagnosis of TTP is essential. However, the diverse clinical signs and symptoms overlap with those of different thrombotic microangiopathies and therefore, the clinical diagnosis remains challenging and presumptive. Due to this complex diagnosis of TTP, the ADAMTS13 parameters need to be evaluated. However, those tests are generally performed in specialized reference centres and require well-trained technicians. The generation of reliable data on the ADAMTS13 parameters is time-consuming and therefore, relatively high mortality rates persist. Rapid and accurate diagnosis remains the corner stone to initiate the appropriate treatment and improve the management of TTP. Therefore, the aim of this master's thesis was to develop easy-to-use diagnostic assays to evaluate several ADAMTS13 parameters.

Since different reference laboratories perform various strategies of the enzyme-linked immunosorbent assay (ELISA) to determine the anti-ADAMTS13 autoantibody titers, the influence of these diverse approaches on the autoantibody levels was assessed first. Thereafter, a fiber optic surface plasmon resonance (FO-SPR) bioassay was developed and optimized to evaluate the anti-ADAMTS13 autoantibody titer, since this easy-to-use technology allows fast and real-time sample analysis with clinical relevant sensitivity. Furthermore, the open ADAMTS13 conformation was recognized as a novel biomarker for subclinical immune-mediated TTP. Although, this ADAMTS13 parameter is currently not evaluated in hospital settings, there is major interest to implement a clinical test for the ADAMTS13 conformation. Therefore, an FO-SPR bioassay, to assess the ADAMTS13 conformation, was also successfully developed and evaluated in patient plasma samples. In the future, the diagnostic tests for the anti-ADAMTS13 autoantibodies, the ADAMTS13 conformation and two other relevant ADAMTS13 parameters (ADAMTS13 activity and ADAMTS13 antigen) will be combined in an easy-to-use FO-SPR combo-assay to evaluate individual patient samples at any hospital intensive care unit.

# Samenvatting

Trombotische trombocytopenische purpura (TTP) is een levensbedreigende, micro-angiopatische zeldzame aandoening, die veroorzaakt wordt door een deficiëntie in ADAMTS13. ADAMTS13 is essentieel voor het bewaren van de balans tijdens hemostase doordat het de omvang van von Willebrand factor multimeren kan aanpassen. Als medische noodsituatie, is een snelle en correcte diagnose van TTP vereist. De verschillende klinische tekens en symptomen overlappen weliswaar met deze van andere trombotische micro-angiopatische aandoeningen, waardoor de medische diagnose doorgaans gebaseerd is op de vermoedens van de uitvoerende arts. Doordat de diagnose van TTP complex is, moet de evaluatie van verschillende ADAMTS13 parameters meer duidelijkheid opleveren. Deze testen moeten echter uitgevoerd worden in gespecialiseerde referentiecentra door opgeleide laboratorium technici. Hierdoor duurt het verzamelen van betrouwbare gegevens over de ADAMTS13 parameters erg lang, waardoor de sterftcijfers voor TTP ook relatief hoog blijven. Snelle en accurate diagnose blijft daarom cruciaal voor het starten van de gepaste behandeling zodat TTP patiënten beter geholpen en opgevolgd kunnen worden. Net om die reden, werden enkele makkelijk toepasbare diagnostische testen voor de ADAMTS13 parameters ontwikkeld.

Diverse referentielaboratoria voor TTP, gebruiken enkele verschillende *enzyme-linked immunosorbent assay* (ELISA) strategieën voor het bepalen van de anti-ADAMTS13 autoantilichaam hoeveelheden. Daarom werd de invloed van deze verschillende benaderingen op de variatie bij het bepalen van anti-ADAMTS13 autoantilichamen als eerste onderzocht. Daarna werd een *fiber optic surface plasmon resonance* (FO-SPR) test ontwikkeld en geoptimaliseerd voor het meten van de anti-ADAMTS13 autoantilichaam hoeveelheden, aangezien deze makkelijk te gebruiken technologie het toelaat om snel en in *real-time* patiënten stalen te analyseren, maar ook een medisch relevante sensitiviteit vertoont. Daarnaast wordt de open ADAMTS13 conformatie beschouwd als een nieuwe indicator voor subklinische immuun-gemedieerde TTP. Hoewel deze ADAMTS13 parameter momenteel niet geëvalueerd wordt in ziekenhuizen, is er toch grote vraag naar een klinisch hanteerbare test voor de ADAMTS13 conformatie. Daarom werd een FO-SPR test voor de ADAMTS13 conformatie succesvol ontwikkeld en getest in patiënten stalen. In de toekomst zullen de diagnostische FO-SPR testen voor de anti-ADAMTS13 autoantilichamen, de ADAMTS13 conformatie en nog twee andere relevante ADAMTS13 parameters (ADAMTS13 activiteit en ADAMTS13 antigeen) samen gebracht worden in een FO-SPR combinatietest om individuele patiënten stalen te kunnen analyseren op de intensieve zorgen afdeling van elk ziekenhuis.

# COVID-19 measures

Due to the outbreak of the novel severe acute respiratory syndrome coronavirus 2 (SARS-CoV-2), all laboratory experiments came to an end in consensus with the promotor and mentor since the 16<sup>th</sup> of march 2020. Therefore, physical presence in the Laboratory of Thrombosis Research was prohibited and we agreed to participate in the weekly lab meeting via online video tools. Although additional experimental work was originally planned during the remaining of the semester and Easter holidays, sufficient data had already been collected during the previous months to write the master's thesis in a normal way. All communication concerning questions and the discussion on the writing part of this master's thesis were performed electronically. Since this master's thesis was performed at KU Leuven Campus Kulak Kortrijk, the experimental work was already started from the beginning of August on a full-time, daily basis to avoid to overload the further course of the master's thesis during this graduation year. From the end of December and during January, a short break from the lab work was provided for studying and taking exams. However, the project was resumed as soon as possible and during the lesson-free week, the lab work was proceeded in consent with both the promotor and mentor on full-time, daily basis.

# List of abbreviations

A (domain)	von Willebrand A domain
ADAMTS13	A disintegrin and metalloprotease with thrombospondin type 1 motif, member 13
ANOVA	Analysis of variance
AuNPs	Gold nanoparticles
Bmp1	Bone morphogenic protein 1
BSA	Bovine serum albumin
C (domain)	Cysteine-rich domain
C1r/C1s	Complement components C1r/C1s
CHO	Chinese hamster ovary
CI	Conformation index
CK	Cysteine knot
cTTP	Congenital TTP
CUB (domain)	C1r/C1s, Uegf and Bmp1 domain
CV	Coefficient of variation
D (domain)	Disintegrin domain
EDC	1-ethyl-3-[3-dimethylaminopropyl] carbodiimide
ELISA	Enzyme-linked immunosorbent assay
FIX	Factor IX; Christmas factor
FL	Full-length
FO	Fiber optic
FO probe	Gold-coated optical fiber
FRETs	Fluorescent resonance energy transfer
FVII	Factor VII; Stable factor
FVIII	Factor VIII
FX	Factor X; Stuart-Prower factor
FXI	Factor XI; Plasma thromboplastin factor
FXII	Factor XII; Hageman factor
FXIII	Factor XIII; Fibrin stabilising factor
GAB	Goat anti-biotin
GAH	Goat anti-human
GPIb $\alpha$	Platelet glycoprotein Ib alpha
GPIIb/IIIa	Glycoprotein IIb/IIIa
HBS	HEPES-buffered saline
HD	Healthy donor
HLA	Human leukocyte antigen
HMW	High molecular weight

HRP	Horseradish peroxidase
HUS	Haemolytic uremic syndrome
IMW	Intermediate molecular weight
iTTP	Immune-mediated TTP
LDH	Lactate dehydrogenase
LMW	Low molecular weight
M (domain)	Metalloprotease domain
MDTCS	Truncated N-terminal part of ADAMTS13
MES	2-(-Morpholino) ethane sulfonic acid
NHP	Normal human plasma
NHS	N-hydroxysuccinimide
OD	Optical density
OPD	O-phenylenediamine
P (domain)	Propeptide domain
PBS	Phosphate-buffered saline
POC	Point-of-care
PVDF	Polyvinylidene fluoride
RGD	Arginine-Glycine-Aspartic acid
rhADAMTS13	Recombinant human ADAMTS13
RT	Room temperature
S (domain)	Spacer domain
SAM	Self-assembling monolayer
SDS-PAGE	Sodium dodecyl sulphate polyacrylamide gel electrophoresis
SP	Signal peptide
SPR	Surface plasmon resonance
T (domain)	Thrombospondin domain
T2C2	Truncated C-terminal part of ADAMTS13
TIL	Trypsin inhibitor-like structure
TMA	Thrombotic microangiopathy
tPA	Tissue plasminogen activator
TPE	Therapeutical plasma exchange
TSR	Thrombospondin type-1 repeat
TTP	Thrombotic thrombocytopenic purpura
Uegf	Urinary epidermal growth factor-related sea urchin protein
UL	Ultra large
VW (domain)	von willebrand domain
VWD	von Willebrand disease
VWF	von Willebrand factor

VWFCP	von Willebrand factor cleaving protease
WPBs	Weibel-Palade bodies
Y1605-M1606	Tyrosine1605 – Methionine1606

# Table of Contents

<b>Acknowledgement</b> .....	I
<b>Summary</b> .....	II
<b>Samenvatting</b> .....	III
<b>COVID-19 measures</b> .....	IV
<b>List of abbreviations</b> .....	V
<b>Table of Contents</b> .....	VIII
<b>Part I - Literature review</b> .....	1
<b>Chapter 1 – Blood &amp; Haemostasis</b> .....	2
<b>Chapter 2 – Von Willebrand Factor</b> .....	4
2.1. VWF biosynthesis.....	4
2.1.1. Primary VWF structure .....	4
2.1.2. Disulphide bridging & Multimerization .....	5
2.1.3. Posttranslational Modifications .....	6
2.2. Functional VWF domains.....	7
2.2.1. D domain.....	7
2.2.2. A domain .....	7
2.2.3. C domain .....	8
2.3. VWF storage & secretion.....	8
<b>Chapter 3 – ADAMTS13</b> .....	9
3.1. ADAMTS13 biosynthesis .....	9
3.2. Functional ADAMTS13 domains.....	11
3.2.1. Propeptide domain .....	11
3.2.2. Metalloprotease domain .....	11
3.2.3. Disintegrin domain.....	12
3.2.4. Cysteine-rich domain.....	12
3.2.5. Spacer domain .....	13
3.2.6. Thrombospondin Type-1 Repeat domain.....	13
3.2.7. CUB domain .....	13
3.3. Open-closed conformation.....	14
3.4. Recognition and cleavage of VWF by ADAMTS13 .....	15

<b>Chapter 4 – Thrombotic thrombocytopenic purpura</b> .....	17
4.1. Pathophysiology .....	17
4.2. Congenital TTP .....	18
4.3. Immune-mediated TTP .....	19
4.4. Diagnosis .....	20
4.4.1. Clinical presentation .....	20
4.4.2. Differential diagnosis .....	21
4.5. Current therapy .....	22
4.5.1. Congenital TTP .....	23
4.5.2. Immune-mediated TTP .....	23
<b>Chapter 5 – FO-SPR</b> .....	25
<b>Part II - Objectives</b> .....	27
2.1. Anti-ADAMTS13 autoantibody levels .....	28
2.2. ADAMTS13 conformation analysis .....	29
<b>Part III – Materials &amp; methods</b> .....	30
3.1. Materials .....	31
3.2. Anti-ADAMTS13 Autoantibody assay .....	31
3.2.1. Recombinant ADAMTS13 .....	31
3.2.2. Recombinant ADAMTS13 variants .....	33
3.2.3. Anti-ADAMTS13 autoantibody ELISA .....	33
3.2.4. Anti-ADAMTS13 autoantibody FO-SPR assay .....	35
3.3. ADAMTS13 conformation assay .....	37
3.3.1. ADAMTS13 conformation ELISA .....	37
3.3.2. ADAMTS13 conformation FO-SPR assay .....	38
3.4. Statistical analysis .....	41
<b>Part IV - Results</b> .....	42
4.1. Anti-ADAMTS13 autoantibody assay .....	43
4.1.1. Evaluation of diverse anti-ADAMTS13 autoantibody ELISA set-ups .....	43
4.1.2. Development of the anti-ADAMTS13 autoantibody FO-SPR assay .....	45
4.2. ADAMTS13 conformation assay .....	47
4.2.1. Development of the ADAMTS13 conformation FO-SPR assay .....	47
4.2.2. Evaluation of the ADAMTS13 conformation FO-SPR assay .....	48

<b>Part V - Discussion</b> .....	50
5.1. Anti-ADAMTS13 autoantibody assay.....	51
5.1.1. Evaluation of diverse anti-ADAMTS13 autoantibody ELISA set-ups ....	51
5.1.2. Development of the anti-ADAMTS13 autoantibody FO-SPR assay.....	52
5.2. ADAMTS13 conformation assay.....	53
<b>References</b> .....	55
<b>Addendum I – Product information</b> .....	A.1
<b>Addendum II – Buffer composition</b> .....	A.3
<b>Addendum III – Laboratory equipment</b> .....	A.5
<b>Addendum IV – Additional experiments</b> .....	A.6
<b>Addendum V – Risk analysis</b> .....	A.7

# **PART I**

## **Literature review**

# Chapter 1 – Blood & Haemostasis

Blood is the human body fluid delivering the fundamental substances, like nutrients and oxygen, towards cells, while removing metabolic waste products. Three major types of cells are suspended in blood: erythrocytes (red blood cells), leukocytes (white blood cells) and thrombocytes (platelets), each of them having their specific properties. Erythrocytes are the most abundant and are responsible for the distribution of oxygen (Gibson et al, 2001). Leukocytes participate in the human immune system by removing cellular debris and attacking foreign pathogens. Thrombocytes, originating from megakaryocytes, are of utmost importance in haemostasis (Boron et al., 2016). During the first step of wound healing, damaged blood vessels manage the bleeding to stop in order to prevent blood loss. This process is called haemostasis and consists of three principal steps: vasoconstriction, platelet plug formation (primary haemostasis) and blood coagulation (secondary haemostasis) (Atluri et al., 2005; Hoehn et al., 2012).

The vascular endothelium controls the first response mechanism when blood vessels are injured by stimulating vasoconstriction in order to reduce the blood flow through the injured area. Hereby, the vascular smooth muscle cells are limiting the quantity of blood loss (Atluri et al., 2005). During primary haemostasis at the site of injury, exposed subendothelial collagen promotes adherence of platelets into a platelet plug, by platelet adhesion (mediated by von Willebrand factor in high shear rate conditions), activation and aggregation (Versteeg et al., 2013). Simultaneously, multiple clotting factors are activated in a sequence of events (Figure 1), which is referred to as secondary haemostasis (Monagle et al., 2011). This cascade leads to the final cleavage of fibrinogen into active fibrin, which consolidates the unstable clot from primary haemostasis (Hoehn et al., 2012). Fibrinolysis is the normal body process that counteracts the mechanisms of haemostasis to prevent growth of problematic blood clots. The primary driver of intravascular fibrinolysis is tissue plasminogen activator (tPA), released by endothelial cells (Cericic et al., 2003). Plasminogen is converted, due to stimulation of tPA, into the physiological active plasmin, regulating the breakdown of fibrin clots. The plasmin enzyme cuts fibrin at diverse places, resulting in smaller circulating clot fragments which are cleared by other proteases or by the liver and kidney (Versteeg et al., 2013).

Although coagulation is essential for wound healing, thrombi have serious health consequences when traveling through the circulatory system after liberation from the vessel wall. When reaching the lungs, brain or heart, released thrombi could provoke respectively pulmonary embolism, stroke or a heart attack (Hoehn et al., 2012). On the other hand, the coagulation mechanism is extremely important to prevent haemorrhage. Insufficient haemostasis provokes problems with wound healing, resulting in uncontrollable, excessive bleeding. The complex processes, involved in the formation of stable blood clots, appear when looking at the multiple regulated mechanisms for all the activators and inhibitors involved in both coagulation and fibrinolysis (Cesarman-Maus et al., 2005; Harbrecht et al., 1967; Tersteeg et al., 2017).

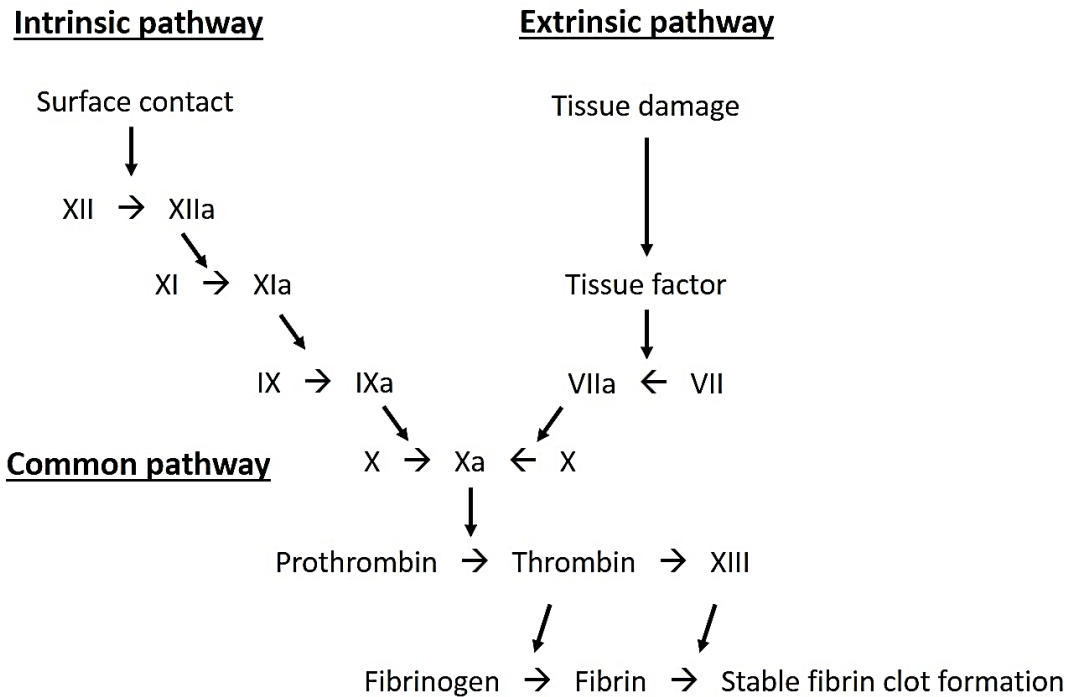


Figure 1: **Coagulation pathway:** The formation process of a stable fibrin clot is multi-regulated by several clotting factors initiating from either the intrinsic or extrinsic pathway. Both pathways stimulate coagulation factor X, which in turn promotes the common coagulation pathway by activating thrombin and fibrin. The processes required to form a stable clot are complex and are influenced by many regulators and feedback mechanisms (XII: Hageman factor; XI: Plasma thromboplastin; IX: Christmas factor; VII: Stable factor; X: Stuart-Prower factor; XIII: Fibrin stabilising factor) (Based on (Pallister et al., 2011)).

# Chapter 2 – von Willebrand factor

Von Willebrand factor (VWF) is a multimeric glycoprotein found in the blood plasma, the subendothelial matrix and in storage granules in endothelial cells and platelets (Sadler et al., 1998). VWF represents one of the main actors of the haemostatic process, since this protein activates platelet adhesion and aggregation, while protecting coagulation factor VIII (FVIII) and introducing it at the site of vascular injury (Sadler et al., 1998). Shortage of VWF reveals extreme haemorrhagic phenotypes, emerging from inadequate platelet plug formation and FVIII deficiency (Lenting et al., 2012). Disorders displaying qualitative or quantitative shortage of VWF are compiled under the collective name of von Willebrand disease (VWD), affecting 0.01% up to 1% of the total population (Sadler et al., 2009).

## 2.1. VWF biosynthesis

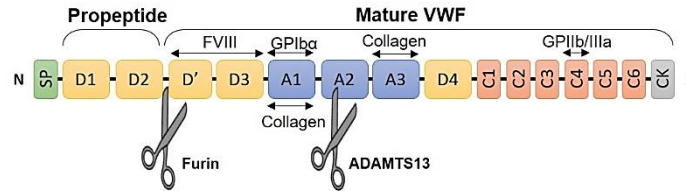
### 2.1.1. Primary VWF structure

The primary protein sequence of VWF was reported in 1986 (Lenting et al., 2015; Sadler et al., 1986), where the repeating domain structure within the protein was immediately observed. Endothelial cells and megakaryocytes produce VWF as a pre-pro-polypeptide composed of 2813 amino acids (Pannekoek et al., 1989). Historically, the multiple domains of VWF were aligned: SP-D1-D2-D'-D3-A1-A2-A3-D4-B1-B2-B3-C1-C2-CK (Figure 2A). From this historical domain alignment, a mature VWF monomer remains after the removal of the signal peptide (SP) and two VWF D domains (D1-D2) from the VWF pre-pro- and pro-polypeptide respectively (Pannekoek et al., 1989; Rauch et al., 2013; Zhou et al., 2012). Recent progresses in structural and bio-informatical protein analysis revealed a reassessment of the VWF structural architecture, submitting an updated domain alignment: SP-D1-D2-D'-D3-A1-A2-A3-D4-C1-C2-C3-C4-C5-C6-CK (Figure 2B). This newly proposed domain organisation consists of a N-terminal signal peptide domain (SP), five von Willebrand D domains (D), three von Willebrand A domains (A), six von Willebrand C domains (C) and a C-terminal cysteine knot domain (CK) (Pannekoek et al., 1989; Rauch et al., 2013; Zhou et al., 2012). Focusing on the protein analysis of the D domains, various explicit structures were revealed (Figure 2C). Each of the D1, D2 and D3 domains incorporate a von Willebrand domain (VW), a C8 fold, a trypsin inhibitor-like structure (TIL) and an E module. However, the D' domain lacks the VW domain and the C8 fold, whereas the E module is absent in the D4 domain, which encloses an unique D4N subdomain (Zhou et al., 2012).

### A) Classical VWF domain alignment



### B) Reassessed VWF structural architecture



### C) Structure alignment of VWF D subdomains

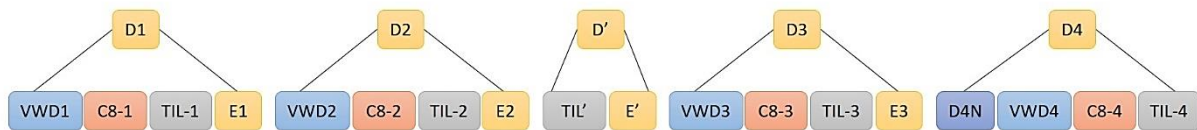


Figure 2: **VWF domain structure:** A) Classical arrangement of the domain structures from the original analysis of the VWF sequence. B) Updated domain alignment after the reassessment of the structural architecture. C) Various independent structure alignments of the VWF D subdomain structures (based on (Lenting et al., 2015)).

## 2.1.2. Disulphide bridging & Multimerization

The *VWF* gene is found on human chromosome 12, where the short chromosome arm comprises about 180 kb that encodes for the 53 exons of the pre-pro-VWF (Reininger et al., 2008). After analysis of the VWF amino acid sequence, an unusually high percentage of cysteine residues (8.3%) was revealed (Shapiro et al., 2014), which is fourfold higher compared to the average cysteine level in human proteins (Lenting et al., 2015). However, these cysteine residues are crucial in the formation of disulphide bridges, promoting dimerization and multimerization in VWF biosynthesis. When entering the endoplasmic reticulum, signal peptidases release the SP domain (Figure 3A) and VWF dimerizes tail-to-tail, showing intra- and interpeptide disulphide bonds in the C-terminal cysteine knot domain (Figure 3B) (Katsumi et al., 2000). The cysteine knot links two  $\beta$  strands perpendicularly by two disulphide bonds, through which a third disulphide bond is threaded (Katsumi et al., 2000; Zhou et al., 2012).

In the Golgi apparatus, the pro-VWF dimers are linked by interchain disulphide bridging, involving cysteines of the D3 domain (Figure 3C). The presence of the propeptide and the D' domains are majorly important in the interchain bridging for two reasons: (1) They align the pro-VWF dimers accurately, facilitating the interdimeric cross-linking by the D3 domain. (2) The formation of disulphide bridges between the D3 domains is catalysed by the propeptide via its disulphide isomerase activity (Mayadas et al., 1989). Moreover, the intermolecular cysteine pairs are protected against disulphide reduction, ensuring the long-term stability of the dimeric conformation (Zhou et al., 2014). The flexibility of the cysteine redox status allows

VWF to further modify its functional properties (Li et al., 2008). Once the propeptide domains are detached by a furin, the VWF dimer subunits (500 kDa) are assembled into a heterogeneous group of differentially sized VWF multimers, varying from 2 to over 100 VWF subunits (Figure 3C). As a result, the VWF multimers are classified in the subdivisions of ultra-large VWF (UL-VWF) (>10,000 kDa), high-molecular weight VWF (HMW-VWF) (5,500-10,000 kDa), intermediate molecular weight VWF (IMW-VWF) (3,000-5,000 kDa) and low-molecular weight VWF (LMW-VWF) (500-2,500 kDa) (Sadler et al., 1998; Stocksclaeder et al., 2014; Wagner et al., 1990).

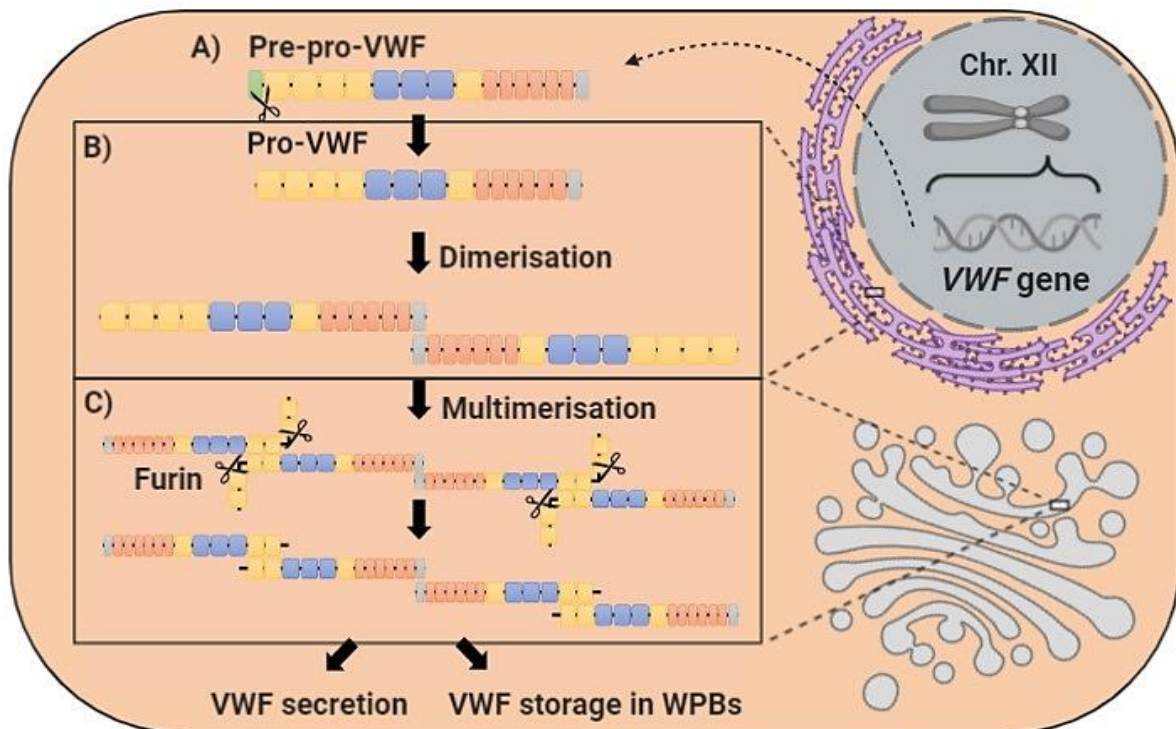


Figure 3: **Biosynthesis of VWF:** A) Removal of the signal peptide is established by signal peptidases during the translocation of pre-pro-VWF to the endoplasmic reticulum. B) CK domains interact tail-to-tail, resulting in the formation of VWF dimers. C) In the Golgi apparatus, VWF multimerizes by head-to-head association of the N-terminal D3 domains. Thereafter, furin releases the D1-D2 propeptide from the mature VWF multimers and post-translational modifications take place (Based on (Luo et al., 2012)).

### 2.1.3. Posttranslational Modifications

To establish a complete VWF life cycle, essential posttranslational modifications take place during the different stages of VWF synthesis. The propeptide is separated by furin, while glycosylation processes occur in the endoplasmic reticulum and Golgi apparatus (Canis et al., 2012; Matsui et al., 1992; Samor et al., 1986). Oligosaccharyltransferase enzymes add *N*- and *O*-linked carbohydrates during the maturation of the VWF core (Canis et al., 2010; Samor et al., 1989). Extensive glycosylation is essential for secretion of VWF, while the presence of glycans also influences VWF proteolysis by ADAMTS13 (Crawley et al., 2011).

## 2.2. Functional VWF domains

### 2.2.1. D domain

The D1 and D2 domains form the VWF propeptide, that assists in VWF multimerization via its disulphide isomerase activity. However, before secretion of mature VWF, the D1-D2 propeptide is cleaved by a furin enzyme (Figure 3C) (Crawley et al., 2011; Lenting et al., 2015). VWF is crucial in secondary haemostasis as it serves as a carrier for coagulation factor VIII (Luo et al., 2012; Sadler et al., 2015). The D<sup>1</sup>-D3 domains interact with FVIII non-covalently resulting in the formation of the VWF/FVIII complex. This binding stabilizes FVIII, brings it to injured sites and protects it from degradation (Rauch et al., 2013). The D4 domain is involved in the side-by-side alignment of VWF monomers, which requires a strong intermonomer interaction to closely associate the monomers (Möller et al., 2016). The D4-D4 interaction tunes the sensitivity of VWF to the hydrodynamic flow as VWF only allows elongation at high shear forces (Möller et al., 2016).

### 2.2.2 A domain

In circulation, VWF is present in its globular conformation under normal shear stress conditions (Crawley et al., 2011; Reininger et al., 2008). While in its globular form, VWF exhibits functional quiescence. Mechanical shear forces in the bloodstream act on the UL-VWF multimers, stretching its conformation, which changes its functional abilities (Crawley et al., 2011). Beside containing an alternative collagen binding site (Rauch et al., 2013), the A1 domain has a binding site enclosed for the platelet receptor GPIIb/IIIa. This receptor is involved in initial platelet adhesion when local shear rates are high (Luo et al., 2012; Reininger et al., 2008). The A2 domain contains the cleavage site for the metalloprotease ADAMTS13 (Figure 2B) at the Tyr1605-Met1606 scissile bond, whereas the A3 domain has a binding site for subendothelial collagen incorporated (Crawley et al., 2011; Lenting et al., 2015; Reininger et al., 2008).

When folded, VWF hides the GPIIb/IIIa and ADAMTS13 interaction sites in the A1 and A2 domains respectively. On the other hand, the binding site for collagen in the A3 domain is constitutively available (Crawley et al., 2011; Reininger et al., 2008). UL-VWF, which can be found circulating or bound to either collagen or endothelial cells, unfolds under high shear stress conditions, unravelling the cryptic binding sites in the A1 and A2 domains. However, the VWF multimers generally obtain the folded conformation in circulation, which makes the ADAMTS13 cleavage site in the A2 domain inaccessible (Reininger et al., 2008; Tersteeg et al., 2015). ADAMTS13 regulates the VWF size by cleaving UL-VWF into smaller and less thrombogenic multimers. The HMW-VWF multimers are essential in primary haemostasis, since they unfold more easily, show higher binding affinity for platelets and expose more binding epitopes compared to smaller multimers (Crawley et al., 2011; Tsai et al., 2012; Vanhoorelbeke et al., 2002).

### 2.2.3. C domain

Initially, VWF tethers platelets through the GPIIb interaction. Conformational changes in the platelet integrin GPIIb/IIIa are caused by platelet activation. This integrin stabilizes platelet-platelet interactions and platelet-vessel adhesion by recognizing the Arginine-Glycine-Aspartic acid (RGD) motif in the VWF C4 domain (Luo et al., 2012; Rauch et al., 2013; Vorchheimer et al., 2006). Therefore, the C4 domain is crucial for the development of a stable cloth (Rauch et al., 2013).

## 2.3. VWF storage & secretion

Once successfully synthesized, the mature VWF is transported and co-packaged into storage organelles, such as  $\alpha$ -granules and Weibel-Palade Bodies (WPBs), respectively found in platelets or endothelial cells (Sporn et al., 1985; Wagner et al., 1982). The inside of the size-varying WPBs is slightly acidified to stimulate the self-assembly of VWF subunits into long helicoidal tubules, called ministacks, compacting the VWF a 100-fold (Lenting et al., 2015). Furthermore, immature WPBs can fuse with each other, which contributes to the heterogeneity of the VWF multimers present in the WPBs (Valentijn et al., 2008). When leaving the Trans-Golgi network, the WPBs mature and several co-resident factors accumulate, which provides the typical rod-shape of the WPBs (Lui-Roberts et al., 2005; Valentijn et al., 2013).

To trigger platelet activation, endothelial cells release VWF via basal or regulated secretory pathways (Sporn et al., 1986). WPBs migrate freely in the cytoplasm and occasionally, a single WPB randomly floats towards the cellular periphery, where it fuses with the cell membrane and releases its VWF content (De Wit et al., 2003). However, this basal secretion mechanism is insufficient to assemble long VWF multimers. Therefore, to generate VWF polymers able to induce platelet aggregation, the stimulation of endothelial cells by cytokines and fluid shear forces regulates the initiation of agonist-induced signalling pathways (Andre et al., 2000; Kremer Hovinga et al., 2017). The regulated multistep WPB exocytosis mechanism generally consists of four steps: tethering, docking, priming and fusion of WPBs with the cell membrane are prior to the release of its content (De Leeuw et al., 1999; Van Breevoort et al., 2014). However, a novel mechanism for regulated VWF secretion, involving both WPBs and autophagosomes, was suggested, since WPBs are repeatedly retrieved nearby autophagosomes and the presence of VWF in those autophagosomes was validated (Torisu et al., 2013). Additionally, VWF is also found to be stored and released from  $\alpha$ -granules in platelets (Wagner et al., 1991).

# Chapter 3 – ADAMTS13

In 1996, a novel plasma metalloprotease, showing VWF cleaving activity, was simultaneously, yet independently described for the first time (Furlan et al., 1996; Tsai et al., 1996). Identification of this VWF-cleaving protease (VWFPC) led to the discovery of hereditary and acquired deficiencies in the activity of this protease, causing thrombotic thrombocytopenic purpura (TTP) (Furlan et al., 1998; Furlan et al., 1997; Tsai et al., 1998). In 2001, this VWFPC was characterized as the 13<sup>th</sup> member of the 'A Disintegrin And Metalloprotease with ThromboSpondin type 1 repeats' (ADAMTS) family of proteases (Fujikawa et al., 2001; Zheng et al., 2001). Therefore, this plasma protein was named ADAMTS13. Various hereditary mutations in the *ADAMTS13* gene generate abnormalities in the VWF-processing capacity of ADAMTS13 (Kokame et al., 2002; Levy et al., 2001), whereas anti-ADAMTS13 autoantibodies clear the plasma protein from circulation or inhibit its enzymatic activity (Zheng et al., 2010; Tsai et al., 1998). When ADAMTS13 is functionally absent, UL-VWF polymers are no longer processed, which bends the balance towards excessive thrombi formation in the microcirculation (Ercig et al., 2018; Feng et al., 2016; Zander et al., 2015). Apart from its role in TTP pathogenesis, ADAMTS13 has been linked with inflammatory diseases, liver diseases, cancer, etc., and has been suggested as a diagnostic and prognostic marker in some of these diseases (Huang et al., 2015; Ikeda et al., 2011; Reuken et al., 2015).

## 3.1. ADAMTS13 biosynthesis

The *ADAMTS13* gene *C9ORF8* spans 37 kb on chromosome 9q34, containing 29 exons (Gerritsen et al., 2001; Zheng et al., 2001). ADAMTS13 is primarily synthesized in hepatic stellate cells and consists of 1427 amino acid residues (Uemura et al., 2005; Zhou et al., 2005). In general, the ADAMTS protein family shows a shared structure, beginning with a N-terminal signal peptide domain (SP), a propeptide domain (P), a zinc-dependent metalloprotease domain (M), a disintegrin domain (D), a first thrombospondin type 1 repeat domain (T1), a cysteine-rich domain (C), a spacer domain (S), seven additional thrombospondin type 1 repeat domains (T2-8) and two complement C1r/C1s, Uegf, Bmp1 domains (CUB) at the C-terminus (Gardner et al., 2009; Petri et al., 2019; Plautz et al., 2018). During ADAMTS13 biosynthesis and secretion (Figure 4), the signal peptide and the propeptide domains are segregated in the endoplasmic reticulum and the Golgi apparatus respectively (Fernandes et al., 2001; Li et al., 2001), resulting in a final glycoprotein of about 180 kDa (Crawley et al., 2011), which is present in a concentration of approximately 1 µg/mL in normal human plasma (Ercig et al., 2018; Feys et al., 2006; Muia et al., 2014; Roose et al., 2018a).

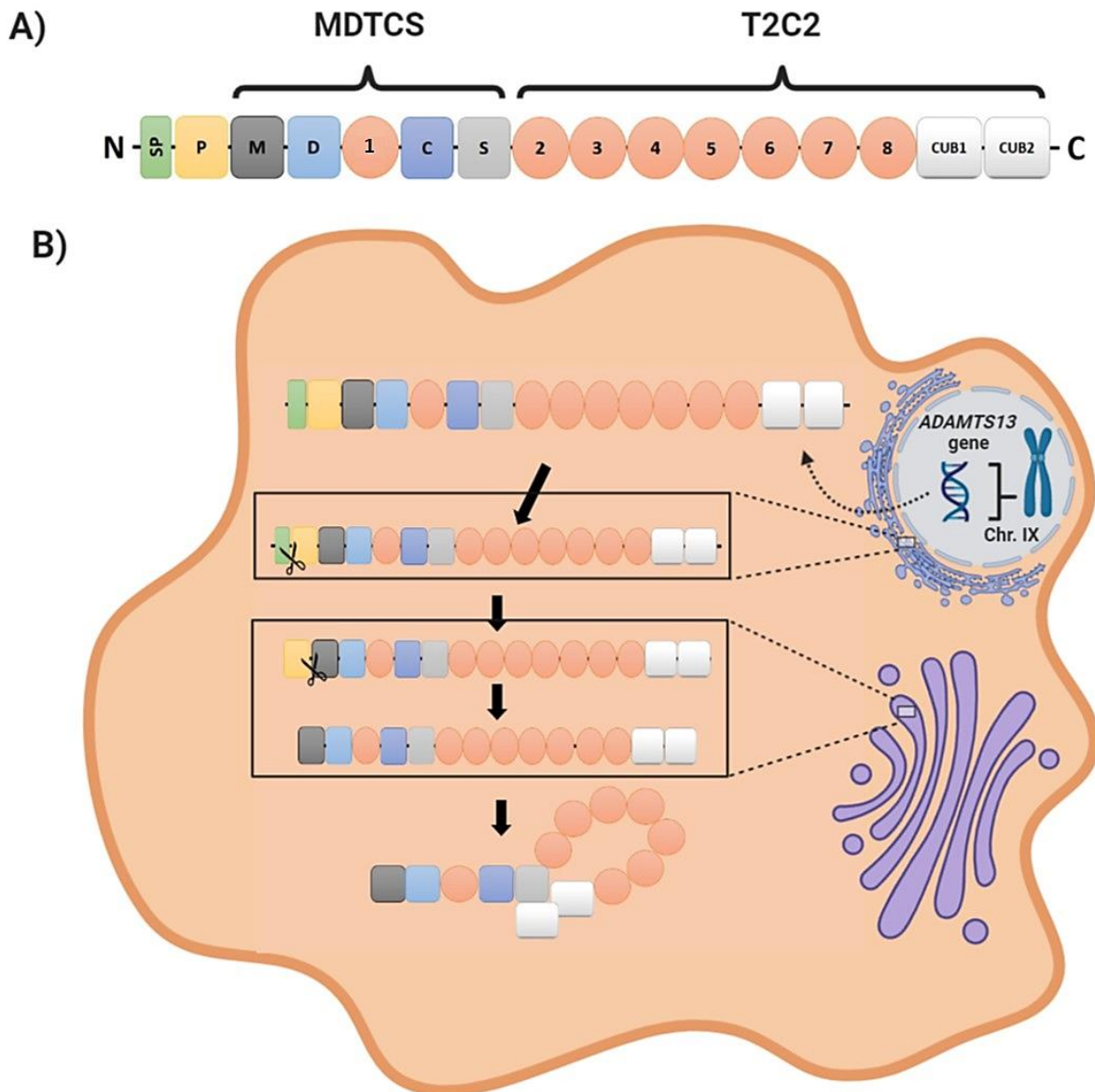


Figure 4: **Domain structure and biosynthesis of ADAMTS13:** A) The alignment of the ADAMTS13 protease domains (Based on (Ercig et al., 2018)). B) Biosynthesis of ADAMTS13 in hepatic stellate cells; when entering the endoplasmic reticulum, the signal peptide domain is removed by signal peptidases. Afterwards the propeptide is removed and proper protein folding occurs in the golgi apparatus, which is followed by the secretion of ADAMTS13 (Based on (Uemura et al., 2005; Watanabe et al., 2009)).

## 3.2. Functional ADAMTS13 domains

### 3.2.1. Propeptide domain

The propeptide of ADAMTS13 is unusually short when comparing to other family members. Yet, this has no adverse effects on its secretion or activation (Zheng et al., 2013). Generally, the propeptide domain of ADAMTS metalloproteases maintains the zymogen form by binding a  $Zn^{2+}$  ion inside the catalytic cleft (Van Wart et al., 1990). The zinc ion binds to a cysteine residue in the catalytic cleft, thereby blocking the active site and maintaining the protease in its zymogen form (Van Wart et al., 1990). However, ADAMTS13 was considered as constitutively active since this so-called 'cysteine switch' mechanism is absent in the ADAMTS13 propeptide (Anderson et al., 2006; Jones et al., 2005; Van Wart et al., 1990; Zhou et al., 2005).

### 3.2.2. Metalloprotease domain

The metalloprotease domain functions as a key role player when focussing on the cleavage of the VWF substrate. Although ADAMTS13 lacks the cysteine-zinc ion interaction, the coordination of metal ions remains essential for the ADAMTS13 activity (Figure 5A) (Ercig et al., 2018). In the catalytic cleft, three histidine residues are present in the conserved HEXXHXXGXXH sequence, which are responsible for the orientation of the  $Zn^{2+}$ -ion (Bode et al., 1993) and allow interaction of the Glu225 residue within the active site to cleave the VWF substrate (Figure 5B) (Shibagaki et al., 2006). Met249 is highly conserved and turns the backbone of the M domain into the so-called Met-turn, which accommodates a hydrophobic setting. This Met-turn supports the histidine residues to regulate the  $Zn^{2+}$  binding (Bode et al., 1993; Ercig et al., 2018).

Homology models revealed the presence of three putative calcium binding sites (Ercig et al., 2018). The first calcium site is coordinated by the side chains of the conserved Asp182 and Glu212 residues, while the  $Ca^{2+}$  ion is stabilized by Leu183, Arg190 and Val192 (Figure 5B) (Gardner et al., 2009; Lancellotti et al., 2016). The calcium site 1 loop is situated near the metalloprotease activity site, which regulates the activity of the ADAMTS13 protease. Since a salt bridge instead of a disulphide bridge is formed close to the site 1 loop, ADAMTS13 significantly differs from other ADAMTS family members (Lancellotti et al., 2016). Calcium sites 2 and 3 are thought to serve as a  $Ca^{2+}$  cluster, which forms the connector loop, consisting of the conserved Glu83, Asp166, Asp173, Cys281 and Asp284 residues (Figure 5B) (Gardner et al., 2009; Lancellotti et al., 2016; Petri et al., 2019).

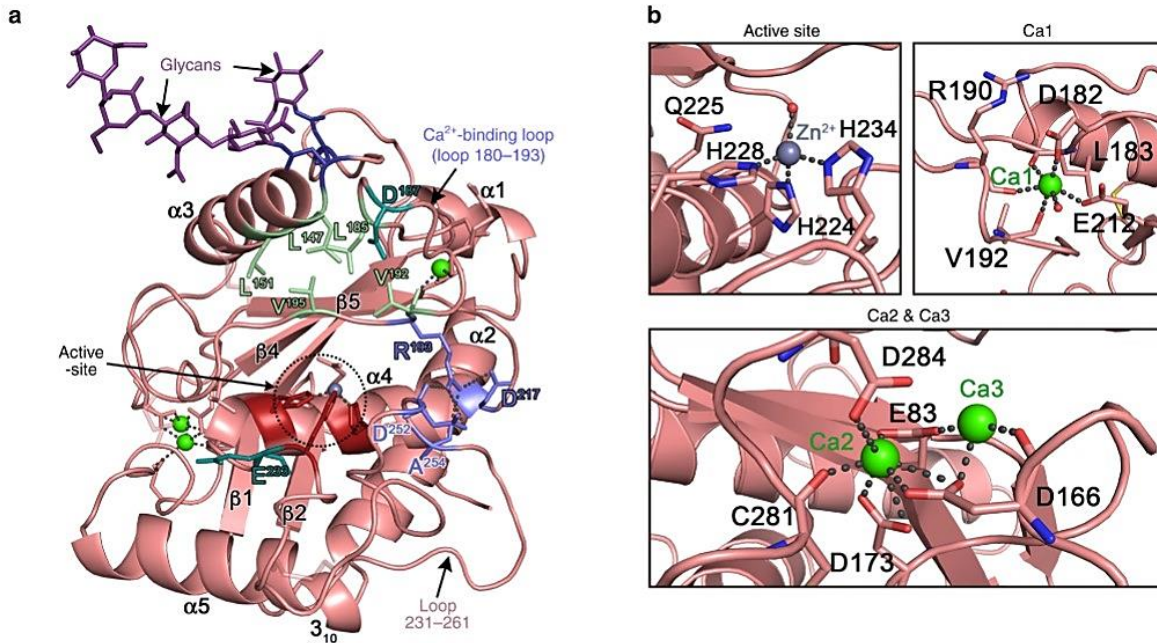


Figure 5: **Metalloprotease domain structure:** A) Crystal structure of the ADAMTS13 metalloprotease domain, with the topology of  $\alpha$ -helices and  $\beta$ -sheets and also the indication of het active site and the Ca<sup>2+</sup> binding loops. B) Detailed representation of the active site and the three Ca<sup>2+</sup> binding sites. Additionally, the amino acid residues required for the coordination of the metal ions at these crucial sites are displayed (Petri et al., 2019).

### 3.2.3. Disintegrin domain

Disintegrins are small soluble polypeptides (47-84 amino acid residues), that can bind the platelet surface protein GPIIb/IIIa (Musial et al., 1990) to serve as platelet aggregation inhibitors. Generally, an RGD sequence approves the high affinity binding of integrin receptors (Ercig et al., 2018; Phillips et al., 1988). However, the ADAMTS13 disintegrin-like domain (D domain) lacks this RGD tripeptide found in other members of the ADAMTS family (De Groot et al., 2009). The D domain of ADAMTS13 possibly obtained an alternative functional architecture through evolution and now plays a combined role in enhancing substrate binding together with the cysteine-rich and spacer domain (De Groot et al., 2015; Zheng et al., 2003). Also, the hydrophobic exosite-1, involved in the recognition of VWF, was identified on the ADAMTS13 D domain (Ercig et al., 2018; Yamaguchi et al., 2011).

### 3.2.4. Cysteine-rich domain

In ADAMTS13, the cysteine-rich domain is situated in between the first thrombospondin type-1 repeat and the spacer domain, containing 10 paired cysteine residues able to form disulphide bonds (Akiyama et al., 2009). The functional part of the ADAMTS13 cysteine-rich domain is not conserved, but harbours the exosite-2 amino acid residues (Ercig et al., 2018). These residues provide a hydrophobic pocket, localised in near proximity to the Pro475 residue (Kokame et al., 2002), which favours interactions with the aromatic side chain of Trp1644 from

the VWF-A2 domain, when exposed due to shear stress induced unfolding (De Groot et al., 2015; Ercig et al., 2018; Zondlo et al., 2013).

### 3.2.5. Spacer domain

The spacer domain, consisting of 130 amino acid residues, is located between the cysteine-rich domain and the second thrombospondin type-1 repeat and mediates essential interactions for complete ADAMTS13 activity (Ercig et al., 2018). MDTCS, a truncated N-terminal ADAMTS13 variant, shows processing activity towards VWF (Ercig et al., 2018). However, complete deletion of the spacer domain from this ADAMTS13 variant, reduces the catalytic activity significantly (Ercig et al., 2018; Tao et al., 2005; Zheng et al., 2003). Exosite-3 of ADAMTS13 is situated in the spacer domain, showing a hydrophobic residue cluster (Akiyama et al., 2009). These surface-exposed residues are involved in ADAMTS13 binding towards the A2 domain of VWF (Jin et al., 2010; Pos et al., 2010), but also turns out to be a major epitope for anti-ADAMTS13 autoantibodies (Luken et al., 2005; Luken et al., 2006; Pos et al., 2011).

### 3.2.6. Thrombospondin Type-1 Repeat domain

In ADAMTS13, the first thrombospondin Type-1 repeat (TSR) is positioned between the disintegrin and the cysteine-rich domains, while seven additional TSRs are consecutively located between the spacer and CUB domains (Akiyama et al., 2009; Petri et al., 2019). Three flexible linker regions are identified between the TSR2/TSR3, TSR4/TSR5 and TSR8/CUB domains (Deforche et al., 2015; Zheng et al., 2001). Structure analysis revealed conserved tryptophan residues promoting ligand interaction and cellular localization (Zheng et al., 2013), although the exact function of each individual TSR domain remains to be elucidated (Tan et al., 2002). Post-translational modification, like O-fucosylation and C-mannosylation, of the TSR domains are shown to have a major impact on ADAMTS13 secretion, stability and VWF binding affinity (Ricketts et al., 2007; Sorvillo et al., 2012; Verbij et al., 2016).

### 3.2.7. CUB domain

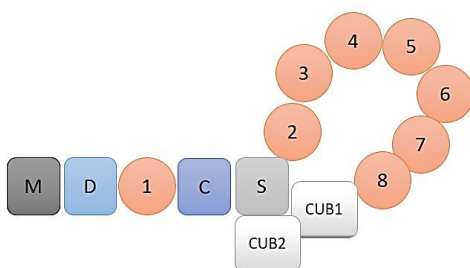
ADAMTS13 is the only ADAMTS family member containing CUB domains, an acronym for complement C1r/C1s, Uegf (epidermal growth factor-related sea urchin protein) and Bmp1 (bone morphogenetic protein 1) (Bork et al., 1993), situated at the C-terminus (Akiyama et al., 2009; Petri et al., 2019). By structural consensus, the two CUB domains respectively consist of 107 and 129 residues (Pimanda et al., 2004) and contain two  $\beta$ -sheets, able to form a  $\beta$ -sandwich architecture, and two disulphide bonds, stabilizing the whole CUB domain (Romero et al., 1997). Homology models show that CUB1 and 2 are highly conserved identities, except for the C-terminal region of CUB2, which displays a rather unconventional structure (Pimanda et al., 2004; Shang et al., 2006).

### 3.3. Open-closed conformation

Metalloproteases of the ADAMTS family bind a  $Zn^{2+}$  ion in their catalytic cleft and use this so-called cysteine switch to maintain their zymogen form (Van Wart et al., 1990). However, ADAMTS13 lacks this regulatory switch and was therefore considered as constitutively active (Gao et al., 2006; Jones et al., 2005). In addition, no natural inhibitors or activators are described for ADAMTS13 and known metalloprotease tissue inhibitors do not inhibit the activity of ADAMTS13 (Guo et al., 2016). However, an alternative regulation mechanism was unravelled, discussing open and closed ADAMTS13 conformations to allosterically regulate the enzymatic activity (Muia et al., 2014; Petri et al., 2019; Roose et al., 2018c; South et al., 2017).

In the closed conformation (Figure 6A), the distal CUB1 and CUB2 domains are folded onto the cysteine-rich and the spacer domain, which represents the inactive ADAMTS13 enzyme. However, to induce its enzymatic activity, the open ADAMTS13 conformation (Figure 6B) is adopted by releasing the CUB domains, which also allows to expose the exosites and cryptic epitopes, found on the spacer domain, to anti-ADAMTS13 autoantibodies (Ercig et al., 2018; Muia et al., 2014; Petri et al., 2019; South et al., 2017). To express its full catalytic function, an effective ligand-enzyme complex is formed, when ADAMTS13 docks on the D4-CK VWF domains, which activates the protease allosterically to stimulate the attachment of ADAMTS13 to the shear stress unfolded VWF A2 domain (Ercig et al., 2018; Muia et al., 2014; Zanardelli et al., 2009). Under normal rheological conditions, ADAMTS13 is found to circulate in its closed form, burying the B-cell epitopes in the spacer domain to protect ADAMTS13 from anti-ADAMTS13 autoantibody recognition (Ercig et al., 2018; South et al., 2014). Although the exact mechanism to modify the ADAMTS13 conformation remains ambiguous, iTTP patients suffering an acute episode typically show elevated levels of the open ADAMTS13 conformation, in combination with higher degrees of anti-ADAMTS13 autoantibodies that target cryptic epitopes (Roose et al., 2018c).

**A) Closed ADAMTS13 conformation**



**B) Open ADAMTS13 conformation**

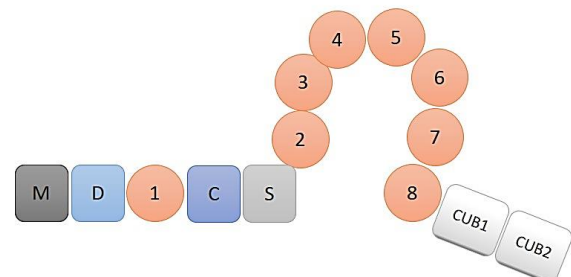


Figure 6: **Conformational states of ADAMTS13:** A) Closed and inactive ADAMTS13 conformation. B) Open, activated ADAMTS13 conformation, which is capable to interact with the VWF A2 domain (based on (Petri et al., 2019; Roose et al., 2018a)).

### 3.4. Recognition and cleavage of VWF by ADAMTS13

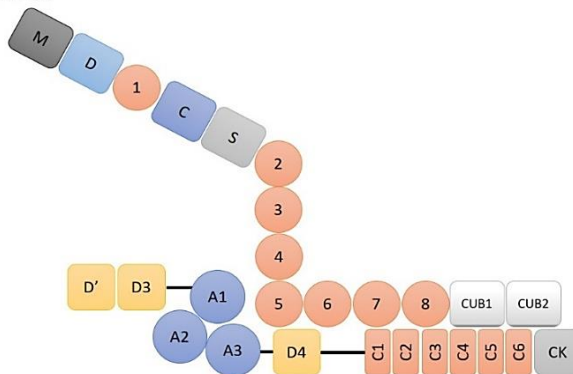
Recognition of VWF by ADAMTS13 is complex and highly specific, requiring several interactions between both substrate and enzyme (Crawley et al., 2011). The process of exactly coordinating the VWF scissile bond towards the ADAMTS13 proteolytic site is referred to as the 'molecular zipper' mechanism (Crawley et al., 2011; Petri et al., 2019). Although ADAMTS13 circulates in a low-activity state and only is completely catalytic active when the open conformation is established (Ercig et al., 2018), small amounts of the plasma ADAMTS13 (~3%) are bound to globular VWF (Crawley et al., 2009; Feys et al., 2009). Since the binding sites within the VWF D4-CK domains are constitutively exposed, reversible ADAMTS13 association, which is mediated by the TSR5-CUB domains, is allowed (Figure 7A) (Ercig et al., 2018; Zhang et al., 2007). However, globular VWF cannot be cleaved (Feys et al., 2009), since other binding sites as well as the scissile bond are hidden inside the enclosed core of the VWF A2 domain (Zanardelli et al., 2006; Zhang et al., 2009). A vicinal disulphide bridge, between the 1669 and 1670 cysteine residues, bends the VWF A2 backbone into the so-called 'molecular plug', establishing an hydrophobic environment surrounding the core of the A2 domain (Crawley et al., 2011; Zhang et al., 2009).

Elevated rheological shear forces take away the molecular plug due to the entrance of water molecules, which destabilize the hydrophobic core and unfolds the VWF A2 domain (Luken et al., 2010). When the A2 domain is stretched, additional binding sites on VWF are revealed and the binding affinity of ADAMTS13 for VWF increases (Crawley et al., 2011; Kokame et al., 2004). The ADAMTS13 spacer domain contributes substantially to the VWF recognition by binding the cryptic Glu1660-Arg1668 exosite residues of the A2 domain (Figure 7B) (Gao et al., 2006). Next, the ADAMTS13 cysteine-rich domain recognizes a functional exosite adjacent to those A2 domain residues (Akiyama et al., 2009; Gao et al., 2008). Furthermore, Arg349 and Leu350 of the ADAMTS13 D domain functionally operate with the Asp1614 exosite of the VWF A2 domain (De Groot et al., 2009; Zanardelli et al., 2006; Zheng et al., 2003), whereas this interaction stimulates the scissile bond to orientate towards the active ADAMTS13 centre (Figure 7C) (De Groot et al., 2009; Zanardelli et al., 2006).

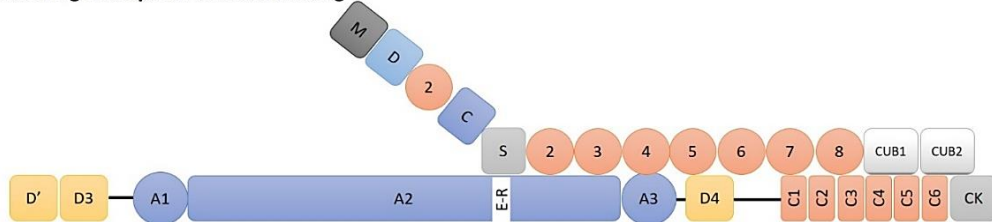
Human ADAMTS13 contains three variable regions: S1, S1' and S3, which provides the substrate specificity (De Groot et al., 2010). The metalloprotease domain harbours these three variable sites to regulate the scissile bond specificity by interacting in close proximity to the cleavage site (Crawley et al., 2011; Pruss et al., 2008). The Tyr1605 (P1) and Met1606 (P1') VWF residues require accommodation in specific ADAMTS13 binding pockets (Pruss et al., 2008; Xiang et al., 2011). The ADAMTS13 S1 pocket interacts with the P1 residue, whereas the S1' binding pocket integrate the P1' residues of VWF (De Groot et al., 2010; Xiang et al., 2011). Both highly specific interactions desire a hydrophobic nature and are assumed to consist of amino acid residues of the Ca<sup>2+</sup>-high-affinity binding site loops (Pruss et al., 2008;

Xiang et al., 2011). An ADAMTS13 docking site is found N-terminal to the scissile bond, which is necessary to cleave VWF enzymatically (Figure 7D) (Crawley et al., 2011; Petri et al., 2019; Xiang et al., 2011). Especially, the VWF 1596-1604 residues harbour a structural determinant essential for proteolysis, which is recognized by the ADAMTS13 S3 subsite. Systematic substitution unravelled that the P3 (Leu1603) residue of VWF play a substantial in the cleavage of the scissile bond (Crawley et al., 2011; Xiang et al., 2011). When the scissile bond is cleaved, ADAMTS13 shows lowered affinity for the smaller VWF multimers, which allows ADAMTS13 to target new UL-VWF fragments or permits the recycling of ADAMTS13 (Crawley et al., 2011).

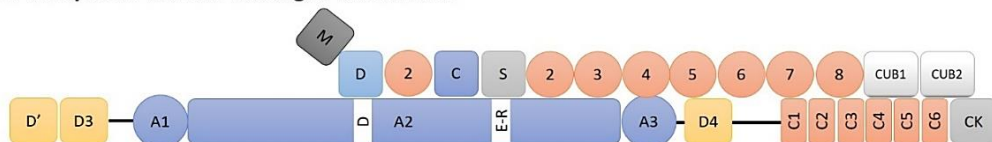
A) Globular VWF-ADAMTS13 complex



B) VWF unravelling and Spacer domain binding



C) Binding of the cysteine-rich and disintegrin-like domains



D) Metalloprotease subsite binding and VWF proteolysis

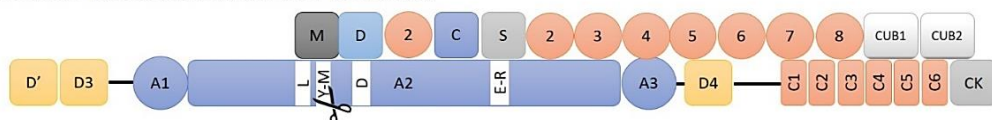


Figure 7: **VWF proteolysis by ADAMTS13:** A) VWF adopts its globular conformation in circulation, allowing ADAMTS13 binding via the TSR(5-8) and CUB domains. B) Increased shear forces remove the molecular plug, unfolding the VWF A2 domain. Cryptic epitopes in the A2 domain grant the ADAMTS13 spacer domain to interact. C) Stepwise, the cysteine-rich and the disintegrin-like domain correctly direct the VWF cleavage site to the ADAMTS13 active site via low-affinity contact. D) The S3 subsite in the metalloprotease domain interacts crucially with the L1603 residue of the VWF A2 domain. Thereafter, the S1 and S1' subsites dock at the Y1605-M1606 residues of the scissile bond, promoting VWF proteolysis (based on (Crawley et al., 2011; Petri et al., 2019)).

# Chapter 4 – Thrombotic thrombocytopenic purpura

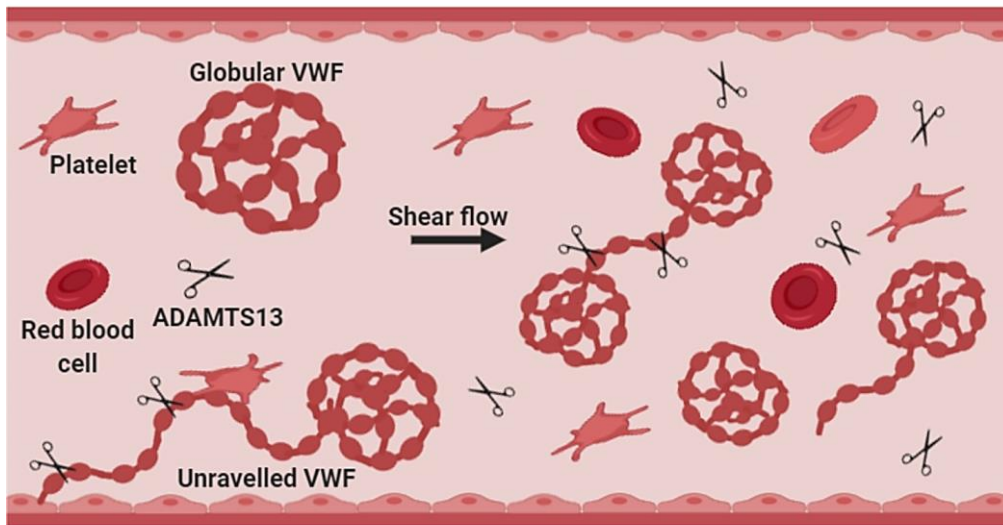
Thrombotic thrombocytopenic purpura (TTP) is a rare and life-threatening disease, which was also called Moschcowitz syndrome, since Dr. Eli Moschcowitz reported this undescribed disorder for the first time in 1924 (Kremer Hovinga et al., 2017). An acute onset of fever, anemia, impairment of the central nervous system and renal dysfunction was presented by his 16-year-old patient (Moschcowitz et al., 1925). However, the cause of TTP remained elusive until 1984, when UL-VWF multimers were found to be involved in chronic relapsing TTP (Moake et al., 1982; Sadler et al., 2017). Therefore, it was hypothesized that plasma of TTP patients lacks a VWF processing factor (Moake et al., 1982). In 1996, ADAMTS13 was discovered as the protease involved in VWF cleavage, which was found to be deficient in plasma samples of TTP patients (Furlan et al., 1996; Tsai et al., 1996). By now, a severe deficiency of ADAMTS13 activity (<10% of its normal activity), resulting from mutations in the *ADAMTS13* gene or anti-ADAMTS13 autoantibodies, specifies TTP (Kremer Hovinga et al., 2017; Moake et al., 2002). Although the knowledge on the pathophysiology of TTP increased enormously during the past decades, proper diagnosis and TTP treatment remains challenging (Kremer Hovinga et al., 2017).

## 4.1. Pathophysiology

In healthy individuals, UL-VWF multimers are either secreted in the circulation or anchored to endothelial cells (Dong et al., 2002; Schneider et al., 2007). Under high local shear forces, the UL-VWF multimers unfold according to the tensile forces of the elongational flow (Sadler et al., 2017; Schneider et al., 2007). When the unfolded cryptic epitopes in VWF are exposed, the Tyr1605-Met1606 site in the VWF A2 domain is proteolysed by ADAMTS13, which results into smaller and less thrombogenic VWF multimers (Figure 8A) (Crawley et al., 2011; Shim et al., 2008; Skipwith et al., 2010). The tensile force-mediated VWF cleavage prevents spontaneous thrombus formation (Sadler et al., 2017). However, when ADAMTS13 is deficient, platelets spontaneously bind to the unprocessed, prothrombotic UL-VWF multimers (Figure 8B) (Arya et al., 2002). The circulating platelets are sequestered in VWF-platelet aggregates, which results in the formation of platelet-rich microthrombi, which is considered as a TTP hallmark (Joly et al., 2017; Kremer Hovinga et al., 2017; Sadler et al., 2017). The blood flow is obstructed and due to scavenging and deprivation of platelets, thrombocytopenia occurs, whereas red blood cells are fragmented into schistocytes, which results in haemolytic anaemia (Kremer Hovinga et al., 2017). Partial occlusion of the microcirculation causes organ ischemia, particularly in the heart, kidneys, brain and gastrointestinal tract (Kremer Hovinga et al., 2012;

Scully et al., 2014). After the disease onset, untreated patients die within days or weeks, since organ failure develops.

### A) Healthy individual



### B) TTP patient

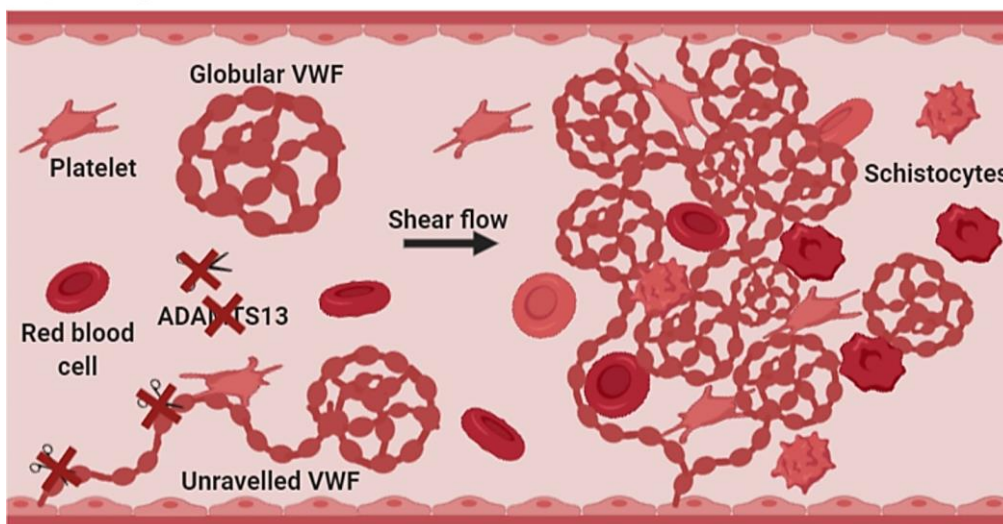


Figure 8: **TTP pathophysiology:** A) Microvessel of a healthy individual. Exposure of cryptic epitopes in UL-VWF allows recognition by ADAMTS13 and cleavage of the Tyr1605-Met1606 scissile bond, resulting into less thrombogenic VWF multimers. B) Microvessel of a TTP patient. Anti-ADAMTS13 autoantibodies or mutations in the *ADAMTS13* gene result in a deficiency of ADAMTS13. Thereby, UL-VWF is no longer cleaved, accumulates platelets and forms excessive microthrombi, which occludes small blood vessels (based on (Kremer Hovinga et al., 2017)).

## 4.2. Congenital TTP

When ADAMTS13 is deficient as a result of homozygous or compound heterozygous mutations in the *ADAMTS13* gene on chromosome 9q34 (Kremer Hovinga et al., 2017; Rossio et al., 2013), patients are typically diagnosed with congenital TTP (cTTP), which is also known as Upshaw-Schulman syndrome (Upshaw et al., 1978). The actual incidence of cTTP remains

uncertain, however, cTTP has been postulated to account for <5% of all acute TTP episodes (Galbusera et al., 2009; Mariotte et al., 2016). During the past decades, over two hundreds of different causative ADAMTS13 mutations including, frameshift, nonsense, splice site and missense mutations, are localised throughout the protein-coding domains of the *ADAMTS13* gene (Kremer Hovinga et al., 2017). Most of the *ADAMTS13* gene mutations inhibit protein secretion, whereas other mutations induce a lack of VWF proteolysis activity (Kokame et al., 2002; Pimanda et al., 2004; Uchida et al., 2004; Underwood et al., 2016). So far, no correlation was found when linking genotypes to a particular phenotype and therefore, clinical disease onset is thought to be triggered by environmental factors in combination with modified genetics (Lämmle et al., 2005; Lotta et al., 2010). Half of the patients present their first TTP episode during childhood, by the age of 2-5, whereas a second TTP onset peak is found in early adulthood with a significant onset for cTTP during first pregnancy (25-66%) (Fujimura et al., 2011; Kremer Hovinga et al., 2017; Taleghani et al., 2013; Scully et al., 2014). Since cTTP is a rare disease and often misdiagnosed, its incidence is possibly underestimated. However, patients risk chronic relapsing TTP episodes and therefore require long-term follow-up (Joly et al., 2017; Kremer Hovinga et al., 2012).

### 4.3. Immune-mediated TTP

In about 95% of TTP patients, the severe ADAMTS13 deficiency is caused by anti-ADAMTS13 autoantibodies and therefore, these patients are diagnosed with the autoimmune disorder, called immune-mediated TTP (iTTP) (Kremer Hovinga et al., 2017). These iTTP patients demonstrate the presence of both inhibitory antibodies, that diminish the ADAMTS13 function, and clearance anti-ADAMTS13 autoantibodies, that remove ADAMTS13 from circulation (Rieger et al., 2006; Scheiflinger et al., 2003; Thomas et al., 2015). Epitope mapping identified that autoantibodies against the ADAMTS13 spacer domain are present in almost all iTTP patients (Klaus et al., 2004; Zheng et al., 2010; Luken et al., 2005). However, as the immune response is polyclonal, antibodies are targeting other domains of the ADAMTS13 enzyme as well (Klaus et al., 2004; Kremer Hovinga et al., 2017; Zheng et al., 2010). Although IgM and IgA autoantibodies are found in some iTTP patients, antibodies of the IgG class are predominantly present (Ferrari et al., 2009; Ferrari et al., 2007; Rieger et al., 2005). Especially, the IgG4 subclass is often found as the only anti-ADAMTS13 isotype and high titers of IgG4 are associated with an increasing risk to relapse (Ferrari et al., 2009; Ferrari et al., 2007). Furthermore, black ethnicity, female sex, obesity and higher frequency of the human leukocyte antigen class II allele (HLA-DRB1\*11) are described as risk factors promoting pathogenic anti-ADAMTS13 autoantibody development in iTTP patients (Coppo et al., 2010; Joly et al., 2017; Kremer Hovinga et al., 2017; Sakai et al., 2020; Scully et al., 2010).

## 4.4. Diagnosis

### 4.4.1. Clinical presentation

After literature screening, the clinical findings, presented in 88 to 98% of the patients, were delineated into a diagnostic pentad for TTP, which includes fever, microangiopathic haemolytic anaemia with schistocytes present in the peripheral blood smear, purpura linked to thrombocytopenia (Figure 9), renal dysfunction and neurological impairment ranging from headaches to seizure and coma (Amorosi et al., 1966; Kremer Hovinga et al., 2017). However, acute onset and severe disease course are often found without the presentation of the complete clinical pentad (Allford et al., 2003; Scully et al., 2012; Veyradier et al., 2005), whereas prodromic symptoms of TTP, like fatigue, flu-like illness or abdominal and lumbar pain, are frequently observed (Coppo et al., 2019; Page et al., 2017). Peripheral thrombocytopenia and microangiopathic haemolytic anaemia are constant TTP features (Coppo et al., 2019), associated with signs of red blood cell fragmentation, such as free serum haemoglobin or increased levels of lactate dehydrogenase (LDH) (Knöbl et al., 2018). Renal injury is in most TTP patients mild or even absent, but still remains significant since kidney failure is described in 10 to 27% of TTP patients (Joly et al., 2017; Kremer Hovinga et al., 2017). Manifestations in cerebral tissue or in the digestive tract are found to be common (Page et al., 2017), while the awareness of cardiac features, involving arrhythmias, congestive heart failure and cardiac arrest, increased over the last few years (Benhamou et al., 2015; Coppo et al., 2019; Hughes et al., 2009). Although all these new insights in TTP epidemiology, these clinical findings are not specific for TTP and other thrombotic microangiopathy (TMA) disorders with similar manifestations, may overlap with the TTP presentation (Coppo et al., 2019; Kremer Hovinga et al., 2017).

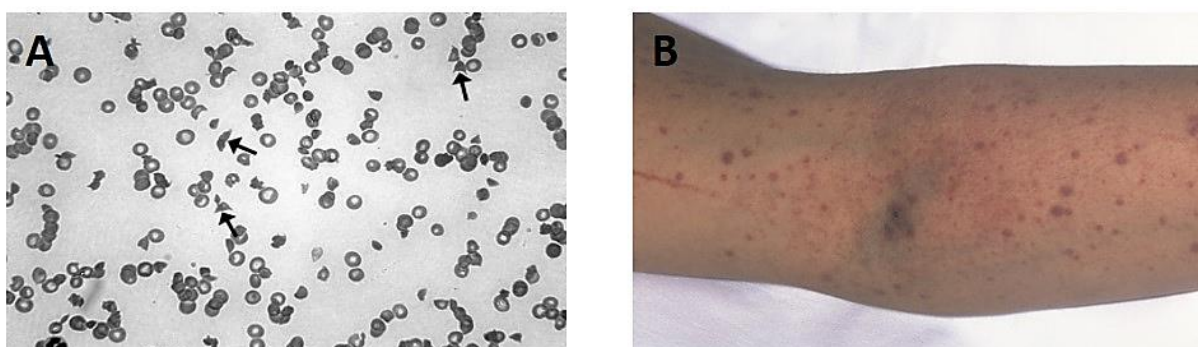


Figure 9: **Clinical symptoms of TTP presentation:** A) Fragmented red blood cells (schistocytes) present in the peripheral blood smear (Lämmle et al., 2005). B) Purpura and petechiae in the forearm linked to thrombocytopenia (Image retrieved from: <https://www.nhlbi.nih.gov/health-topics/thrombotic-thrombocytopenic-purpura>).

#### 4.4.2. Differential diagnosis

The clinical signs during TTP presentation are variable and overlap with a series of other TMAs, even when the complete clinical pentad is simultaneously present. Therefore, accurate TTP diagnosis is difficult (Grall et al., 2017). Similar clinical manifestations are observed in several differentially diagnosed TMAs, including Shiga toxin-associated and atypical haemolytic uraemic syndrome (HUS), connective tissue disorders and drug-associated TMAs (Kremer Hovinga et al., 2017). Therefore, a presumptive diagnosis, following sensitive clinical criteria, is mandatory, since the initiation of appropriate treatment cannot be postponed (Kremer Hovinga et al., 2017). When thrombocytopenia and microangiopathic haemolytic anaemia are presented, the patient is diagnosed with a TMA. However, TTP is only confirmed when ADAMTS13 activity is below 10%, since ADAMTS13 deficiency is the only specific biomarker and thus diagnostic feature to discriminate TTP from other TMAs (Figure 10) (Joly et al., 2017). When anti-ADAMTS13 autoantibodies are detected during an acute TTP episode, patients are generally diagnosed with iTTP. However, when no anti-ADAMTS13 autoantibodies are detected, but the ADAMTS13 activity is measureable during remission, patients are recognized with acquired TTP with unknown mechanism (Kremer Hovinga et al., 2017). Congenital TTP is considered when ADAMTS13 activity is always below 10%, no anti-ADAMTS13 antibodies are detected and homozygous or compound heterozygous mutations result from *ADAMTS13* gene analysis. Only when the ADAMTS13 activity is always <10%, but no autoantibodies and no *ADAMTS13* mutations were found, the exceptional diagnosis of TTP with unknown aetiology is made (Joly et al., 2017; Knöbl et al., 2018). Major concerns in TTP diagnosis are misdiagnosis and the delay of the diagnosis due to the unavailability of essential ADAMTS13 assays in hospital settings (Sadler et al., 2015), since ADAMTS13 activity assays are generally performed in specialized reference laboratories (Coppo et al., 2019; Grall et al., 2017).

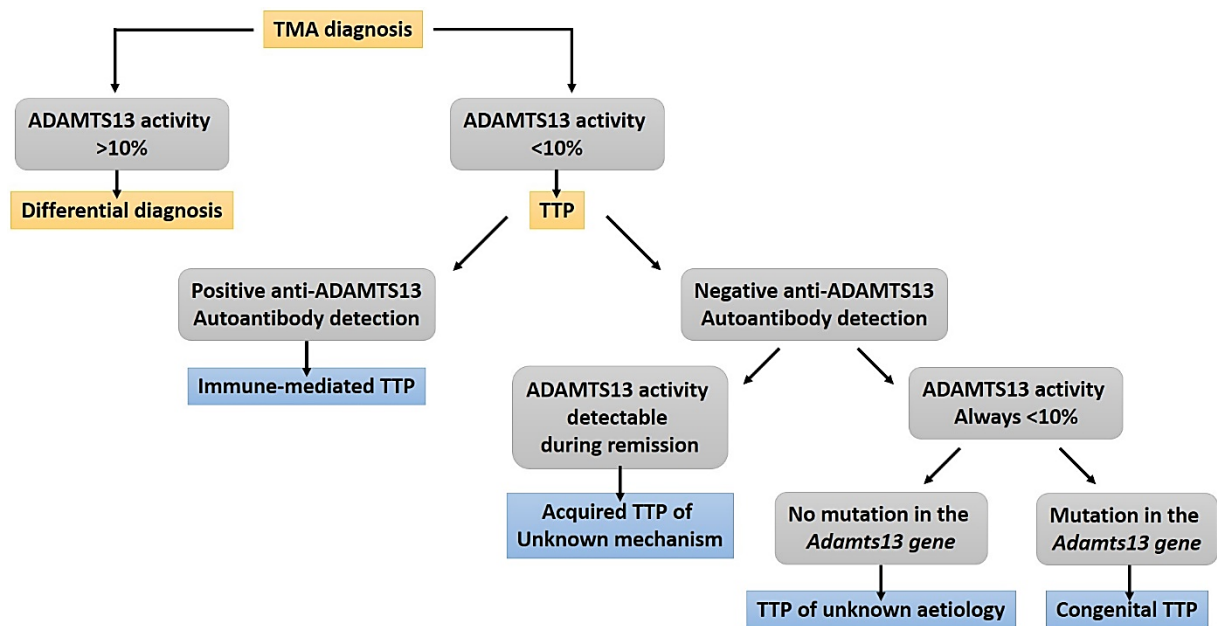


Figure 10: **Flowchart for TTP diagnosis:** First, ADAMTS13 activity is determined, since this is the only specific biomarker that discriminates TTP from other TMAs. When the ADAMTS13 activity is lower than 10% of the normal activity, TTP is diagnosed. Patients are diagnosed with iTTP if anti-ADAMTS13 autoantibodies are detected. However, when no anti-ADAMTS13 autoantibodies are present and the enzymatic activity recovers during remission, the distinct diagnosis is acquired TTP with an unknown underlying mechanism. On the other hand, congenital TTP is recognized when the ADAMTS13 activity always remains below 10% and mutations in the *ADAMTS13* gene are found. However, when no mutations are detected but the activity is <10%, TTP of unknown aetiology is described (bases on (Joly et al., 2017)).

## 4.5. Current therapy

As an medical emergency, TTP demands proper diagnosis and effective management since a delay in treatment results in severe consequences like organ failure and even death (Joly et al., 2017; Veyradier et al., 2005). Historically, the TTP mortality rate reached up to 90% since no proper treatment was available yet. Therefore, the universal prognosis of TTP was fatal until plasmapheresis was introduced in the 1970s. Plasma therapy includes plasma infusions to treat cTTP, whereas therapeutical plasma exchange (TPE) is provided to iTTP patients. As a result, the survival rate of TTP patients increased up to 80% (Lämmle et al., 2005; Sadler et al., 2017). At present, plasma therapy remains the cornerstone in the treatment of patients with a severe ADAMTS13 deficiency, even though additional immunosuppressive drugs are administered since the understanding of the underlying pathophysiology increased (Lämmle et al., 2005).

### 4.5.1. Congenital TTP

Regular plasma infusions (every 2-3 weeks) are generally considered as satisfactory in the treatment of cTTP patients to effectively prevent acute episodes, since the infusions provide sufficient functional ADAMTS13 (Fujimura et al., 2011; Fujimura et al., 2009; Scully et al., 2014). Since lifelong plasma treatment is inconvenient and ADAMTS13 was characterized as the missing key in TTP, a recombinant ADAMTS13 (rADAMTS13) enzyme was developed and its tolerability and safety are screened in an ongoing phase 3 clinical trial (ClinicalTrials.gov NCT03393975) (Kremer Hovinga et al., 2017). The previous phase 1 clinical trial gained insights on the rADAMTS13 activity, since the larger VWF multimers are effectively cleared, whereas no adverse effects of the recombinant enzyme were detected (Coppo et al., 2017). However, the expensive cost for rADAMTS13 synthesis remains a significant concern (Coppo et al., 2019; Knöbl et al., 2018). More recently, gene therapy was evaluated in mice models, since it is considered as an alternative therapy for long-term prevention of cTTP by curing the underlying monogenetic defects (Verhenne et al., 2017).

### 4.5.2. Immune-mediated TTP

The front-line treatment for iTTP patients with an acute episode is TPE, in which the patient plasma is removed and replaced by large infusions of donor plasma (Knöbl et al., 2018; Kremer Hovinga et al., 2017). The donor plasma restores the ADAMTS13 activity while anti-ADAMTS13 autoantibodies, inflammatory cytokines, HMW-VWF multimers and immune complexes are removed (Kremer Hovinga et al., 2017). Therefore, as soon as TTP is diagnosed, TPE treatment should be started until clinical recovery and complete remission is obtained (Joly et al., 2017; Rock et al., 1991). However, TPE turns out to be insufficient in order to abolish the auto-immune character of iTTP (Furlan et al., 1998; Tsai et al., 1998). Consequently, immunomodulating drugs, which interferes with and blocks the production of anti-ADAMTS13 autoantibodies, are co-administered (George et al., 2012; Knöbl et al., 2018; Sayani et al., 2015; Scully et al., 2016). Corticosteroids, such as methylprednisolone, are introduced as a routine adjunctive therapy to TPE due to its anti-inflammatory and immunosuppressive contribution (Balduini et al., 2010; Joly et al., 2017). Intracellular glucocorticoid receptors regulate gene expression in order to inhibit the biosynthesis of inflammatory mediators or to promote apoptosis of leukocytes (Murphy et al., 2018). Since the use of Rituximab, a humanized antibody against the CD20 epitope on B cells, is effective in several antibody-mediated autoimmune disease, clinical studies assessed its role in the treatment of iTTP patients (Coppo et al., 2019; Scully et al., 2014). Generally, Rituximab is considered as a safe and effective treatment that reduces the autoimmune nature of iTTP, since the production of anti-ADAMTS13 autoantibodies is suppressed by the depletion of peripheral B cells (Benhamou et al., 2016; Coppo et al., 2019; Scully et al., 2014). However, TPE removes Rituximab from the circulation, therefore, its mode of action is maximized by

Rituximab administration subsequent to TPE. Moreover, the optimal therapeutic effect against the autoimmune antibody production is delayed after applying Rituximab (Froissart et al., 2012; Westwood et al., 2013). Caplacizumab, commercially available as Cablivi, is a humanized nanobody with origin from heavy chain immunoglobulins from *Camelidae*, that does not target the autoimmune response, but prevents platelet binding towards VWF by blocking the VWF A1 domain interaction with GPIb $\alpha$  (Cataland et al., 2012; Jilma-Stohlawetz et al., 2011). As a result of supplemental Caplacizumab treatment, platelet counts normalize more rapidly, and other biomarkers found for organ injury also restore faster (Peyvandi et al., 2016).

# Chapter 5 – FO-SPR

The current diagnosis of TTP, through enzyme-linked immunosorbent assays (ELISA) and fluorescence resonance energy transfer assays (FRETs), is time-consuming and need to be performed in specialized laboratories. To monitor the relevant ADAMTS13 parameters, such as the enzyme activity, conformation, antigen and autoantibody levels, an easy-to-use diagnostic assay is required to maximize the therapeutic outcome of the disease management. To generate a proper point- of-care diagnosis technique, an easy-to-use, single-sample testing platform is required, which is inexpensive and has good accuracy, a short detection time and minimal sample preparation (Corstjens et al., 2013; Van Stappen et al., 2017).

Therefore, the innovative fiber-optic surface plasmon resonance (FO-SPR) technology is used to develop the rapid diagnostic tests for the validation of the ADAMTS13 parameters from patient plasma samples. The SPR biosensors detect the change of the local refractive index when immobilized biomolecules capture a specific analyte. Even though these standard SPR biosensors provide ultrasensitive, specific analyte measurements in real-time, they remain large, expensive and inconvenient to work with. Therefore, the novel FO-SPR technique was recently developed, which offers a robust, cost-effective and easy-to-use alternative for the standard SPR technology. This FO-SPR platform permits single-sample testing with fast analysis time combined to clinical relevant sensitivity (Lu et al., 2017). A light source transmits light through a bifurcated optic fiber (Figure 11A), that is coated with a thin gold layer at its pigtail end to enable light reflection through the probe back to a spectrometer sensor. Bioreceptor molecules are immobilized on the gold layered fiber surface and when target analytes bind, a shift occurs in the refractive index of the reflected light (Figure 11B) (Homola et al., 2008; Nguyen et al., 2015). Moreover, the optic fibers are compatible with gold nanoparticles (AuNPs), which increases the sensitivity and specificity due to a signal amplification of the shift after molecular interactions (Bedford et al., 2012; Hounkhamhang et al., 2018; Pollet et al., 2009). The robustness and versatility of the FO-SPR biosensor was illustrated by the screening of clinical patient samples (e.g.: Infliximab in inflammatory bowel disease (Lu et al., 2017), Adalimumab in Crohn's disease (Bian et al., 2018)), thereby proving its value as a diagnostic tool for the detection of various small molecules, like DNA and proteins (Bian et al., 2018; Daems et al., 2017; Lu et al., 2017; Lu et al., 2016).

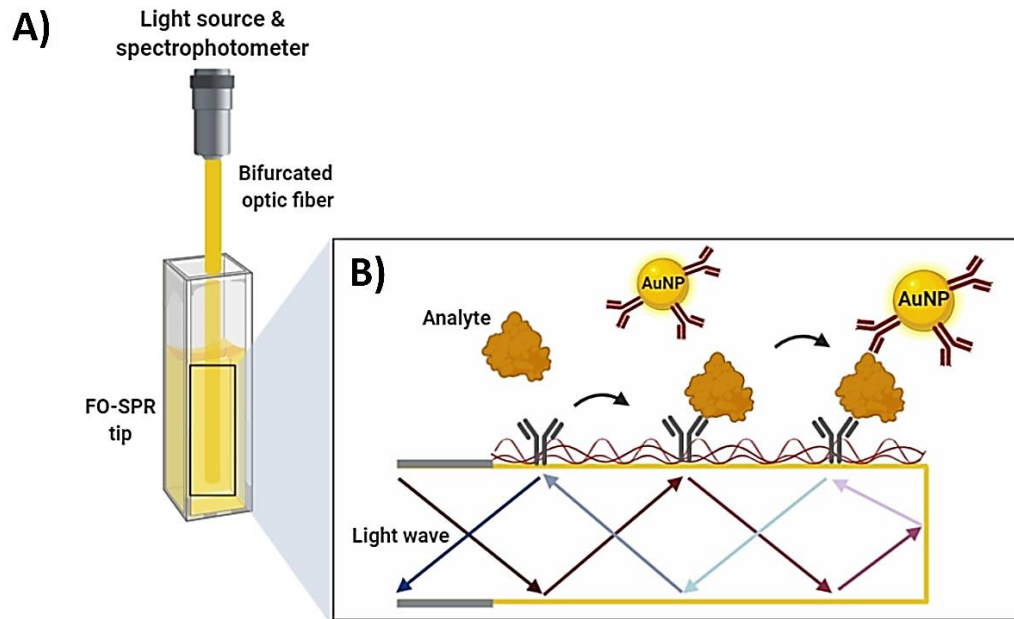


Figure 11: **FO-SPR bioassay**: A) FO-SPR biosensor set-up; a light source is connected through a bifurcated optical fiber to a spectrometer, which functions as an optic sensor probe. The optical fiber tip is successively submerged in microliter volumes containing receptor or target biomolecules. B) Biomolecular interaction analysis; labelled or label-free (not shown) sensor technology is used to analyse small biomolecules, generating information on binding kinetics and quantification of target molecules.

# **Part II**

# **Objectives**

Since iTTP is a rare and life-threatening disease, rapid and appropriate diagnosis is essential for the initiation of proper disease management, which could enhance the therapeutic outcome significantly. It is paramount that the diagnosis can be made quickly to deliver the correct therapy, but due to the diversity of the clinical signs that overlap with those of other TMAs, urgent diagnosis of iTTP remains challenging. Therefore, this master's thesis generally focused on the development of easy-to-use bioassays to monitor several ADAMTS13 parameters (anti-ADAMTS13 autoantibodies and ADAMTS13 conformation) to accelerate and improve the diagnosis and overall therapeutic outcome of iTTP patients.

## 2.1. Anti-ADAMTS13 autoantibody levels

An acute TTP episode is considered as an emergency setting and therefore, treatment is immediately initiated from the very moment that the diagnosis of TTP is suspected. Nevertheless, this decisive diagnosis is generally substantiated with the presentation of clinical signs and symptoms rather than based on the monitored ADAMTS13 parameters. The evaluation of anti-ADAMTS13 autoantibody levels enables the differential diagnosis between the different TTP forms and facilitates the adjustment of the disease management, since both iTTP and cTTP patients present reduced ADAMTS13 activity. Therefore, as a part of the standard diagnostic tests, the levels of anti-ADAMTS13 autoantibodies (both inhibitory and clearance antibodies) are quantitatively evaluated by in-house developed or commercial anti-ADAMTS13 autoantibody ELISA assays. Multiple studies attempted to associate the anti-ADAMTS13 autoantibody titers with the clinical outcome (Hughes et al., 2009; Peyvandi et al., 2008; Scully et al., 2007), but only recently, elevated autoantibody levels were linked to enhanced cardiac involvement and increased mortality rates (Alwan et al., 2017). However, it remains challenging to translate these observations to the routine clinical practice since different reference laboratories perform different in-house or commercial ELISAs that vary in their approach of presenting recombinant ADAMTS13 (e.g.: full-length or truncated ADAMTS13; captured ADAMTS13) and detection method of the anti-ADAMTS13 autoantibodies (e.g.: poly- or monoclonal). Since the influence of these different approaches is currently not known, several of the experimental anti-ADAMTS13 autoantibody ELISA set-ups (coated ADAMTS13; coated MDTCS and T2C2; captured ADAMTS13; polyclonal vs. monoclonal detection antibodies) were performed to assess the variation on the anti-ADAMTS13 autoantibody titers (**AIM 1**).

Up till now, all ADAMTS13 characteristics (enzymatic activity, open/closed conformation, antigen and autoantibody levels) were generally evaluated by in-house developed ELISAs and FRET assays. Nevertheless, three major concerns are involved with both techniques: (1) The assays need to be run by well-trained lab technicians in highly specialized laboratories, (2) It takes relatively long to generate reliable results for all ADAMTS13 characteristics, (3) Multiple patient samples need to be collected in a central laboratory prior to the distribution of the

samples to the reference laboratories that perform the different assays (Lu et al., 2017). To generate a proper point-of-care (POC) diagnosis technique, an inexpensive platform for single-sample testing with minimal sample preparation is required (Corstjens et al., 2013; Van Stappen et al., 2017). Therefore, an FO-SPR immunoassay for the determination of anti-ADAMTS13 autoantibody levels was developed and optimized, since this easy-to-use technique permits real-time sample monitoring in combination with a clinical relevant sensitivity (Lu et al., 2017) (**AIM 2**).

## 2.2. ADAMTS13 conformation analysis

Recently, ADAMTS13 was found to circulate in its open conformation during acute and remission phases of iTTP and was therefore considered as a hallmark and novel biomarker for iTTP (Roose et al., 2018a; Roose et al., 2020). Although the multifactorial cause of the switch from closed to open conformation is not strictly defined yet, anti-ADAMTS13 autoantibodies were found to induce the open conformation (Jestin et al., 2018; Roose et al., 2018b; Roose et al., 2020). The ADAMTS13 conformation ELISA assay, using the anti-ADAMTS13 antibody 1C4 that targets a cryptic epitope in the spacer domain, was developed in-house (Laboratory for Thrombosis Research, KU Leuven Campus Kulak Kortrijk) to discriminate between the open (conformation index (CI) > 0.5) and closed (CI ≤ 0.5) conformation (Roose et al., 2018a). Despite the fact that the ADAMTS13 conformation could be successfully screened in patient plasma samples, this ADAMTS13 conformation ELISA suffers from the same controversies as described above. Accordingly, the easy-to-use FO-SPR technology provides a promising alternative to improve the ADAMTS13 conformation test by overcoming these ELISA-related limitations (Bian et al., 2018; Lu et al., 2017). Therefore, an ADAMTS13 conformation FO-SPR assay was developed and optimized to generate an easy-to-use test, which potentially could accomplish the current clinical needs of all TTP patients in the near future (**AIM 3**).

**Part III**  
**Materials**  
**&**  
**methods**

## 3.1. Materials

Detailed description of all used chemicals, plasma samples and laboratory equipment is respectively provided in Addendum I and II. Alongside, more information on the composition of the different buffers can be found in Addendum III. Furthermore, Addendum IV gives an overview of the experimental work that was performed alongside the lab work for this master's thesis. At last, the risk analysis for working in the Laboratory for Thrombosis Research at the KU Leuven Campus Kulak Kortrijk is described in Addendum V.

## 3.2. Anti-ADAMTS13 Autoantibody assay

### 3.2.1. Recombinant ADAMTS13

Full-length recombinant human (FL-rh)ADAMTS13 (Roose et al., 2018a), with C-terminal 6xHis and V5 tags, was produced in-house using an inducible T-Rex™ system for mammalian cells lines. Purification was facilitated by applying Zn<sup>2+</sup> affinity chromatography on an ÄKTA device. Ultrafiltration and dialysis were performed with a Vivaflow® 200, 50 000 MWCO, PES system to concentrate the expression medium. The concentrated sample was loaded on the Zn<sup>2+</sup> Histrap™ HP column and after elution, the positive fractions, verified by sodium dodecyl sulfate polyacrylamide gel electrophoresis (SDS-PAGE), were merged for dialysis against HEPES-buffered saline (HBS, All.4.). This protein purification protocol was performed under guidance of one of the lab technicians (Aline Vandenbulcke or Inge Pareyn).

#### 3.2.1.1. ADAMTS13 antigen ELISA

To accomplish the quality control assessment, the exact concentration of FL-rhADAMTS13 and the efficiency of the purification was evaluated by performing an in-house developed ADAMTS13 antigen ELISA assay (Figure 12). The monoclonal antibody 3H9 (5 µg/mL in (bi)carbonate, All.2.), targeting the human ADAMTS13 metalloprotease domain (Figure AI.3.), was coated on a 96-well microtiter plate and stored overnight in a wet chamber at 4°C. Next, the plate was washed three times using phosphate buffered saline (PBS, All.1.) with 0.1% Tween20 and blocked for two hours at RT using PBS/3% milk. Again, the plate was washed three times and then, different dilutions of the purified FL-rhADAMTS13 were serially diluted in a 1.5/2.5 ratio in PBS/0.3% milk and incubated for 1.5 hours at 37°C. Thereafter, the microtiter plate was washed six times and was incubated with a mixture of the biotinylated anti-human ADAMTS13 antibodies 17G2 and 19H4 (each at 1.5 µg/mL in PBS/0.3% milk, Figure AI.3.) during one hour at RT. After washing six times, detection was performed using horse radish peroxidase (HRP)-labelled streptavidin, which was 1/10 000 diluted in PBS/0.3% milk and incubated for one hour at RT. Lastly, the plate was again washed six times and in order to initiate the colorimetric reaction, the colouring solution (160 µL/well), consisting of *O*-phenylenediamine (OPD) and hydrogen peroxide (H<sub>2</sub>O<sub>2</sub>) in phosphate and citric acid buffer, was added to the microtiter plate. Exactly 10 minutes later, the reaction was stopped by adding 50 µL/well of 4 M sulfuric acid (H<sub>2</sub>SO<sub>4</sub>) and the absorbance was measured at 492 nm and 630

nm using the FLUOstar OPTIMA reader. In this sandwich ELISA assay, pooled normal human plasma (NHP) served as calibrator (set at 5.7 nM) to determine the specific concentration of the purified FL-rhADAMTS13 (nM) and the samples taken during the purification and filtration process. As a negative control, a non-coated well was included for all samples.

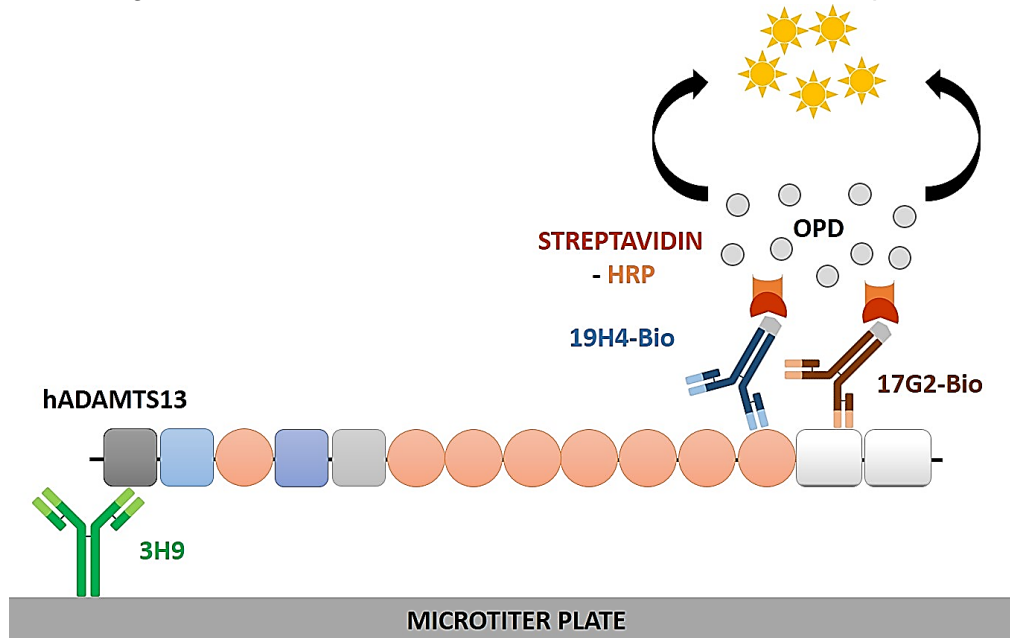


Figure 12: **Experimental ELISA set-up of the human ADAMTS13 antigen ELISA:** A 96-well microtiter plate was coated with the monoclonal anti-human ADAMTS13 antibody 3H9 (Green). After blocking, the plasma calibrator, containing human ADAMTS13, and the rhADAMTS13 samples were incubated. After incubation with the biotinylated anti-human ADAMTS13 antibodies 19H4 (Blue) and 17G2 (Brown), detection was performed by using HRP-labelled streptavidin (Red/Orange). During the colorimetric reaction, HRP converts the OPD and H<sub>2</sub>O<sub>2</sub> present in the colouring solution from transparent to a yellow-coloured mixture. Finally, the absorbance is determined at 492 nm and 630 nm.

### 3.2.1.2. SDS-PAGE & Western Blot

To assess the quality and purity of the FL-rhADAMTS13, SDS-PAGE and western blot analysis were performed. Firstly, two small plates and two plates with 1 mm spacer were assembled on a casting stand. Then, a 7.5% running gel (AII.5.) and a 4% stacking gel (AII.6.) were consecutively prepared and polymerised. Non-reducing sample buffer (1/5 diluted) was added to the prepared protein samples, containing 30 nM FL-rhADAMTS13 in PBS, and these were heated in a water bath at 100°C. Once the vertical electrophoresis cell was assembled, the inner and outer chamber were filled with electrophoresis buffer (AII.7.) and subsequently, the samples and a protein standard were loaded. After connecting the electrical leads to the power supply, electrophoresis was performed for 30 minutes at 20 mA and for one hour at 40 mA in the stacking and running gel respectively.

Thereafter, the gels were removed from the SDS-PAGE device and put in transfer buffer (All.8.). First, a polyvinylidene fluoride (PVDF) membrane was soaked in methanol and distilled water, which was later washed in transfer buffer, together with the Novablot filter paper. Thereafter, the filter paper, the PVDF membrane and the SDS-PAGE gels were successively piled on the blotting device and covered with another bundle of filter paper, that was saturated with transfer buffer. After blotting (1.5 hours; 16 V), the PVDF membrane was blocked overnight in PBS/3% milk. Detection of the blotted proteins was performed by incubating the monoclonal mouse anti-human ADAMTS13 antibody 19H4 and HRP-labelled polyclonal goat-anti-mouse antibodies sequentially for one hour at room temperature (RT). After washing the PVDF membrane ten times with PBS/0.05%Tween80, the western blot was developed using TMB III solution.

### 3.2.2. Recombinant ADAMTS13 variants

Recombinant human (rh)MDTCS and (rh)T2C2 (see Literature review, Chapter 3 ADAMTS13), both truncated ADAMTS13 variants with C-terminal 6xHis and V5 tags, were expressed and cultivated in CHO-derived CHOEBNALT85 cells (European Patent EP1851319B1). These ADAMTS13 variants were purified using Ni<sup>2+</sup> affinity chromatography and filtered overnight on a Ni<sup>2+</sup> HisTrap™ excel column. After washing and eluting the column, the positive fractions containing the purified protein variants were exchanged into HBS medium by performing gel filtration. For both truncated variants of ADAMTS13, the quality control was analogously assessed as for the purification of FL-rhADAMTS13 by performing SDS-PAGE, western blot and the ADAMTS13 antigen ELISA assay, including minor protocol modifications. However, the purification of both proteins and their quality assessment was kindly performed by Kadri Kangro (PhD student, performed at Icosagen).

### 3.2.3 Anti-ADAMTS13 autoantibody ELISA

The levels of anti-ADAMTS13 autoantibodies in iTTP and healthy donor (HD) plasma samples were evaluated quantitatively by performing an in-house developed ELISA, based on (Roose et al., 2018c). Overnight, FL-rhADAMTS13 was coated at a concentration of 15 nM in PBS on a 96-well microtiter plate and stored in a wet chamber at 4°C. After blocking for 2 hours with PBS/3% milk, iTTP patient or HD plasma samples, starting from a 1/40 dilution in PBS/0.3% milk, were ½ diluted and incubated for 1 hour at 37°C. The detection of anti-ADAMTS13 autoantibodies, present in the plasma samples, was performed with HRP-labelled anti-human IgG (Fc specific) antibodies (1/10 000 diluted in PBS/0.3% milk), which were incubated for 1 hour at RT. The washing steps and the colouring reaction were performed as described above. After exactly ten minutes, the colorimetric reaction was stopped and the absorbance was measured at 492 nm and 630 nm. This ELISA set-up is considered as the standard in-house developed anti-ADAMTS13 autoantibody ELISA (Figure 13A).

However, three different ELISA methods with major modifications of the standard set-up were also investigated to evaluate the effects of the ADAMTS13 presentation (coated rhMDTCS + rhT2C2 and captured FL-rhADAMTS13) and the autoantibody detection (IgG<sub>1,2,3,4</sub> mixture) method on the variation between the diverse approaches. In contrast to the standard in-house developed ELISA set-up, the anti-ADAMTS13 autoantibody levels were measured by coating the combination of both truncated ADAMTS13 variants, rhMDTCS and rhT2C2 (each at 1.25 µg/mL), instead of FL-rhADAMTS13 (Figure 13B). In addition, the amount of anti-ADAMTS13 autoantibodies were determined using captured rhADAMTS13. Therefore, the antibody 17C7 (5 µg/mL in (bi)carbonate buffer, pH 9.6), targeting the metalloprotease domain of ADAMTS13 (Figure A1.3.), was coated on a 96-well plate and stored overnight at 4°C in a wet chamber. After blocking the microtiter plate for at least 2 hours at RT, FL-rhADAMTS13 (15 nM in PBS/0.3% milk) was incubated for 1 hour at 37°C. From there on, the protocol of the standard in-house ELISA was pursued (Figure 13C). At last, a mixture of HRP-labeled monoclonal anti-human IgG<sub>1</sub> (1/20 000 in PBS/0.3% milk), anti-human IgG<sub>2</sub>, anti-human IgG<sub>3</sub>, anti-human IgG<sub>4</sub> (1/2000 in PBS/0.3% milk) was used for the detection of anti-ADAMTS13 autoantibodies instead of polyclonal anti-human IgG antibodies (Figure 13D). Throughout these four approaches of the anti-ADAMTS13 autoantibody ELISA set-up, a ½ dilution series of a high-titer iTTP patient plasma sample served as calibrator and was set as 100% in order to determine the anti-ADAMTS13 autoantibody titers (%). For each plasma sample, a negative control (1/40 diluted in PBS/0.3% milk) was included by providing a non-coated well.

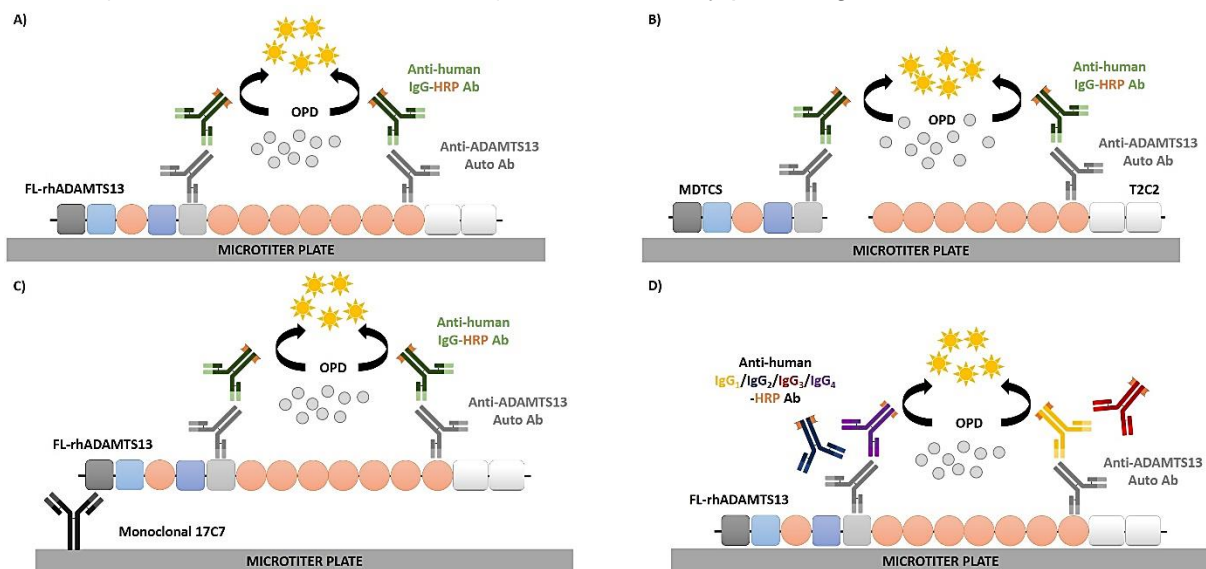


Figure 13: **Experimental set-up of the anti-ADAMTS13 autoantibody ELISA:** A) The standard in-house developed anti-ADAMTS13 autoantibody ELISA set-up; A 96-well microtiter plate was coated with FL-rhADAMTS13. Thereafter, plasma samples containing anti-ADAMTS13 autoantibodies (grey) were incubated and detected by HRP-labelled anti-human antibodies (green). During the colorimetric reaction, HRP converts the OPD and H<sub>2</sub>O<sub>2</sub> from the colouring solution and finally, the absorbance is determined at 492 nm and 630 nm (based on (Roose et al., 2018c)). B) Alternative anti-ADAMTS13 autoantibody set-up using both truncated ADAMTS13

variants, namely MDTCS and T2C2. C) Variant of the anti-ADAMTS13 autoantibody assay with the monoclonal 17C7 (black) antibody coated on the 96-well microtiter plate to capture FL-rhADAMTS13 via the metalloprotease domain. D) Substitution of the polyclonal HRP-labelled detection antibodies by a mixture of monoclonal HRP-labelled anti-human IgG<sub>1</sub> (Yellow)/IgG<sub>2</sub> (Blue)/IgG<sub>3</sub> (Red)/IgG<sub>4</sub> (purple) detection antibodies.

### 3.2.4. Anti-ADAMTS13 autoantibody FO-SPR assay

Gold coated optical fibers (FO probes), containing a carboxyl self-assembling monolayer (SAM) on the gold coated surface, were stored until use in 2-*N*-morpholino-ethanesulfonic acid (MES) buffer at 4 °C. First, the carboxylic groups of the SAM-functionalized FO probes were activated by 1-ethyl-3-[-3-dimethylaminopropyl] carbodiimide (EDC)/*N*-hydroxysuccinimide (NHS) chemistry and therefore, the FO probes were immersed in a mixture of 0.4 M EDC/0.1 M NHS, dissolved in MES buffer (50 mM; pH 6.0). As a capturing antibody, the monoclonal anti-human ADAMTS13 antibody 3H9 (20 µg/mL in 10 mM NaAc pH 5.5, Figure AI.3.) was covalently immobilized on the activated SAM layer. Next, the FO probes were submerged in glycine (10 mM; pH 2.0) regeneration buffer to remove non-covalently bound antibodies. After blocking, using Superblock™ blocking buffer, the FO probes were immersed in rhADAMTS13 (0.5 µg/mL in PBS/0.01%Tween20). In the next step, the probes were immersed in TTP patient plasma (1/100 dilution in PBS/0.01%Tween20) containing anti-ADAMTS13 autoantibodies. The detection of these autoantibodies was performed by goat anti-human antibodies, conjugated to 40 nm gold nanoparticles (GAH-AuNPs) (OD1 in PBS/bovine serum albumin (BSA) 0.5%), which result in an increased final endpoint shift (nm) measurement. This protocol sequence (Table 1) provides our standard anti-ADAMTS13 autoantibody FO-SPR assay (Figure 14), since only some minor set-up modifications were used to evaluate the capturing anti-ADAMTS13 antibody and rhADAMTS13 concentration.

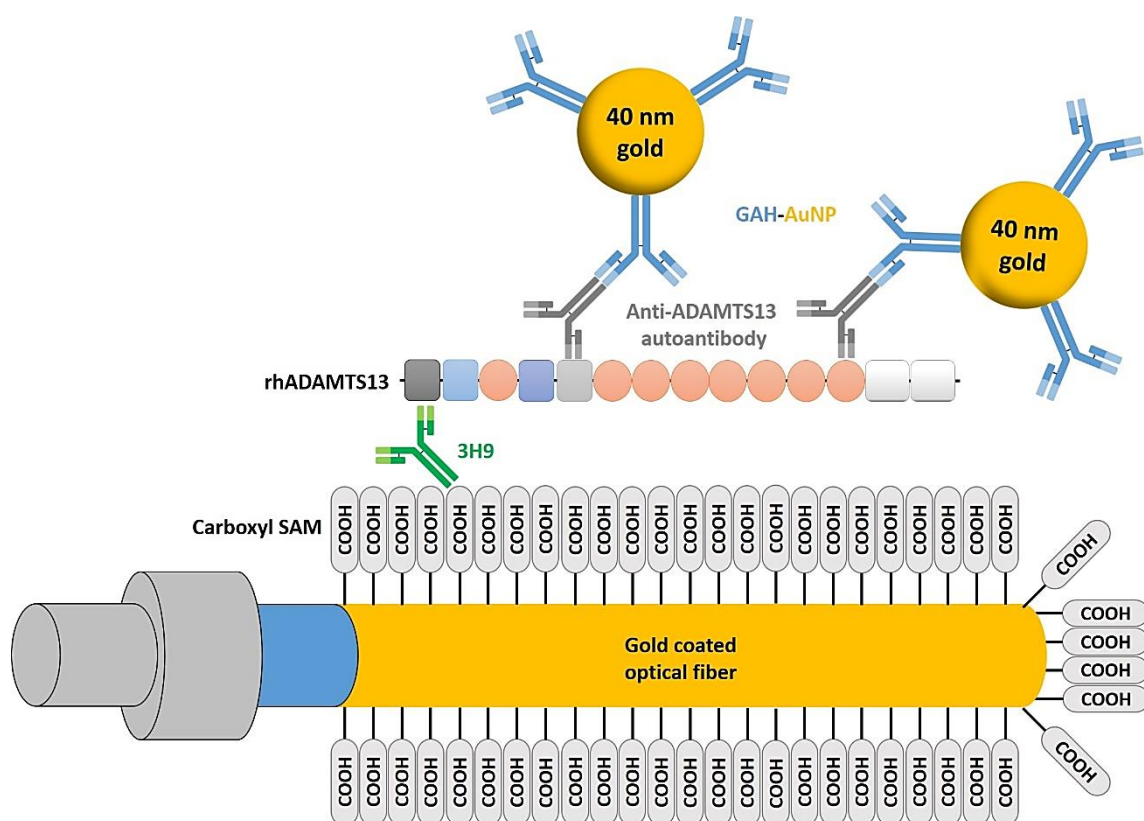


Figure 14: **Anti-ADAMTS13 autoantibody FO-SPR assay:** EDC/NHS chemistry was used to activate pre-functionalised, gold-coated FO probes, allowing the covalent immobilisation of the monoclonal anti-ADAMTS13 antibody 3H9 (Green). After regeneration and blocking with respectively glycine and Superblock™ blocking buffer, rhADAMTS13 was captured, which supports the binding of anti-ADAMTS13 autoantibodies (Grey) present in plasma samples. Afterwards, these autoantibodies were detected by GAH-AuNPs (Blue/Gold).

Table 1: **Sequence of the protocol of the anti-ADAMTS13 autoantibody FO-SPR assay**

STEP	TIME (Sec.)	AGENT	SHAKING	ACTION
1	600	MES (50 mM; pH 6.0)	/	/
2	900	0.4 M EDC/0.1 M NHS	/	Activation of SAM carboxylic groups
3	300	NaAc (10 mM; pH 5.5)	/	/
4	1800	3H9 (20 µg/mL) in NaAc (10 mM; pH 5.5)	400 rpm	Immobilisation of capture antibody
5	180	NaAc (10 mM; pH 5.5)	/	/
6	30	Glycine (10 mM; pH 2.0)	/	Regeneration

7	30	Glycine (10 mM; pH 2.0)	/	Regeneration
8	60	NaAc (10 mM; pH 2.0)	/	/
9	480	Superblock™ Blocking Buffer	/	Blocking
10	180	PBS/0.01%Tween20	/	/
11	1200	rhADAMTS13 (0.5 µg/mL) in PBS/0.01%Tween20	400 rpm	Interaction with capture antibody
12	180	PBS/0.01%Tween20	/	/
13	1200	Plasma sample (1/100) in PBS/0.01%Tween20	400 rpm	Interaction with captured rhADAMTS13
14	60	PBS/0.01%Tween20	/	/
15	240	PBS/BSA 0.5%	/	/
16	1200	GAB-AuNPs (OD1) in PBS/BSA 0.5%	400 rpm	Interaction with anti-ADAMTS13 autoantibody
17	60	PBS/BSA 0.5%	/	/

### 3.3. ADAMTS13 conformation assay

#### 3.3.1. ADAMTS13 conformation ELISA

To determine the conformation of ADAMTS13 in samples from TTP patients or healthy individuals, the in-house developed 1C4 conformation ELISA (Roose et al., 2018a) was performed (Figure 15). The 96-well microtiter plate was coated with the monoclonal anti-ADAMTS13 antibody 1C4 (5 µg/mL in (bi)carbonate), which targets a cryptic epitope in the spacer domain (Figure AI.3.). So, this cryptic epitope was only available for 1C4 binding when ADAMTS13 adopted its open conformation, for example in TTP patient samples, or by the addition of opening anti-CUB1 (e.g. 17G2) antibodies (Roose et al., 2018a; South et al., 2014). In this ADAMTS13 conformation ELISA, the monoclonal anti-ADAMTS13 CUB1 domain antibody 17G2 (2.5 µg/mL in PBS/0.3% milk, Figure AI.3.) was *in vitro* pre-incubated with the plasma samples (¼ dilution in PBS/0.3% milk) for half an hour at 37°C, to force the open conformation of ADAMTS13. Detection was performed using biotinylated 3H9 (1.5 µg/mL in PBS/0.3% milk), followed by HRP-labelled high-sensitivity-streptavidin (1/10 000 diluted in

PBS/0.3% milk), which were both incubated for an hour at RT. The washing steps in between and the colorimetric reaction were uniformly executed as described above. The optical density (OD) was determined at 492 nm and 630 nm after ten minutes of colouring. By correcting the  $OD_{492nm}$  values for the ADAMTS13 antigen levels found for each plasma sample and normalizing the ADAMTS13 antigen-corrected  $OD_{492nm}$  values using an intra-assay control ( $\frac{1}{4}$  diluted NHP with 17G2), the data could be expressed as CI. When the CI is  $\leq 0.5$ , a closed ADAMTS13 conformation is indicated, supposing that the open ADAMTS13 conformation is defined by  $CI > 0.5$  (Roose et al., 2018a).

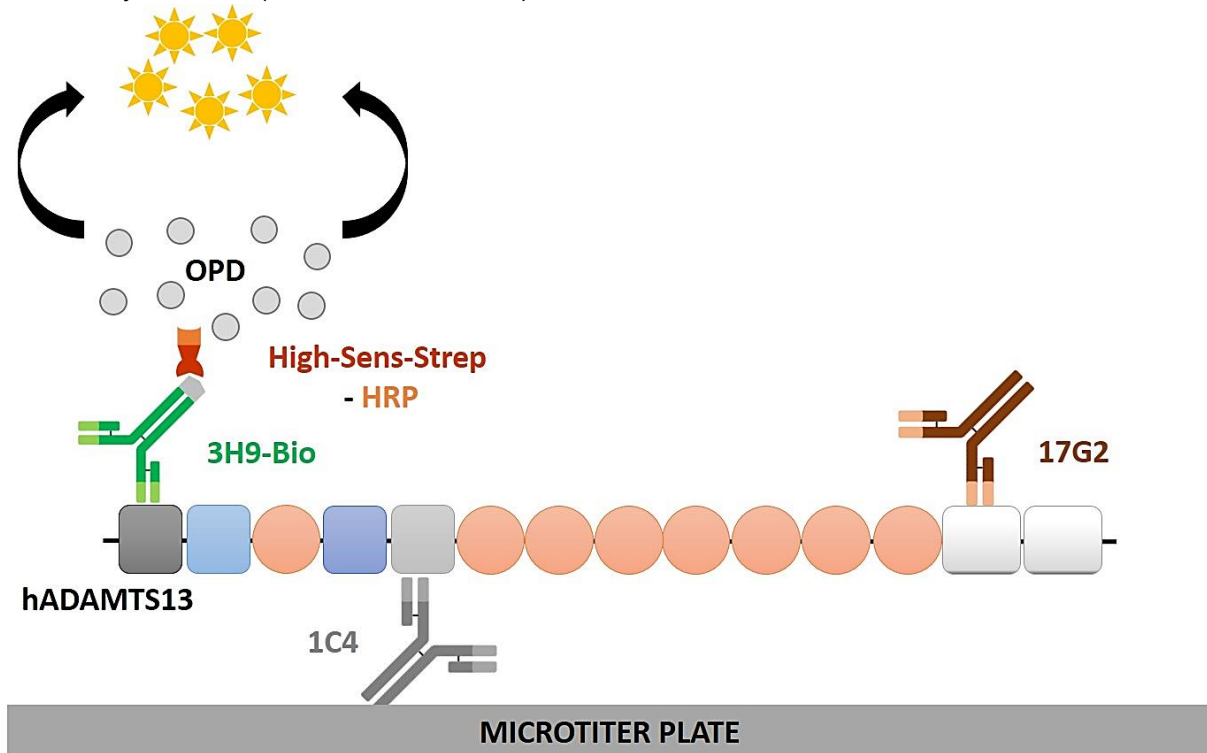


Figure 15: **Experimental set-up of the human ADAMTS13 conformation ELISA:** The in-house developed ADAMTS13 conformation ELISA set-up. A 96-well microtiter plate was coated with the monoclonal anti-human ADAMTS13 antibody 1C4 (Grey). Thereafter, plasma samples (in the presence or absence of the opening 17G2 antibody (Brown)) containing human ADAMTS13 were incubated. Once biotinylated 3H9 (Green) antibodies were added, detection was performed by using HRP-labelled high-sensitivity-streptavidin (Red/Orange). During the colorimetric reaction, HRP converts the OPD and  $H_2O_2$  into a yellowish solution. Then, the absorbance is determined at 492 nm and 630 nm.

### 3.3.2. ADAMTS13 Conformation FO-SPR assay

Besides the evaluation of the ADAMTS13 conformation through the 1C4 ELISA, an analogous bioassay using the FO-SPR technology was developed, accordingly to the anti-ADAMTS13 autoantibody FO-SPR assay, to allow the future assessment of the ADAMTS13 conformation in a clinical setting. Briefly, the monoclonal antibody 1C4 was covalently immobilized using EDC/NHS chemistry on the carboxyl-SAM layer of the FO probes. After regeneration and

blocking, the FO probes were submerged in a plasma sample, which was ½ diluted in buffer (PBS/0.01%Tween20) or in the 17G2 antibody (2.5 µg/mL in ½ diluted plasma in PBS/0.01%Tween20), to capture ADAMTS13. Thereafter, the detection was performed using biotinylated 3H9 antibodies that bind to the captured ADAMTS13. Lastly, goat anti-biotin gold nanoparticles (GAB-AuNPs) (OD1 in PBS/BSA 0.5%) interact with the biotinylated 3H9 antibodies, which gives the final endpoint shift (nm). Different concentrations and pH values for the different anti-ADAMTS13 antibodies were tested and the optimized protocol sequence for the ADAMTS13 conformation is provided in Table 2 (Figure 16).

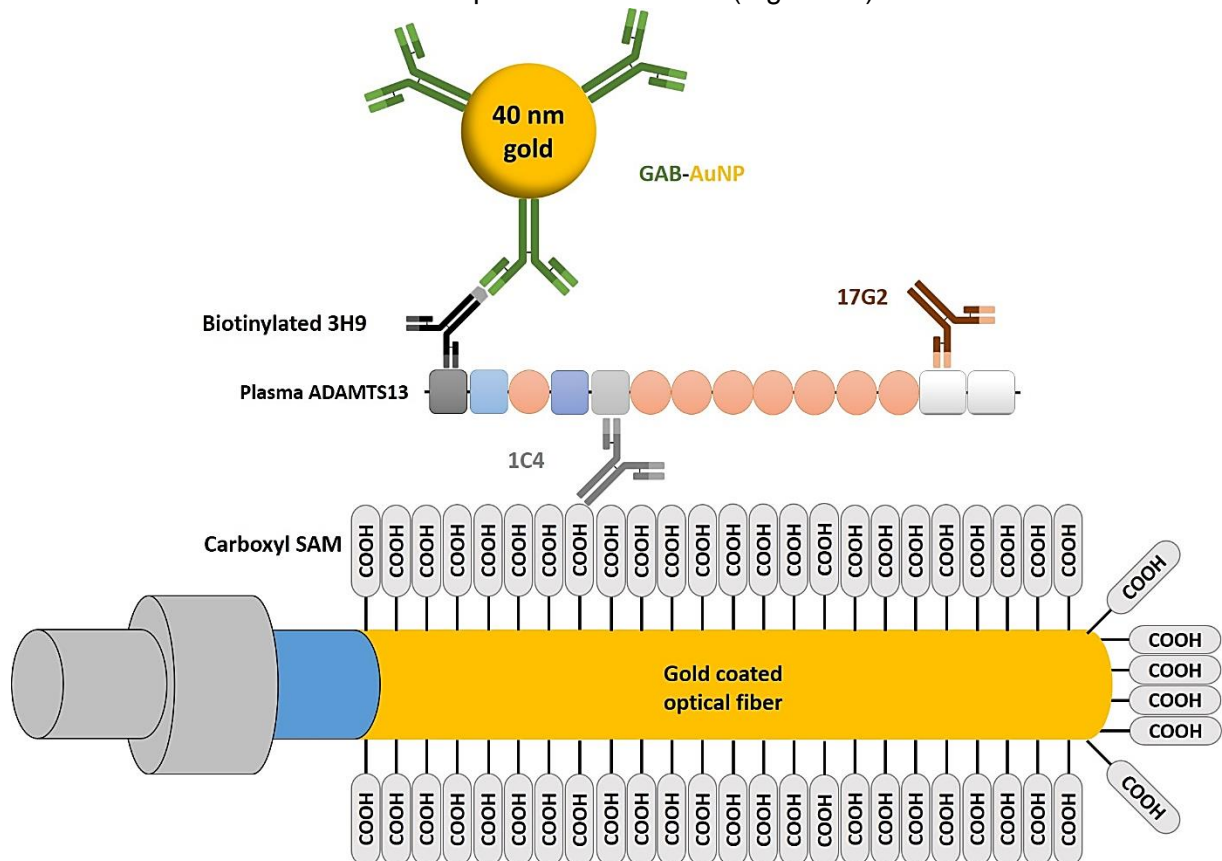


Figure 16: **ADAMTS13 conformation FO-SPR assay:** A mixture of EDC/NHS was used to activate the pre-functionalized carboxyl SAM layer of gold-coated FO probes, stimulating the covalent binding of 1C4 (Grey) capturing antibody. After regeneration and blocking, ADAMTS13 from plasma samples was captured, whether or not pre-incubated with 17G2 (Brown) antibodies. Biotinylated 3H9 (Black) antibodies and GAB-AuNPs (Green/Gold) were used to detect the captured open ADAMTS13, resulting in the final endpoint shift (nm).

Table 2: Sequence of the protocol for the ADAMTS13 conformation assay

STEP	TIME (Sec.)	AGENT	SHAKING	ACTION
1	600	MES (50 mM; pH 6.0)	/	/
2	900	0.4 M EDC/0.1 M NHS	/	Activation of SAM carboxylic groups
3	300	NaAc (10 mM; pH 5.5)	/	/
4	1800	1C4 (20 µg/mL) in NaAc (10 mM; pH 5.5)	400 rpm	Immobilisation of capture antibody
5	180	NaAc (10 mM; pH 5.5)	/	/
6	30	Glycine (10 mM; pH 2.0)	/	Regeneration
7	30	Glycine (10 mM; pH 2.0)	/	Regeneration
8	60	NaAc (10 mM; pH 2.0)	/	/
9	480	Superblock™ Blocking Buffer	/	Blocking
10	180	PBS/0.01%Tween20	/	/
11	1200	Plasma sample (1/2) in 2.5 µg/mL 17G2 or in PBS/0.01%Tween20	400 rpm	Interaction with capture antibody
12	180	PBS/0.01%Tween20	/	/
13	1200	Biotinylated 3H9 (5 µg/mL) in PBS/0.01%Tween20	400 rpm	Interaction with captured protein
14	60	PBS/0.01%Tween20	/	/
15	240	PBS/BSA 0.5%	/	/
16	1200	GAB-AuNPs (OD1) in PBS/BSA 0.5%	400 rpm	Interaction with detection antibody
17	60	PBS/BSA 0.5%	/	/

### 3.4. Statistical analysis

GraphPad Prism 5.03 (GraphPad Software, San Diego, California) was used to perform the statistical analysis. During the optimization experiments for both FO-SPR bioassays, the mean SPR shift, standard deviation and coefficient of variation (CV) were determined through basic column statistics, whereas the statistical comparison between more than two groups was performed with a one-way analysis of variance (ANOVA) followed by a Bonferroni's Multiple Comparison test. To evaluate if the data from the various plasma samples was normally distributed, a Shapiro-Wilk Normality test was performed. When normally distributed, a Pearson Correlation test accomplished the evaluation of the correlation between different experimental set-ups, whereas a Spearman Correlation test was used when the data was not normally distributed.

# **Part IV**

# **Results**

## 4.1. Anti-ADAMTS13 autoantibody assay

### 4.1.1. Evaluation of diverse anti-ADAMTS13 autoantibody ELISA set-ups

The anti-ADAMTS13 autoantibody ELISA was included as a diagnostic test to appoint the differential diagnosis between both iTTP and cTTP patients. However, different reference laboratories use diverse commercial or in-house developed ELISA set-ups to measure anti-ADAMTS13 autoantibody levels. Generally, the distinct approaches differed in the ADAMTS13 presentation or the anti-ADAMTS13 autoantibody detection methods. As yet, the influence of those discrepancies on anti-ADAMTS13 autoantibody level determination was unknown. Therefore, the anti-ADAMTS13 autoantibody levels were assessed in 18 iTTP plasma samples by in-house developed anti-ADAMTS13 autoantibody ELISAs. These iTTP plasma samples have been shown to be positive for anti-ADAMTS13 autoantibodies in the commercial Technozym® ADAMTS-13 inhibitor ELISA (Aix-Marseille Université, Marseille, France). Firstly, our in-house developed standard ELISA was performed using coated FL-rhADAMTS13 and polyclonal anti-human IgG (Fc specific) detection antibodies (Figure 17Ai). In addition, the anti-ADAMTS13 autoantibody titers were determined by three alternative approaches using: 1) coated rhMDTCS and rhT2C2 with polyclonal detection antibodies (Figure 17Aii), 2) captured FL-rhADAMTS13 with polyclonal detection antibodies (Figure 17Aiii) and 3) coated FL-rhADAMTS13 with a mixture of monoclonal anti-human IgG<sub>1-4</sub> detection antibodies (Figure 17Aiv). For all anti-ADAMTS13 autoantibody ELISA approaches a high-titer iTTP patient plasma sample served as calibrator, which was set as 100%, to determine the anti-ADAMTS13 autoantibody titers (%) of individual iTTP plasma samples. Anti-ADAMTS13 autoantibody levels determined using the standard ELISA set-up strongly correlated (Spearman  $r=0.936$ ,  $p<0.0001$ ) with the set-up that used the coated MDTCS and T2C2 (Figure 17B). Furthermore, strong statistical correlation (Spearman  $r=0.9216$ ,  $p<0.0001$ ) was found when comparing the anti-ADAMTS13 autoantibody titers, evaluated by using coated or captured FL-rhADAMTS13 (Figure 17C). Lastly, when monoclonal HRP-labelled anti-human IgG<sub>1-4</sub> antibodies were used instead of the polyclonal HRP-labelled anti-human Fc specific detection antibodies for the detection of autoantibody binding to coated FL-rhADAMTS13, only moderate statistical correlation (Spearman  $r=0.7234$ ,  $p=0.0007$ ) was observed for the anti-ADAMTS13 autoantibody levels (Figure 17D).

Thereafter, the sensitivity of the different anti-ADAMTS13 autoantibody ELISA approaches was assessed. For this purpose, the 97.5 percentile of the anti-ADAMTS13 autoantibody levels was determined by means of 72 HD plasma samples for each ELISA set-up, except for the set-up using the alternative autoantibody detection method with monoclonal anti-IgG<sub>1-4</sub> detection antibodies, since these antibodies were no longer commercially available. The cut-off value for the positivity of anti-ADAMTS13 autoantibodies was delineated at 12.21% and 14.00% for the ELISA set-ups using coated and captured FL-rhADAMTS13 respectively.

However, the cut-off for the ELISA design with coated rhMDTCS and T2C2 was indicated at 19.43%, which illustrates the higher sensitivity of both methods using FL-rhADAMTS13 compared to the set-up using rhMDTCS and rhT2C2. When comparing to the reference Technozym® ADAMTS-13 inhibitor kit, 17 out of the 18 screened iTTP plasma samples (94%) were positive when using coated FL-rhADAMTS13, whereas anti-ADAMTS13 autoantibodies were measurable in only 15 out of 18 plasma samples (83%) using rhMDTCS and rhT2C2. Additionally, anti-ADAMTS13 autoantibodies were detectable in 15 out of 18 (83%) plasma samples when evaluating the ELISA set-up with captured FL-rhADAMTS13, despite having a comparable assay sensitivity as when FL-rhADAMTS13 is coated.

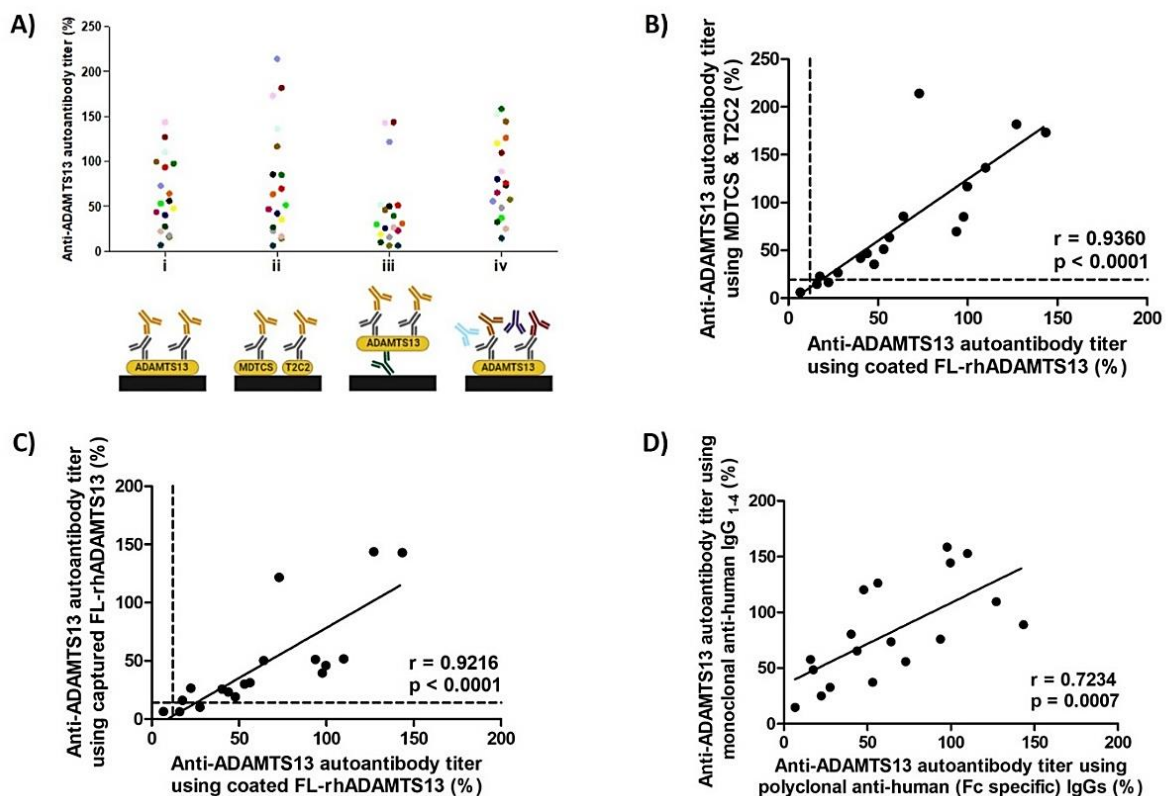


Figure 17: **Correlation between anti-ADAMTS13 autoantibody ELISA designs:** A) Anti-ADAMTS13 autoantibody titers (%) from iTTP (n=18) patient plasma samples determined in the standard (i) and three diverse ELISA set-ups (ii, coated rhMDTCS and rhT2C2; iii, captured FL-rhADAMTS13; iv, mixture of monoclonal detection antibodies), using a high-titer plasma sample as calibrator that was set as 100%. B) Correlation between the anti-ADAMTS13 autoantibody levels (n=18), measured using coated FL-rhADAMTS13 (i) or coated MDTCS and T2C2 (ii) (Spearman  $r=0.936$ ,  $p<0.0001$ ). C) Correlation between the anti-ADAMTS13 autoantibody titers (n=18), which were assessed applying coated (i) or captured FL-rhADAMTS13 (iii) (Spearman  $r=0.9216$ ,  $p<0.0001$ ). D) Correlation between the anti-ADAMTS13 autoantibody levels (n=18), determined using monoclonal HRP-labelled anti-human IgG<sub>1-4</sub> antibodies (iv) or polyclonal HRP-labelled anti-human Fc specific detection antibodies (i) (Spearman  $r=0.7234$ ,  $p=0.0007$ ).

#### 4.1.2. Development of the anti-ADAMTS13 autoantibody FO-SPR assay

As described above, ELISA bioassays show considerable limitations to be used as a diagnostic test in clinical settings. Therefore, the anti-ADAMTS13 autoantibody assay was developed using the easy-to-use diagnostic FO-SPR platform. First, the carboxyl SAM layer of FO probes was activated using EDC/NHS chemistry to immobilize the ADAMTS13 capturing antibody (3H9). Thereafter, FL-rhADAMTS13 was captured, which allowed the binding of anti-ADAMTS13 autoantibodies, present in iTTP patient plasma samples. Finally, these autoantibodies were detected using goat anti-human antibodies conjugated to gold nanoparticles (Figure 14). The course of the different steps in the FO-SPR assay are depicted in the typical sensorgram (Figure 18A). Firstly, two different ADAMTS13 capturing antibodies were evaluated and the FL-rhADAMTS13 concentration was assessed. Generally, two parameters were considered in the evaluation of these different conditions: 1) a high goat anti-human AuNP endpoint shift (nm, final read-out anti-ADAMTS13 autoantibody assay) and 2) a low CV. Both anti-metalloprotease domain antibodies 3H9 and 17C7 were assessed in triplicate to test their ability to capture FL-rhADAMTS13 (Figure 18B). The antibody 3H9 was preferred above 17C7 to use in further experiments ( $p=0.0295$ ), since this conditions exhibited a higher goat anti-human AuNP endpoint shift (mean values of 20.00 nm and 15.93 nm for respectively 3H9 and 17C7) in combination with a lower CV (5.68% vs. 11.46% for 3H9 vs 17C7). Subsequently, different concentrations of FL-rhADAMTS13 (0.5, 1 or 5  $\mu\text{g/mL}$ ) were evaluated. Based on its highest final goat anti-human AuNP shift ( $p<0.0001$ ) and low CV (Figure 18C), 0.5  $\mu\text{g/mL}$  was determined as the favourable FL-rhADAMTS13 concentration to continue experiments. Remarkably, although higher FL-rhADAMTS13 concentrations show increasing shifts for the binding of FL-rhADAMTS13 to the capturing antibody 3H9 (Figure 18D), decreasing goat anti-human endpoint shifts were noticed (Figure 18C). These observations could potentially be explained by steric hindrance effects, since these higher FL-rhADAMTS13 concentrations take too much space, so that the goat anti-human labelled gold nanoparticles have not enough place to properly bind and detect the anti-ADAMTS13 autoantibodies. Next, a calibration curve was developed using a high-titer iTTP patient plasma sample (Figure 18E) and plasma samples from healthy individuals ( $n=3$ ) were screened as negative controls, since anti-ADAMTS13 autoantibodies are not present in healthy donors. Thereafter, the further development of the anti-ADAMTS13 autoantibody FO-SPR assay was interrupted, since the goat anti-human AuNPs were temporary not available.

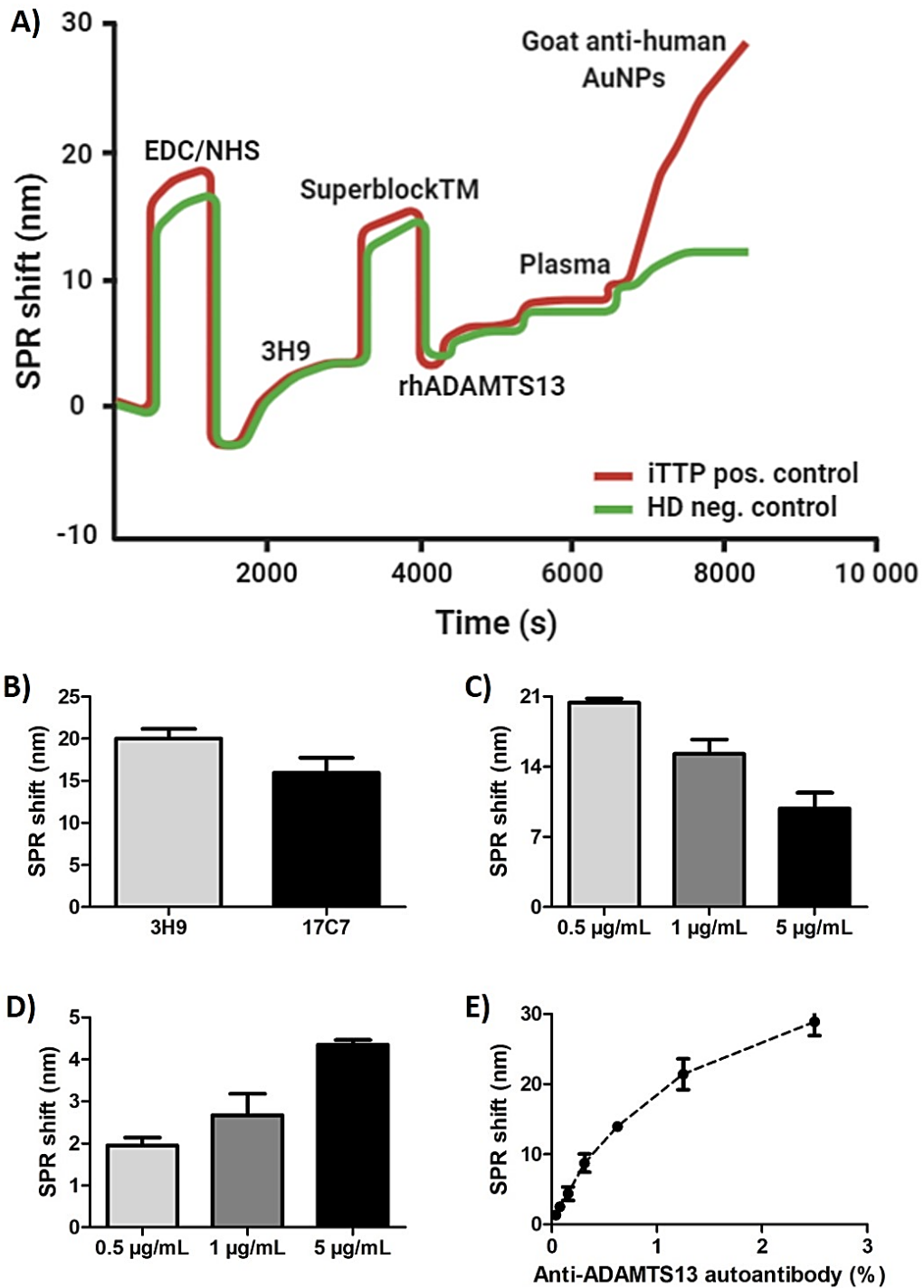


Figure 18: **Development of the anti-ADAMTS13 autoantibody FO-SPR assay:** A) Typical FO-SPR sensorgram that symbolizes the complete sequence of the anti-ADAMTS13 autoantibody FO-SPR assay, evaluating plasma samples from iTTP patients (Red) or healthy individuals (Green). B) Assessment of the goat anti-human AuNP endpoint shift (nm) using the anti-metalloprotease capturing antibodies 3H9 and 17C7, which are covalently immobilised at the carboxyl-SAM layer. C) Goat anti-human endpoint shift for the optimisation of the FL-rhADAMTS13 concentration (0.5, 1 or 5 µg/mL). D) SPR shift for the diverse FL-rhADAMTS13 concentrations (0.5, 1, 5 µg/mL), when FL-rhADAMTS13 binds to the capturing antibody 3H9. E) Calibration curve of a dilution series from a high-titer iTTP patient plasma sample, based on the final goat anti-human AuNP endpoint shift.

## 4.2. ADAMTS13 conformation assay

### 4.2.1. Development of the ADAMTS13 conformation FO-SPR assay

Since the assessment of the ADAMTS13 conformation in clinical settings requires an easy-to-use single-sample testing technique, a bioassay using the FO-SPR technology was developed. An ADAMTS13 capturing antibody (1C4) was first immobilized to the carboxyl SAM layer of FO probes using EDC/NHS chemistry. This antibody can only capture ADAMTS13 in its open conformation and therefore plasma samples were pre-incubated in the presence or absence of an opening antibody (17G2) to induce the open ADAMTS13 conformation *in vitro*. Thereafter, the captured open ADAMTS13 was detected by biotinylated antibodies (3H9), followed by goat anti-biotin antibodies conjugated to gold nanoparticles (Figure 16). During the optimization of the anti-ADAMTS13 autoantibody FO-SPR assay, three parameters were taken into account to evaluate the different conditions: 1) a high goat anti-biotin AuNP endpoint shift (nm, final read-out ADAMTS13 conformation assay), 2) a large signal-to-noise ratio (i.e. signal of NHP+17G2/NHP-17G2) and 3) a low CV. Firstly, the favourable conditions for the immobilisation of 1C4 to the carboxyl-SAM layer were assessed: 1) the concentration of the capturing antibody 1C4 (5, 10, 20 µg/mL) and 2) the pH of the sodium acetate (NaAc) buffer (pH 4.5, 5.0, 5.5). The effects of these different 1C4 immobilisation conditions on the final goat anti-biotin AuNP endpoint SPR shift were evaluated in the presence (n=3) and absence (n=3) of the opening antibody 17G2 (Figure 19B). Immobilisation of 1C4 at 20 µg/mL in pH 5.5 NaAc buffer generated a robust goat anti-biotin AuNP endpoint shift, delivered reliable signal-to-noise ratios and additionally showed the lowest CV. Therefore, this condition was used in further experiments for the immobilization of 1C4, even though no statistical significant difference was demonstrated between most of the evaluated conditions. Next, the appropriate concentration (1.25, 2.5, 5 µg/mL) of the biotinylated 3H9 detection antibody was determined (n=3) in the presence and absence of 17G2 (Figure 19C). In further experiments, 5 µg/mL biotinylated 3H9 was opted for as detection antibody concentration, since this concentration demonstrated the highest endpoint SPR shift and a beneficial NHP+17G2/NHP ratio compared to the other screened conditions. Moreover, when 17G2 was present, this 5 µg/mL 3H9 concentration showed the smallest CV. Finally, the concentration (1.25, 2.5, 5 µg/mL) of the antibody 17G2, which induces the open ADAMTS13 conformation, was assessed (n=3) (Figure 19D). In further experiments, the opening antibody 17G2 was used in a concentration of 2.5 µg/mL. This antibody concentration showed the smallest CV and additionally, a proper endpoint SPR shift was observed for this condition. After evaluation of the 1C4 immobilisation condition and the concentrations of 17G2 and biotinylated 3H9, the ADAMTS13 conformation was tested in plasma samples from both healthy individuals and iTTP patients using the following conditions: 20 µg/mL 1C4 in pH 5.5 NaAc buffer, 2.5 µg/mL 17G2 and 5 µg/mL

biotinylated 3H9, which results in a typical sensorgram for the ADAMTS13 conformation FO-SPR assay (Figure 19A).

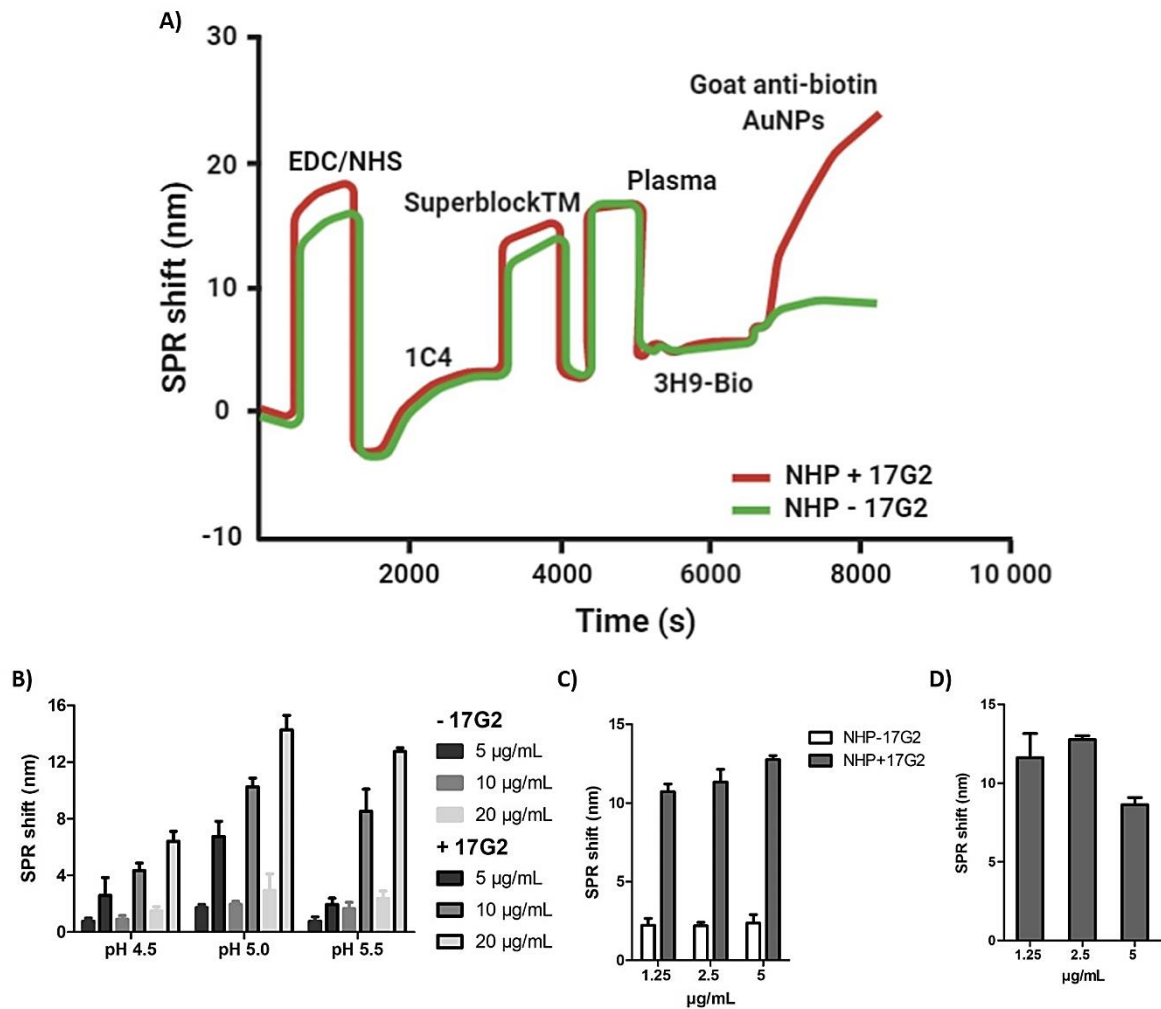


Figure 19: **Optimization of the ADAMTS13 conformation FO-SPR assay:** A) Typical FO-SPR sensorgram that symbolizes the complete sequence of the ADAMTS13 conformation FO-SPR assay, evaluating a NHP plasma sample in the presence (Red) or absence (Green) of 17G2. B) Goat anti-biotin AuNP endpoint shifts for the optimization of the ADAMTS13 capturing antibody 1C4 (5,10 and 20 µg/mL in NaAc buffer with pH 4.5, 5.0 or 5.5) in NHP without 17G2 (closed ADAMTS13 conformation, n=3) or NHP with 17G2 (induced open ADAMTS13 conformation, n=3). C) Goat anti-biotin endpoint shifts for the optimization of the biotinylated 3H9 (1.25, 2.5, 5 µg/mL) detection antibody in NHP with (Grey bars, n=3) or without (White bars, n=3) 17G2. D) Goat anti-biotin endpoint shifts in addition of 1.25, 2.5 or 5 µg/mL 17G2 antibody (n=3) to induce the open ADAMTS13 conformation.

#### 4.2.2. Evaluation of the ADAMTS13 conformation FO-SPR assay

Since the open ADAMTS13 conformation is recognized as a novel biomarker for iTTP, the in-house developed ADAMTS13 conformation ELISA was performed to evaluate the conformation of ADAMTS13 in plasma samples from HDs and iTTP patients. Moreover, this in-house ELISA is currently the standard method for the evaluation of the ADAMTS13

conformation (Roose et al., 2018a; Roose et al., 2020) and therefore, the ADAMTS13 conformation, determined by the optimized ADAMTS13 conformation FO-SPR assay, needs to be compared with the ADAMTS13 conformation, determined by the ADAMTS13 conformation ELISA. The ADAMTS13 conformation, in absence or presence of the opening anti-CUB1 antibody 17G2 (Figure 16), was assessed using the optimized FO-SPR assay (and ELISA) in plasma samples of both healthy individuals (Figure 20A, n=20) and iTTP patients (Figure 20B, n=19). In general, when the opening 17G2 antibody was pre-incubated with the plasma samples, the final goat anti-biotin AuNP endpoint shifts for HD samples showed a strong increase, whereas the endpoint shift of iTTP plasma samples remained almost unaltered. Next, the data for both HD (n=20, Green) and iTTP (n=18, Red) plasma samples, was expressed as a conformation index (CI) (Figure 20C) by correcting the goat anti-biotin AuNP endpoint shifts for the ADAMTS13 antigen levels, which were determined using the human ADAMTS13 antigen ELISA. The cut-off value, which allows to distinguish the open and closed conformation, was set at the highest value of the HDs (CI =10.13, *Dashed line*). This cut-off value confirmed the open ADAMTS13 conformation in all but one (CI =5.16) iTTP plasma sample, which also showed the closed ADAMTS13 conformation in ELISA. Also, one other iTTP patient was excluded from the data set, since no ADAMTS13 was present. Lastly, the CI determined in ELISA and FO-SPR were compared by performing a correlation test (Figure 20D), which indicated a statistical significant correlation ( $p < 0.0001$ , Pearson  $r = 0.8161$ ) between both assays.

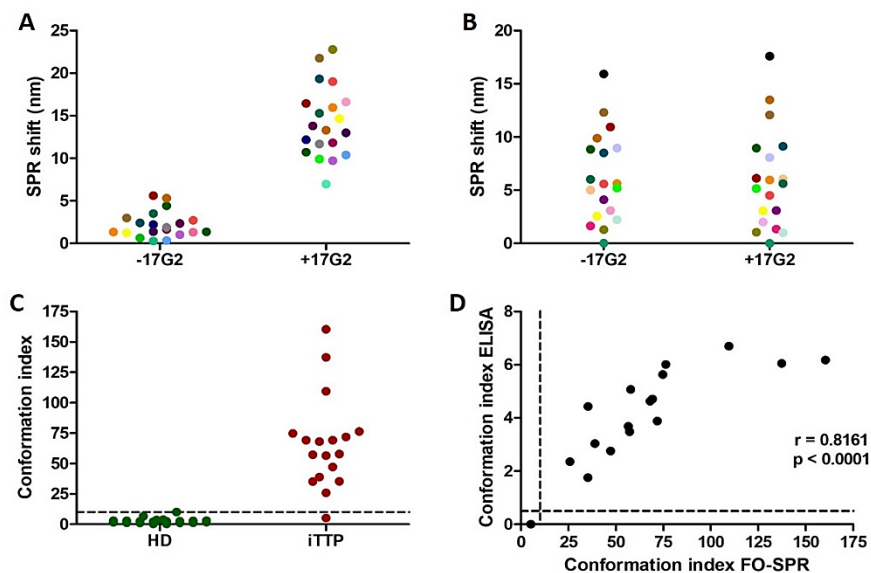


Figure 20: **Evaluation of the ADAMTS13 conformation FO-SPR assay:** A) FO-SPR endpoint shifts from HD plasma samples (n=20) with and without the opening anti-CUB1 antibody 17G2. B) FO-SPR endpoint shifts from iTTP patients (n=19) in the absence and presence of 17G2. C) ADAMTS13 conformation index from HD (n=20) and iTTP (n=18) plasma samples in absence of 17G2 by correcting the FO-SPR endpoint shifts for the ADAMTS13 antigen levels. D) Correlation between the conformation indices, assessed in ELISA and FO-SPR, of iTTP patient (n=18) plasma samples in absence of 17G2.

# **Part V**

# **Discussion**

## 5.1. Anti-ADAMTS13 autoantibody assay

Since the clinical signs and symptoms of TTP are similar to those of several other TMAs, the clinical diagnosis remains challenging and presumptive. However, since TTP is a clinical emergency, the initiation of appropriate treatment cannot be postponed. Therefore, as the only specific biomarker for TTP, the evaluation of the ADAMTS13 activity remains crucial for the discrimination of TTP (ADAMTS13 activity <10%) from other TMAs (ADAMTS13 activity >10%) (Kremer Hovinga et al., 2017). However, to guide the disease management of TTP patients, anti-ADAMTS13 autoantibody assays are pivotal to differentially diagnose between the immune-mediated and the congenital form of the disease, particularly since *ADAMTS13* mutational analysis is exclusively done when no anti-ADAMTS13 autoantibodies are detected (Joly et al., 2017). However, different laboratories have their own approach to determine anti-ADAMTS13 autoantibody levels, which makes it challenging to compare autoantibody titers between different centres. Moreover, the transition of the anti-ADAMTS13 autoantibody assay from ELISA to the FO-SPR device will improve the diagnosis of TTP disease and boost the management and subsequently the therapeutic outcome of TTP patients.

### 5.1.1. Evaluation of diverse anti-ADAMTS13 autoantibody ELISA set-ups

In the reference laboratories for TTP, diverse approaches of the anti-ADAMTS13 autoantibody assay are performed. Both commercial (e.g.: Technozym®, Imubind®) and in-house developed ELISAs are used, which differs in terms of the ADAMTS13 presentation (coated and captured FL-rhADAMTS13 or coated truncated forms of ADAMTS13) or the autoantibody detection method (polyclonal anti-human (Fc specific) antibodies vs. a mixture of monoclonal anti-human IgG antibodies). In the Laboratory for Thrombosis Research, the current in-house developed anti-ADAMTS13 autoantibody ELISA uses coated FL-rhADAMTS13 combined with polyclonal anti-human (Fc specific) detection antibodies. Up till now, the effect of these various approaches on the anti-ADAMTS13 autoantibody levels remained elusive and therefore, the aim was to assess the variation between the different experimental set-ups on the determination of the anti-ADAMTS13 autoantibody titers.

Strong correlation was observed when comparing the anti-ADAMTS13 autoantibody levels using diverse methods of ADAMTS13 presentation (coated and captured FL-rhADAMTS13 or coated rhMDTCS and rhT2C2), whereas only moderate correlation was identified regarding the alternative approach for the anti-ADAMTS13 autoantibody detection (a mixture of monoclonal anti-human IgG or polyclonal anti-human (Fc specific) antibodies). Thereafter, the sensitivity of the anti-ADAMTS13 autoantibody ELISA set-ups, measured using the different ADAMTS13 presentations, was assessed. A cut-off value, determined by means of 72 HD plasma samples, was delineated for the positivity of anti-ADAMTS13 autoantibodies, which indicated a higher sensitivity for both methods using coated or captured FL-rhADAMTS13 compared to the approach using the combination of coated rhMDTCS and rhT2C2. However,

some discrepancies were observed in all diverse ELISA approaches when focusing on plasma samples containing lower anti-ADAMTS13 autoantibody levels. Therefore, the anti-ADAMTS13 autoantibody titers, assessed in the different reference centres, can only be compared when identical ELISA approaches are performed.

Importantly, the inter-laboratory comparison of anti-ADAMTS13 autoantibody levels is additionally complicated since the different commercial and in-house developed assays use different reference plasma samples as a calibrator and express the anti-ADAMTS13 autoantibody titer in different units. Therefore, a new project was started to develop a universal calibrator for anti-ADAMTS13 autoantibody assays.

### 5.1.2. Development of the anti-ADAMTS13 autoantibody FO-SPR assay

Currently, ADAMTS13 parameters are assessed by in-house developed or commercial ELISAs and FRETs assays in order to diagnose TTP patients. Nevertheless, the use of the current assays is restricted by some major limitations: 1) The ADAMTS13 assays are not easy to perform and are therefore only run in specialized laboratories in the reference centres; 2) The complex assays are labor-intensive and require the expertise of well-trained lab technicians; 3) The generation of reliable results for all ADAMTS13 characteristic is time-consuming (Lu et al., 2017). Since the ADAMTS13 bioassays are only performed in reference centres, physicians base their diagnosis on the presented clinical signs and standard biological parameters, which leads to the misdiagnosis of TTP disease and increases the mortality rates. Therefore, the transition from the current standard assays to the easy-to-use FO-SPR platform is favoured to maximize the therapeutic outcome of the disease management, as this technology allows simple, real-time single-sample testing with minimal sample preparation and clinical relevant sensitivity (Lu et al., 2017). Therefore, an anti-ADAMTS13 autoantibody FO-SPR assay was developed. Gold-coated optical fibers were used to immobilize an ADAMTS13-capturing antibody to its carboxyl-SAM layer, which in turn catches FL-rhADAMTS13. Thereafter, the FO probes are simply immersed in an iTTP patient plasma sample that contains anti-ADAMTS13 autoantibodies, which are detected using goat anti-human antibodies that are conjugated to gold nanoparticles.

The anti-metalloprotease domain antibodies 3H9 and 17C7 were screened for their ability to capture FL-rhADAMTS13 in the FO-SPR assay and subsequently, different amounts of FL-rhADAMTS13 were evaluated. Based on a high goat anti-human AuNP endpoint shift and a low CV, the anti-ADAMTS13 antibody 3H9 in combination with a FL-rhADAMTS13 concentration of 0.5 µg/mL was preferred to use in further experiments. Higher FL-rhADAMTS13 concentrations showed increasing immobilisation shifts, whereas the final goat anti-human AuNP endpoint shift surprisingly decreased significantly. Plausibly, steric hindrance effects contribute to these observations. After establishing a calibration curve, based

on the dilutions of a high-titer iTTP patient plasma sample, some HD plasma samples were screened as a negative control. Thereby, the anti-ADAMTS13 autoantibody FO-SPR assay was confirmed to be operational. However, further development and optimization of this bioassay was interrupted since the goat anti-human AuNPs were temporary not available. Therefore, the favourable concentration of the anti-ADAMTS13 antibody 3H9, the pH of the NaAc buffer and the preferred plasma sample dilution remains to be determined. Thereafter, the anti-ADAMTS13 autoantibody FO-SPR assay needs to be validated in plasma samples from both iTTP patients and healthy individuals to delineate the cut-off for the positivity of anti-ADAMTS13 autoantibodies.

## 5.2. ADAMTS13 conformation assay

ADAMTS13 circulates in the closed conformation, in which the CUB domains are folded onto the cysteine-rich and spacer domain, under normal rheological conditions in order to regulate its functional activity (Ercig et al., 2018; South et al., 2014). The induction of the open conformation is required to fully activate ADAMTS13, which thereby also regulates the exposure of cryptic epitopes that are recognized by anti-ADAMTS13 autoantibodies (Muia et al., 2014). Typically, iTTP patients present increased levels of the open ADAMTS13 conformation, which is demonstrated with the in-house developed ADAMTS13 conformation ELISA and therefore, the open ADAMTS13 conformation was depicted as a hallmark for acute iTTP (Roose et al., 2018a). Furthermore, the open ADAMTS13 conformation was recently observed in most plasma samples from iTTP patients in remission when ADAMTS13 activity levels were <50%, which supports the open ADAMTS13 conformation as a novel biomarker for subclinical iTTP (Roose et al., 2020). Although the ADAMTS13 conformation bioassay is currently not performed in hospital settings, there is a lot of interest to implement this test in a clinical context. However, the current ELISA assay encounters the same drawbacks as described above and therefore, the ADAMTS13 conformation ELISA was transferred to the easy-to-use FO-SPR platform as illustrated for the FO-SPR anti-ADAMTS13 autoantibody assay.

First, the immobilisation (the 1C4 antibody concentration and the pH of the NaAc buffer) of the anti-spacer domain antibody 1C4 to the carboxyl-SAM layer was optimized based on a high goat anti-biotin AuNP endpoint shift, large signal-to-noise ratio and low CV. Next, the favourable concentrations of the biotinylated antibody 3H9 and the opening anti-CUB1 antibody 17G2 were determined based on the same parameters. Thereafter, the conformational status of ADAMTS13 was screened in plasma samples from both iTTP patients and healthy individuals in presence and absence of the opening antibody 17G2. By means of 20 plasma samples from healthy individuals, a cut-off value was established to distinguish between the open and closed conformation. All samples characterized with an open ADAMTS13 conformation in ELISA, were analogously indicated with the open conformation

by the FO-SPR bioassay, whereas a single iTTP sample was registered with the closed ADAMTS13 conformation in both ELISA and FO-SPR. Furthermore, statistical significant correlation was demonstrated between the ADAMTS13 conformation index in plasma from iTTP patients, which was determined in ELISA and FO-SPR.

The successful transition of both the anti-ADAMTS13 autoantibody and the ADAMTS13 conformation assay from ELISA to the easy-to-use FO-SPR platform will positively impact the testing of ADAMTS13. Additionally, FO-SPR bioassays for the evaluation of the ADAMTS13 activity and the ADAMTS13 antigen levels are currently under development in the Laboratory for Thrombosis Research. In the future, the assessment of all four relevant ADAMTS13 parameters will be combined in a quantitative and easy-to-perform combo-assay, which allows rapid evaluation of individual samples when patients arrive at a hospital intensive care unit. Since no ADAMTS13 test currently combines these features, the combo-assay will decrease the misdiagnosis of TTP and allow the initiation of the correct treatment, resulting in an improved disease management.

# References

- Akiyama, M., Takeda, S., Kokame, K., Takagi, J., & Miyata, T. (2009). Crystal structures of the noncatalytic domains of ADAMTS13 reveal multiple discontinuous exosites for von Willebrand factor. *Proceedings of the National Academy of Sciences of the United States of America*. <https://doi.org/10.1073/pnas.0909755106>
- Allford, S. L., Hunt, B. J., Rose, P., & Machin, S. J. (2003). Guidelines on the diagnosis and management of the thrombotic microangiopathic haemolytic anaemias. *British Journal of Haematology*. <https://doi.org/10.1046/j.1365-2141.2003.04049.x>
- Alwan, F., Vendramin, C., Vanhoorelbeke, K., Langley, K., McDonald, V., Austin, S., ... Scully, M. (2017). Presenting ADAMTS13 antibody and antigen levels predict prognosis in immune-mediated thrombotic thrombocytopenic purpura. *Blood*. <https://doi.org/10.1182/blood-2016-12-758656>
- Amorosi, E. L., & Ultmann, J. E. (1966). Thrombotic thrombocytopenic purpura: Report of 16 cases and review of the literature. *Medicine (United States)*. <https://doi.org/10.1097/00005792-196603000-00003>
- Anderson, P. J., Kokame, K., & Sadler, J. E. (2006). Zinc and calcium ions cooperatively modulate ADAMTS13 activity. *Journal of Biological Chemistry*. <https://doi.org/10.1074/jbc.M504540200>
- Arya, M., Anvari, B., Romo, G. M., Cruz, M. A., Dong, J. F., McIntire, L. V., ... López, J. A. (2002). Ultralarge multimers of von Willebrand factor form spontaneous high-strength bonds with the platelet glycoprotein Ib-IX complex: Studies using optical tweezers. *Blood*. <https://doi.org/10.1182/blood-2001-11-0060>
- Atluri, P. (2005). *The surgical review: an integrated basic and clinical science study guide*. Lippincott Williams & Wilkins.
- Balduini, C. L., Gugliotta, L., Luppi, M., Laurenti, L., Klersy, C., Pieresca, C., ... Ascari, E. (2010). High versus standard dose methylprednisolone in the acute phase of idiopathic thrombotic thrombocytopenic purpura: A randomized study. *Annals of Hematology*. <https://doi.org/10.1007/s00277-009-0877-5>
- Bedford, E. E., Spadavecchia, J., Pradier, C. M., & Gu, F. X. (2012). Surface Plasmon Resonance Biosensors Incorporating Gold Nanoparticles. *Macromolecular Bioscience*. <https://doi.org/10.1002/mabi.201100435>
- Benhamou, Y., Boelle, P. Y., Baudin, B., Ederhy, S., Gras, J., Galicier, L., ... Coppo, P. (2015). Cardiac troponin-i on diagnosis predicts early death and refractoriness in acquired thrombotic thrombocytopenic purpura. experience of the french thrombotic microangiopathies reference center. *Journal of Thrombosis and Haemostasis*. <https://doi.org/10.1111/jth.12790>
- Benhamou, Ygal, Paintaud, G., Azoulay, E., Poullin, P., Galicier, L., Desvignes, C., ... Coppo, P. (2016). Efficacy of a rituximab regimen based on B cell depletion in thrombotic thrombocytopenic purpura with suboptimal response to standard treatment: Results of a phase II, multicenter noncomparative study. *American Journal of Hematology*. <https://doi.org/10.1002/ajh.24559>
- Bian, S., Lu, J., Delpont, F., Vermeire, S., Spasic, D., Lammertyn, J., & Gils, A. (2018). Development and validation of an optical biosensor for rapid monitoring of adalimumab in serum of patients with Crohn's disease. *Drug Testing and Analysis*, 10(3), 592–596. <https://doi.org/10.1002/dta.2250>

- Bode, W., Gomis-Rüth, F. X., & Stöckler, W. (1993). Astacins, serralysins, snake venom and matrix metalloproteinases exhibit identical zinc-binding environments (HEXXHXXGXXH and Met-turn) and topologies and should be grouped into a common family, the "metzincins." *FEBS Letters*. [https://doi.org/10.1016/0014-5793\(93\)80312-1](https://doi.org/10.1016/0014-5793(93)80312-1)
- Bork, P., & Beckmann, G. (1993). The CUB domain: A widespread module in developmentally regulated proteins. *Journal of Molecular Biology*. <https://doi.org/10.1006/jmbi.1993.1305>
- Boron, Walter, F., & Boulpaep, E. L. (2016). Medical Physiology 3rd edition. In *US Elsevier Health Bookshop*.
- Canis, K., Mckinnon, T. A. J., Nowak, A., Panico, M., Morris, H. R., Laffan, M., & Dell, A. (2010). The plasma von Willebrand factor O-glycome comprises a surprising variety of structures including ABH antigens and disialosyl motifs. *Journal of Thrombosis and Haemostasis*. <https://doi.org/10.1111/j.1538-7836.2009.03665.x>
- Canis, Kevin, Mckinnon, T. A. J., Nowak, A., Haslam, S. M., Panico, M., Morris, H. R., ... Dell, A. (2012). Mapping the N-glycome of human von Willebrand factor. *Biochemical Journal*. <https://doi.org/10.1042/BJ20120810>
- Cataland, S. R., Peyvandi, F., Mannucci, P. M., Lämmle, B., Kremer Hovinga, J. A., Machin, S. J., ... Knoebl, P. (2012). Initial experience from a double-blind, placebo-controlled, clinical outcome study of ARC1779 in patients with thrombotic thrombocytopenic purpura. *American Journal of Hematology*. <https://doi.org/10.1002/ajh.23106>
- Cerinic, M. M., Valentini, G., Sorano, G. G., D'Angelo, S., Cuomo, G., Fenu, L., ... Marongiu, F. (2003). Blood coagulation, fibrinolysis, and markers of endothelial dysfunction in systemic sclerosis. *Seminars in Arthritis and Rheumatism*, 32(5), 285–295. <https://doi.org/10.1053/sarh.2002.50011>
- Cesarman-Maus, G., & Hajjar, K. A. (2005). Molecular mechanisms of fibrinolysis. *British Journal of Haematology*, 129(3), 307–321. <https://doi.org/10.1111/j.1365-2141.2005.05444.x>
- Coppo, P. (2017). Management of thrombotic thrombocytopenic purpura. *Transfusion Clinique et Biologique*. <https://doi.org/10.1016/j.tracli.2017.05.015>
- Coppo, P., Busson, M., Veyradier, A., Wynckel, A., Poullin, P., Azoulay, E., ... Loiseau, P. (2010). HLA-DRB1\*11: A strong risk factor for acquired severe ADAMTS13 deficiency-related idiopathic thrombotic thrombocytopenic purpura in Caucasians. *Journal of Thrombosis and Haemostasis*. <https://doi.org/10.1111/j.1538-7836.2010.03772.x>
- Coppo, Paul, Cuker, A., & George, J. N. (2019). Thrombotic thrombocytopenic purpura: Toward targeted therapy and precision medicine. *Research and Practice in Thrombosis and Haemostasis*. <https://doi.org/10.1002/rth2.12160>
- Corstjens, P. L. A. M., Fidler, H. H., Wiesmeijer, K. C., De Dood, C. J., Rispen, T., Wolbink, G. J., ... Tanke, H. J. (2013). A rapid assay for on-site monitoring of infliximab trough levels: A feasibility study. *Analytical and Bioanalytical Chemistry*. <https://doi.org/10.1007/s00216-013-7154-0>
- Crawley, J. T B, De Groot, R., & Luken, B. M. (2009). Circulating ADAMTS-13-von Willebrand factor complexes: An enzyme on demand. *Journal of Thrombosis and Haemostasis*. <https://doi.org/10.1111/j.1538-7836.2009.03621.x>
- Crawley, James T.B., De Groot, R., Xiang, Y., Luken, B. M., & Lane, D. A. (2011). Unraveling the scissile bond: How ADAMTS13 recognizes and cleaves von Willebrand factor. *Blood*, 118(12), 3212–3221. <https://doi.org/10.1182/blood-2011-02-306597>

- Daems, D., Peeters, B., Delpoort, F., Remans, T., Lammertyn, J., & Spasic, D. (2017). Identification and quantification of celery allergens using fiber optic surface plasmon resonance PCR. *Sensors (Switzerland)*. <https://doi.org/10.3390/s17081754>
- De Groot, R., Bardhan, A., Ramroop, N., Lane, D. A., & Crawley, J. T. B. (2009). Essential role of the disintegrin-like domain in ADAMTS13 function. *Blood*. <https://doi.org/10.1182/blood-2008-11-187914>
- De Groot, R., Lane, D. A., & Crawley, J. T. B. (2010). The ADAMTS13 metalloprotease domain: Roles of subsites in enzyme activity and specificity. *Blood*. <https://doi.org/10.1182/blood-2009-12-258780>
- De Groot, R., Lane, D. A., & Crawley, J. T. B. (2015). The role of the ADAMTS13 cysteine-rich domain in VWF binding and proteolysis. *Blood*. <https://doi.org/10.1182/blood-2014-08-594556>
- Deforche, L., Roose, E., Vandenbulcke, A., Vandeputte, N., Feys, H. B., Springer, T. A., ... Vanhoorelbeke, K. (2015). Linker regions and flexibility around the metalloprotease domain account for conformational activation of ADAMTS-13. *Journal of Thrombosis and Haemostasis*. <https://doi.org/10.1111/jth.13149>
- Dong, J. fei, Moake, J. L., Nolasco, L., Bernardo, A., Arceneaux, W., Shrimpton, C. N., ... López, J. A. (2002). ADAMTS-13 rapidly cleaves newly secreted ultralarge von Willebrand factor multimers on the endothelial surface under flowing conditions. *Blood*. <https://doi.org/10.1182/blood-2002-05-1401>
- Ercig, B., Wichapong, K., Reutelingsperger, C. P. M., Vanhoorelbeke, K., Voorberg, J., & Nicolaes, G. A. F. (2018). Insights into 3D Structure of ADAMTS13: A Stepping Stone towards Novel Therapeutic Treatment of Thrombotic Thrombocytopenic Purpura. *Thrombosis and Haemostasis*. <https://doi.org/10.1160/TH17-06-0404>
- Feng, Y., Li, X., Xiao, J., Li, W., Liu, J., Zeng, X., ... Chen, S. (2016). ADAMTS13: more than a regulator of thrombosis. *International Journal of Hematology*. <https://doi.org/10.1007/s12185-016-2091-2>
- Fernandes, R. J., Hirohata, S., Engle, J. M., Colige, A., Cohn, D. H., Eyre, D. R., & Apte, S. S. (2001). Procollagen II amino propeptide processing by ADAMTS-3. Insights on dermatosparaxis. *Journal of Biological Chemistry*. <https://doi.org/10.1074/jbc.M103466200>
- Ferrari, S., Mudde, G. C., Rieger, M., Veyradier, A., Kremer Hovinga, J. A., & Scheifflinger, F. (2009). IgG subclass distribution of anti-ADAMTS13 antibodies in patients with acquired thrombotic thrombocytopenic purpura. *Journal of Thrombosis and Haemostasis*. <https://doi.org/10.1111/j.1538-7836.2009.03568.x>
- Ferrari, Silvia, Scheifflinger, F., Rieger, M., Mudde, G., Wolf, M., Coppo, P., ... Veyradier, A. (2007). Prognostic value of anti-ADAMTS13 antibody features (Ig isotype, titer, and inhibitory effect) in a cohort of 35 adult French patients undergoing a first episode of thrombotic microangiopathy with undetectable ADAMTS13 activity. *Blood*. <https://doi.org/10.1182/blood-2006-02-006064>
- Feys, H. B., Anderson, P. J., Vanhoorelbeke, K., Majerus, E. M., & Sadler, J. E. (2009). Multi-step binding of ADAMTS-13 to von Willebrand factor. *Journal of Thrombosis and Haemostasis*. <https://doi.org/10.1111/j.1538-7836.2009.03620.x>
- Feys, H. B., Liu, F., Dong, N., Pareyn, I., Vauterin, S., Vandeputte, N., ... Vanhoorelbeke, K. (2006). ADAMTS-13 plasma level determination uncovers antigen absence in acquired thrombotic thrombocytopenic purpura and ethnic differences. *Journal of Thrombosis and Haemostasis*. <https://doi.org/10.1111/j.1538-7836.2006.01833.x>

- Froissart, A., Buffet, M., Veyradier, A., Poullin, P., Provôt, F., Malot, S., ... Coppo, P. (2012). Efficacy and safety of first-line rituximab in severe, acquired thrombotic thrombocytopenic purpura with a suboptimal response to plasma exchange. Experience of the French Thrombotic Microangiopathies Reference Center. *Critical Care Medicine*. <https://doi.org/10.1097/CCM.0b013e31822e9d66>
- Fujikawa, K., Suzuki, H., McMullen, B., & Chung, D. (2001). Purification of human von Willebrand factor-cleaving protease and its identification as a new member of the metalloproteinase family. *Blood*. <https://doi.org/10.1182/blood.V98.6.1662>
- Fujimura, Y., Matsumoto, M., Isonishi, A., Yagi, H., Kokame, K., Soejima, K., ... Miyata, T. (2011). Natural history of Upshaw-Schulman syndrome based on ADAMTS13 gene analysis in Japan. *Journal of Thrombosis and Haemostasis*. <https://doi.org/10.1111/j.1538-7836.2011.04341.x>
- Fujimura, Yoshihiro, Matsumoto, M., Kokame, K., Isonishi, A., Soejima, K., Akiyama, N., ... George, J. N. (2009). Pregnancy-induced thrombocytopenia and TTP, and the risk of fetal death, in Upshaw-Schulman syndrome: A series of 15 pregnancies in 9 genotyped patients. *British Journal of Haematology*. <https://doi.org/10.1111/j.1365-2141.2008.07515.x>
- Furlan, M., Robles, R., Galbusera, M., Remuzzi, G., Kyrle, P. A., Brenner, B., ... Lämmle, B. (1998). Von Willebrand factor-cleaving protease in thrombotic thrombocytopenic purpura and the hemolytic-uremic syndrome. *New England Journal of Medicine*. <https://doi.org/10.1056/NEJM199811263392202>
- Furlan, M., Robles, R., & Lämmle, B. (1996). Partial purification and characterization of a protease from human plasma cleaving von Willebrand factor to fragments produced by in vivo proteolysis. *Blood*.
- Furlan, M., Robles, R., Solenthaler, M., & Lämmle, B. (1998). Acquired deficiency of von Willebrand factor-cleaving protease in a patient with thrombotic thrombocytopenic purpura. *Blood*.
- Furlan, M., Rubles, R., Solenthaler, M., Wassmer, M., Sandoz, P., & Lämmle, B. (1997). Deficient activity of von Willebrand factor-cleaving protease in chronic relapsing thrombotic thrombocytopenic purpura. *Blood*.
- Galbusera, M., Noris, M., & Remuzzi, G. (2009). Inherited thrombotic thrombocytopenic purpura. *Haematologica*. <https://doi.org/10.3324/haematol.2008.002493>
- Gao, W., Anderson, P. J., Majerus, E. M., Tuley, E. A., & Sadler, J. E. (2006). Exosite interactions contribute to tension-induced cleavage of von Willebrand factor by the antithrombotic ADAMTS13 metalloprotease. *Proceedings of the National Academy of Sciences of the United States of America*. <https://doi.org/10.1073/pnas.0607264104>
- Gao, W., Anderson, P. J., & Sadler, J. E. (2008). Extensive contacts between ADAMTS13 exosites and von Willebrand factor domain A2 contribute to substrate specificity. *Blood*. <https://doi.org/10.1182/blood-2008-04-148759>
- Gardner, M. D., Chion, C. K. N. K., Groot, R. De, Shah, A., Crawley, J. T. B., & Lane, D. A. (2009). Afunctional calcium-binding site in the metalloprotease domain of ADAMTS13. *Blood*. <https://doi.org/10.1182/blood-2008-03-144683>
- George, J. N. (2012). Corticosteroids and rituximab as adjunctive treatments for thrombotic thrombocytopenic purpura. *American Journal of Hematology*. <https://doi.org/10.1002/ajh.23126>
- Gerritsen, H. E., Robles, R., Lämmle, B., & Furlan, M. (2001). Partial amino acid sequence of

- purified von Willebrand factor-cleaving protease. *Blood*.  
<https://doi.org/10.1182/blood.V98.6.1654>
- Gibson, J. S. (2001). Oxygen-sensitive cation transport in sickle cells. *Blood Cells, Molecules, and Diseases*. <https://doi.org/10.1006/bcmd.2000.0361>
- Grall, M., Azoulay, E., Galicier, L., Provôt, F., Wynckel, A., Poullin, P., ... Benhamou, Y. (2017). Thrombotic thrombocytopenic purpura misdiagnosed as autoimmune cytopenia: Causes of diagnostic errors and consequence on outcome. Experience of the French thrombotic microangiopathies reference centre. *American Journal of Hematology*.  
<https://doi.org/10.1002/ajh.24665>
- Guo, C., Tsigkou, A., & Lee, M. H. (2016). ADAMTS13 and 15 are not regulated by the full length and N-terminal domain forms of TIMP-1, -2, -3 and -4. *Biomedical Reports*.  
<https://doi.org/10.3892/br.2015.535>
- Harbrecht, P. J. M. D. (1967). *Fibrinolysis* (pp. 209–2014). pp. 209–2014. Louisville: Southern Medical Journal.
- Hoehn, K., & Marieb, E. N. (2012). Human Anatomy & Physiology. *Benjamin-Cummings Publishing Company*. <https://doi.org/10.1007/BF00845519>
- Homola, J. (2008). Surface plasmon resonance sensors for detection of chemical and biological species. *Chemical Reviews*. <https://doi.org/10.1021/cr068107d>
- Houngkamhang, N., Charoensuwan, S., Sonthipakdee, O., Nawattanapaiboon, K., Somboonkaew, A., & Amarit, R. (2018). Gold-nanoparticle-based fiber optic sensor for sensing the refractive index of environmental solutions. *Chiang Mai Journal of Science*.
- Huang, Y., Zhang, S. D., McCrudden, C., Chan, K. W., Lin, Y., & Kwok, H. F. (2015). The prognostic significance of PD-L1 in bladder cancer. *Oncology Reports*.  
<https://doi.org/10.3892/or.2015.3933>
- Hughes, C., Mcewan, J. R., Longair, I., Hughes, S., Cohen, H., Machin, S., & Scully, M. (2009). Cardiac involvement in acute thrombotic thrombocytopenic purpura: Association with troponin T and IgG antibodies to ADAMTS 13. *Journal of Thrombosis and Haemostasis*. <https://doi.org/10.1111/j.1538-7836.2009.03285.x>
- Ikeda, H., Tateishi, R., Enooku, K., Yoshida, H., Nakagawa, H., Masuzaki, R., ... Yatomi, Y. (2011). Prediction of hepatocellular carcinoma development by plasma ADAMTS13 in chronic hepatitis B and C. *Cancer Epidemiology Biomarkers and Prevention*.  
<https://doi.org/10.1158/1055-9965.EPI-11-0464>
- Jestin, M., Benhamou, Y., Schelpe, A. S., Roose, E., Provôt, F., Galicier, L., ... Coppo, P. (2018). Preemptive rituximab prevents long-term relapses in immune-mediated thrombotic thrombocytopenic purpura. *Blood*. <https://doi.org/10.1182/blood-2018-04-840090>
- Jilma-Stohlawetz, P., Gorczyca, M. E., Jilma, B., Siller-Matula, J., Gilbert, J. C., & Knöbl, P. (2011). Inhibition of von Willebrand factor by ARC1779 in patients with acute thrombotic thrombocytopenic purpura. *Thrombosis and Haemostasis*. <https://doi.org/10.1160/TH10-08-0520>
- Jin, S. Y., Skipwith, C. G., & Zheng, X. L. (2010). Amino acid residues Arg659, Arg660, and Tyr 661 in the spacer domain of ADAMTS13 are critical for cleavage of von Willebrand factor. *Blood*. <https://doi.org/10.1182/blood-2009-07-235101>
- Joly, B. S., Coppo, P., & Veyradier, A. (2017). Thrombotic thrombocytopenic purpura. *Blood*.  
<https://doi.org/10.1182/blood-2016-10-709857>

- Joly, B. S., Vanhoorelbeke, K., & Veyradier, A. (2017). Understanding therapeutic targets in thrombotic thrombocytopenic purpura. *Intensive Care Medicine*. <https://doi.org/10.1007/s00134-016-4662-3>
- Jones, G. C., & Riley, G. P. (2005). ADAMTS proteinases: A multi-domain, multi-functional family with roles in extracellular matrix turnover and arthritis. *Arthritis Research and Therapy*. <https://doi.org/10.1186/ar1783>
- Katsumi, A., Tuley, E. A., Bodo, I., & Sadler, J. E. (2000). Localization of disulfide bonds in the cystine knot domain of human von Willebrand factor. *Journal of Biological Chemistry*. <https://doi.org/10.1074/jbc.M002654200>
- Klaus, C., Plaimauer, B., Studt, J. D., Dorner, F., Lämmle, B., Mannucci, P. M., & Scheiflinger, F. (2004). Epitope mapping of ADAMTS13 autoantibodies in acquired thrombotic thrombocytopenic purpura. *Blood*. <https://doi.org/10.1182/blood-2003-12-4165>
- Knöbl, P. (2018). Thrombotic thrombocytopenic purpura. *Memo - Magazine of European Medical Oncology*. <https://doi.org/10.1007/s12254-018-0429-6>
- Kokame, K., Matsumoto, M., Fujimura, Y., & Miyata, T. (2004). VWF73, a region from D1596 to R1668 of von Willebrand factor, provides a minimal substrate for ADAMTS-13. *Blood*. <https://doi.org/10.1182/blood-2003-08-2861>
- Kokame, K., Matsumoto, M., Soejima, K., Yagi, H., Ishizashi, H., Funato, M., ... Fujimura, Y. (2002). Mutations and common polymorphisms in ADAMTS13 gene responsible for von Willebrand factor-cleaving protease activity. *Proceedings of the National Academy of Sciences of the United States of America*. <https://doi.org/10.1073/pnas.172277399>
- Kremer Hovinga, J. A., Coppo, P., Lämmle, B., Moake, J. L., Miyata, T., & Vanhoorelbeke, K. (2017). Thrombotic thrombocytopenic purpura. *Nature Reviews Disease Primers*. <https://doi.org/10.1038/nrdp.2017.20>
- Kremer Hovinga, J. A., & Lämmle, B. (2012). Role of ADAMTS13 in the pathogenesis, diagnosis, and treatment of thrombotic thrombocytopenic purpura. *Hematology / the Education Program of the American Society of Hematology. American Society of Hematology. Education Program*. <https://doi.org/10.1182/asheducation.v2012.1.610.3798654>
- Lämmle, B., Kremer Hovinga, J. A., & Alberio, L. (2005). Thrombotic thrombocytopenic purpura. *Journal of Thrombosis and Haemostasis*. <https://doi.org/10.1111/j.1538-7836.2005.01425.x>
- Lancellotti, S., Peyvandi, F., Pagliari, M. T., Cairo, A., Abdel-Azeim, S., Chermak, E., ... De Cristofaro, R. (2016). The D173G mutation in ADAMTS-13 causes a severe form of congenital thrombotic thrombocytopenic purpura: A clinical, biochemical and in silico study. *Thrombosis and Haemostasis*. <https://doi.org/10.1160/TH15-02-0119>
- Lenting, P. J., Casari, C., Christophe, O. D., & Denis, C. V. (2012). von Willebrand factor: The old, the new and the unknown. *Journal of Thrombosis and Haemostasis*. <https://doi.org/10.1111/jth.12008>
- Lenting, Peter J., Christophe, O. D., & Denis, C. V. (2015). Von Willebrand factor biosynthesis, secretion, and clearance: Connecting the far ends. *Blood*, 125(13), 2019–2028. <https://doi.org/10.1182/blood-2014-06-528406>
- Levy, G. G., Nichols, W. C., Lian, E. C., Foroud, T., McClintick, J. N., McGee, B. M., ... Tsai, H. M. (2001). Mutations in a member of the ADAMTS gene family cause thrombotic thrombocytopenic purpura. *Nature*. <https://doi.org/10.1038/35097008>

- Li, S. W., Arita, M., Fertala, A., Bao, Y., Kopen, G. C., Långsjö, T. K., ... Prockop, D. J. (2001). Transgenic mice with inactive alleles for procollagen N-proteinase (ADAMTS-2) develop fragile skin and male sterility. *Biochemical Journal*.  
<https://doi.org/10.1042/0264-6021:3550271>
- Li, Y., Choi, H., Zhou, Z., Nolasco, L., Pownall, H. J., Voorberg, J., ... Dong, J. F. (2008). Covalent regulation of ULVWF string formation and elongation on endothelial cells under flow conditions. *Journal of Thrombosis and Haemostasis*.  
<https://doi.org/10.1111/j.1538-7836.2008.02991.x>
- Long Zheng, X., Wu, H. M., Shang, D., Falls, E., Skipwith, C. G., Cataland, S. R., ... Kwaan, H. C. (2010). Multiple domains of ADAMTS13 are targeted by autoantibodies against ADAMTS13 in patients with acquired idiopathic thrombotic thrombocytopenic purpura. *Haematologica*. <https://doi.org/10.3324/haematol.2009.019299>
- Lotta, L. A., Garagiola, I., Palla, R., Cairo, A., & Peyvandi, F. (2010). ADAMTS13 mutations and polymorphisms in congenital thrombotic thrombocytopenic purpura. *Human Mutation*. <https://doi.org/10.1002/humu.21143>
- Lu, J., Spasic, D., Delpont, F., Van Stappen, T., Detrez, I., Daems, D., ... Lammertyn, J. (2017). Immunoassay for Detection of Infliximab in Whole Blood Using a Fiber-Optic Surface Plasmon Resonance Biosensor. *Analytical Chemistry*, 89(6), 3664–3671.  
<https://doi.org/10.1021/acs.analchem.6b05092>
- Lu, J., Van Stappen, T., Spasic, D., Delpont, F., Vermeire, S., Gils, A., & Lammertyn, J. (2016). Fiber optic-SPR platform for fast and sensitive infliximab detection in serum of inflammatory bowel disease patients. *Biosensors and Bioelectronics*.  
<https://doi.org/10.1016/j.bios.2015.11.087>
- Luken, B. M., Turenhout, E. A. M., Hulstein, J. J. J., Van Mourik, J. A., Fijnheer, R., & Voorberg, J. (2005). The spacer domain of ADAMTS13 contains a major binding site for antibodies in patients with thrombotic thrombocytopenic purpura. *Thrombosis and Haemostasis*. <https://doi.org/10.1160/TH04-05-0301>
- Luken, B. M., Turenhout, E. A. M., Kaijen, P. H. P., Greuter, M. J., Pos, W., van Mourik, J. A., ... Voorberg, J. (2006). Amino acid regions 572-579 and 657-666 of the spacer domain of ADAMTS13 provide a common antigenic core required for binding of antibodies in patients with acquired TTP. *Thrombosis and Haemostasis*.  
<https://doi.org/10.1160/TH06-03-0135>
- Luken, B. M., Winn, L. Y. N., Emsley, J., Lane, D. A., & Crawley, J. T. B. (2010). The importance of vicinal cysteines, C1669 and C1670, for von Willebrand factor A2 domain function. *Blood*. <https://doi.org/10.1182/blood-2009-12-257949>
- Luo, G. P., Ni, B., Yang, X., & Wu, Y. Z. (2012). Von Willebrand factor: More than a regulator of hemostasis and thrombosis. *Acta Haematologica*. <https://doi.org/10.1159/000339426>
- Mansouri Taleghani, M., von Krogh, A. S., Fujimura, Y., George, J. N., Hrachovinova, I., Knöbl, P. N., ... Kremer Hovinga, J. A. (2013). Hereditary thrombotic thrombocytopenic purpura and the hereditary TTP registry. *Hamostaseologie*.  
<https://doi.org/10.5482/HAMO-13-04-0026>
- Mariotte, E., Azoulay, E., Galicier, L., Rondeau, E., Zouiti, F., Boisseau, P., ... Veyradier, A. (2016). Epidemiology and pathophysiology of adulthood-onset thrombotic microangiopathy with severe ADAMTS13 deficiency (thrombotic thrombocytopenic purpura): A cross-sectional analysis of the French national registry for thrombotic microangiopathy. *The Lancet Haematology*. [https://doi.org/10.1016/S2352-3026\(16\)30018-7](https://doi.org/10.1016/S2352-3026(16)30018-7)

- Matsui, T., Titani, K., & Mizuochi, T. (1992). Structures of the Asparagine-linked oligosaccharide chains of human von Willebrand factor. *J Biol Chem*.
- Mayadas, T. N., & Wagner, D. D. (1989). In vitro multimerization of von Willebrand factor is triggered by low pH. Importance of the propolypeptide and free sulfhydryls. *Journal of Biological Chemistry*.
- Moake, J. L. (2002). Thrombotic microangiopathies. *New England Journal of Medicine*. <https://doi.org/10.1056/NEJMra020528>
- Moake, J. L., Rudy, C. K., Troll, J. H., Weinstein, M. J., Colannino, N. M., Azocar, J., ... Deykin, D. (1982). Unusually Large Plasma Factor VIII: Von Willebrand Factor Multimers in Chronic Relapsing Thrombotic Thrombocytopenic Purpura. *New England Journal of Medicine*. <https://doi.org/10.1056/NEJM198212023072306>
- Möller, J. P., Mielke, S., Löf, A., Obser, T., Beer, C., Bruetzel, L. K., ... Benoit, M. (2016). Force sensing by the vascular protein von Willebrand factor is tuned by a strong intermonomer interaction. *Proceedings of the National Academy of Sciences of the United States of America*. <https://doi.org/10.1073/pnas.1516214113>
- Monagle, P., & Massicotte, P. (2011). Developmental haemostasis: Secondary haemostasis. *Seminars in Fetal and Neonatal Medicine*. <https://doi.org/10.1016/j.siny.2011.07.007>
- Moschcowitz, E. (1925). An acute febrile pleiochromic anemia with hyaline thrombosis of the terminal arterioles and capillaries: An undescribed disease. *Archives of Internal Medicine*. <https://doi.org/10.1001/archinte.1925.00120130092009>
- Muia, J., Zhu, J., Gupta, G., Haberichter, S. L., Friedman, K. D., Feys, H. B., ... Sadler, J. E. (2014). Allosteric activation of ADAMTS13 by von Willebrand factor. *Proceedings of the National Academy of Sciences of the United States of America*. <https://doi.org/10.1073/pnas.1413282112>
- Murphy, K., & Weaver, C. (2018). Janeway's Immunobiology. Ninth Edition. *The Quarterly Review of Biology*. <https://doi.org/10.1086/696793>
- Musial, J., Niewiarowski, S., Rucinski, B., Stewart, G. J., Cook, J. J., Williams, J. A., & Edmunds, L. H. (1990). Inhibition of platelet adhesion to surfaces of extracorporeal circuits by distintegrins. RGD-containing peptides from viper venoms. *Circulation*. <https://doi.org/10.1161/01.CIR.82.1.261>
- Nguyen, H. H., Park, J., Kang, S., & Kim, M. (2015). Surface plasmon resonance: A versatile technique for biosensor applications. *Sensors (Switzerland)*. <https://doi.org/10.3390/s150510481>
- Page, E. E., Kremer Hovinga, J. A., Terrell, D. R., Vesely, S. K., & George, J. N. (2017). Thrombotic thrombocytopenic purpura: Diagnostic criteria, clinical features, and long-term outcomes from 1995 through 2015. *Blood Advances*. <https://doi.org/10.1182/bloodadvances.2017005124>
- Pallister, C. J., & Watson, M. S. (2011). Haematology 2nd edition. In *Scion*.
- Pannekoek, H., & Voorberg, J. (1989). 5 Molecular cloning, expression and assembly of multimeric von Willebrand factor. *Bailliere's Clinical Haematology*. [https://doi.org/10.1016/S0950-3536\(89\)80050-2](https://doi.org/10.1016/S0950-3536(89)80050-2)
- Petri, A., Kim, H. J., Xu, Y., de Groot, R., Li, C., Vandenbulcke, A., ... Crawley, J. T. B. (2019). Crystal structure and substrate-induced activation of ADAMTS13. *Nature Communications*. <https://doi.org/10.1038/s41467-019-11474-5>
- Peyvandi, F., Lavoretano, S., Palla, R., Feys, H. B., Vanhoorelbeke, K., Battaglioli, T., ...

- Mannucci, P. M. (2008). ADAMTS13 and anti-ADAMTS13 antibodies as markers for recurrence of acquired thrombotic thrombocytopenic purpura during remission. *Haematologica*. <https://doi.org/10.3324/haematol.11739>
- Peyvandi, F., Scully, M., Kremer Hovinga, J. A., Cataland, S., Knöbl, P., Wu, H., ... Tersago, D. (2016). Caplacizumab for acquired thrombotic thrombocytopenic purpura. *New England Journal of Medicine*. <https://doi.org/10.1056/NEJMoa1505533>
- Phillips, D. R., Charo, I. F., Parise, L. V., & Fitzgerald, L. A. (1988). The platelet membrane glycoprotein IIb-IIIa complex. *Blood*.
- Pimanda, J. E., Maekawa, A., Wind, T., Paxton, J., Chesterman, C. N., & Hogg, P. J. (2004). Congenital thrombotic thrombocytopenic purpura in association with a mutation in the second CUB domain of ADAMTS13. *Blood*. <https://doi.org/10.1182/blood-2003-04-1346>
- Plautz, W. E., Raval, J. S., Dyer, M. R., Rollins-Raval, M. A., Zuckerbraun, B. S., & Neal, M. D. (2018). ADAMTS13: origins, applications, and prospects. *Transfusion*. <https://doi.org/10.1111/trf.14804>
- Pollet, J., Delport, F., Janssen, K. P. F., Jans, K., Maes, G., Pfeiffer, H., ... Lammertyn, J. (2009). Fiber optic SPR biosensing of DNA hybridization and DNA-protein interactions. *Biosensors and Bioelectronics*. <https://doi.org/10.1016/j.bios.2009.08.045>
- Pos, W., Crawley, J. T. B., Fijnheer, R., Voorberg, J., Lane, D. A., & Luken, B. M. (2010). An autoantibody epitope comprising residues R660, Y661, and Y665 in the ADAMTS13 spacer domain identifies a binding site for the A2 domain of VWF. *Blood*. <https://doi.org/10.1182/blood-2009-06-229203>
- Pos, W., Sorvillo, N., Fijnheer, R., Feys, H. B., Kaijen, P. H. P., Vidarsson, G., & Voorberg, J. (2011). Residues arg568 and phe592 contribute to an antigenic surface for anti-adamts13 antibodies in the spacer domain. *Haematologica*. <https://doi.org/10.3324/haematol.2010.036327>
- Pruss, C. M., Notley, C. R. P., Hegadorn, C. A., O'Brien, L. A., & Lillicrap, D. (2008). ADAMTS13 cleavage efficiency is altered by mutagenic and, to a lesser extent, polymorphic sequence changes in the A1 and A2 domains of von Willebrand factor. *British Journal of Haematology*. <https://doi.org/10.1111/j.1365-2141.2008.07266.x>
- Rauch, A., Wohner, N., Christophe, O. D., Denis, C. V., Susen, S., & Lenting, P. J. (2013). On the versatility of von Willebrand factor. *Mediterranean Journal of Hematology and Infectious Diseases*. <https://doi.org/10.4084/mjhid.2013.046>
- Reininger, A. J. (2008). Function of von Willebrand factor in haemostasis and thrombosis. *Haemophilia*. <https://doi.org/10.1111/j.1365-2516.2008.01848.x>
- Reuken, P. A., Kussmann, A., Kiehntopf, M., Budde, U., Stallmach, A., Claus, R. A., & Bruns, T. (2015). Imbalance of von Willebrand factor and its cleaving protease ADAMTS 13 during systemic inflammation superimposed on advanced cirrhosis. *Liver International*. <https://doi.org/10.1111/liv.12657>
- Ricketts, L. M., Dlugosz, M., Luther, K. B., Haltiwanger, R. S., & Majerus, E. M. (2007). O-fucosylation is required for ADAMTS13 secretion. *Journal of Biological Chemistry*. <https://doi.org/10.1074/jbc.M700317200>
- Rieger, M., Ferrari, S., Kremer Hovinga, J. A., Konetschny, C., Herzog, A., Koller, L., ... Scheifflinger, F. (2006). Relation between ADAMTS13 activity and ADAMTS13 antigen levels in healthy donors and patients with thrombotic microangiopathies (TMA). *Thrombosis and Haemostasis*. <https://doi.org/10.1160/TH05-08-0550>

- Rieger, M., Mannucci, P. M., Kremer Hovinga, J. A., Herzog, A., Gerstenbauer, G., Konetschny, C., ... Scheiflinger, F. (2005). ADAMTS13 autoantibodies in patients with thrombotic microangiopathies and other immunomediated diseases. *Blood*. <https://doi.org/10.1182/blood-2004-11-4490>
- Rock, G. A., Shumak, K. H., Buskard, N. A., Blanchette, V. S., Kelton, J. G., Nair, R. C., & Spasoff, R. A. (1991). Comparison of plasma exchange with plasma infusion in the treatment of thrombotic thrombocytopenic purpura. *New England Journal of Medicine*. <https://doi.org/10.1056/NEJM199108083250604>
- Romero, A., Romao, M. J., Varela, P. F., Kölln, I., Dias, J. M., Carvalho, A. L., ... Calvete, J. J. (1997). The crystal structures of two spermadhesins reveal the CUB domain fold. *Nature Structural Biology*. <https://doi.org/10.1038/nsb1097-783>
- Roose, E., Schelpe, A. S., Joly, B. S., Peetermans, M., Verhamme, P., Voorberg, J., ... Vanhoorelbeke, K. (2018a). An open conformation of ADAMTS-13 is a hallmark of acute acquired thrombotic thrombocytopenic purpura. *Journal of Thrombosis and Haemostasis*. <https://doi.org/10.1111/jth.13922>
- Roose, Elien, Schelpe, A.-S. M. B., Tellier, E., Sinkovits, G., Joly, B. S., Dekimpe, C., ... Vanhoorelbeke, K. (2020). Open ADAMTS13, induced by antibodies, is a biomarker for subclinical immune-mediated thrombotic thrombocytopenic purpura. *Blood*. <https://doi.org/10.1182/blood.2019004221>
- Roose, Elien, Schelpe, A.-S., Tellier, E., Sinkovits, G., Kaplanski, G., Le Besnerais, M., ... Vanhoorelbeke, K. (2018b). Open ADAMTS13 Conformation in Immune-Mediated Thrombotic Thrombocytopenic Purpura Is Induced By Anti-ADAMTS13 Autoantibodies and Corresponds with an Ongoing ADAMTS13 Pathology. *Blood*. <https://doi.org/10.1182/blood-2018-99-113762>
- Roose, Elien, Vidarsson, G., Kangro, K., Verhagen, O. J. H. M., Mancini, I., Desender, L., ... Vanhoorelbeke, K. (2018c). Anti-ADAMTS13 Autoantibodies against Cryptic Epitopes in Immune-Mediated Thrombotic Thrombocytopenic Purpura. *Thrombosis and Haemostasis*. <https://doi.org/10.1055/s-0038-1669459>
- Rossio, R., Ferrari, B., Cairo, A., Mancini, I., Pisapia, G., Palazzo, G., & Peyvandi, F. (2013). Two novel heterozygote missense mutations of the ADAMTS13 gene in a child with recurrent Thrombotic thrombocytopenic purpura. *Blood Transfusion*. <https://doi.org/10.2450/2012.0029-12>
- Sadler, J. E., Shelton-Inloes, B. B., Sorace, J. M., & Titani, K. (1986). Cloning of cDNA and genomic DNA for human von Willebrand factor. *Cold Spring Harbor Symposia on Quantitative Biology*. <https://doi.org/10.1101/sqb.1986.051.01.063>
- Sadler, J. Evan. (1998). BIOCHEMISTRY AND GENETICS OF VON WILLEBRAND FACTOR. *Annual Review of Biochemistry*. <https://doi.org/10.1146/annurev.biochem.67.1.395>
- Sadler, J. Evan. (2009). Low von Willebrand factor: sometimes a risk factor and sometimes a disease. *Hematology / the Education Program of the American Society of Hematology. American Society of Hematology. Education Program*. <https://doi.org/10.1182/asheducation-2009.1.106>
- Sadler, J. Evan. (2015). What's new in the diagnosis and pathophysiology of thrombotic thrombocytopenic purpura. *Hematology*. <https://doi.org/10.1182/asheducation-2015.1.631>
- Sadler, J. Evan. (2017). Pathophysiology of thrombotic thrombocytopenic purpura. *Blood*. <https://doi.org/10.1182/blood-2017-04-636431>

- Sakai, K., Kuwana, M., Tanaka, H., Hosomichi, K., Hasegawa, A., Uyama, H., ... Matsumoto, M. (2020). HLA loci predisposing to immune TTP in Japanese: potential role of the shared ADAMTS13 peptide bound to different HLA-DR. *Blood*. <https://doi.org/10.1182/blood.2020005395>
- Samor, B., Michalski, J. -C, Debray, H., Mazurier, C., Goudemand, M., Van Halbeek, H., ... Montreuil, J. (1986). Primary structure of a new tetraantennary glycan of the N-acetyllactosaminic type isolated from human factor VIII/von Willebrand factor. *European Journal of Biochemistry*. <https://doi.org/10.1111/j.1432-1033.1986.tb09750.x>
- Samor, B., Michalski, J. C., Mazurier, C., Goudemand, M., De Waard, P., Vliegenthart, J. F. G., ... Montreuil, J. (1989). Primary structure of the major O-glycosidically linked carbohydrate unit of human von Willebrand factor. *Glycoconjugate Journal*. <https://doi.org/10.1007/BF01047846>
- Sayani, F. A., & Abrams, C. S. (2015). How I treat refractory thrombotic thrombocytopenic purpura. *Blood*. <https://doi.org/10.1182/blood-2014-11-551580>
- Scheiflinger, F., Knöbl, P., Trattner, B., Plaimauer, B., Mohr, G., Dockal, M., ... Rieger, M. (2003). Nonneutralizing IgM and IgG antibodies to von Willebrand factor-cleaving protease (ADAMTS-13) in a patient with thrombotic thrombocytopenic purpura. *Blood*. <https://doi.org/10.1182/blood-2003-05-1616>
- Schneider, S. W., Nuschele, S., Wixforth, A., Gorzelanny, C., Alexander-Katz, A., Netz, R. R., & Schneider, M. F. (2007). Shear-induced unfolding triggers adhesion of von Willebrand factor fibers. *Proceedings of the National Academy of Sciences of the United States of America*. <https://doi.org/10.1073/pnas.0608422104>
- Scully, M., Brown, J., Patel, R., Mcdonald, V., Brown, C. J., & Machin, S. (2010). Human leukocyte antigen association in idiopathic thrombotic thrombocytopenic purpura: Evidence for an immunogenetic link. *Journal of Thrombosis and Haemostasis*. <https://doi.org/10.1111/j.1538-7836.2009.03692.x>
- Scully, Marie, & Blombery, P. (2014). Management of thrombotic thrombocytopenic purpura: current perspectives. *Journal of Blood Medicine*. <https://doi.org/10.2147/jbm.s46458>
- Scully, Marie, Cohen, H., Cavenagh, J., Benjamin, S., Starke, R., Killick, S., ... Machin, S. J. (2007). Remission in acute refractory and relapsing thrombotic thrombocytopenic purpura following rituximab is associated with a reduction in IgG antibodies to ADAMTS-13. *British Journal of Haematology*. <https://doi.org/10.1111/j.1365-2141.2006.06448.x>
- Scully, Marie, Hunt, B. J., Benjamin, S., Liesner, R., Rose, P., Peyvandi, F., ... Machin, S. J. (2012). Guidelines on the diagnosis and management of thrombotic thrombocytopenic purpura and other thrombotic microangiopathies. *British Journal of Haematology*. <https://doi.org/10.1111/j.1365-2141.2012.09167.x>
- Scully, Marie, Knoebl, P., Kentouche, K., Rice, L., Windyga, J., Schneppenheim, R., ... Ewenstein, B. M. (2016). Pharmacodynamic Profile of a Recombinant ADAMTS13 (BAX930) in Hereditary Thrombotic Thrombocytopenic Purpura (Upshaw-Schulman Syndrome (USS)). *Blood*.
- Scully, Marie, Thomas, M., Underwood, M., Watson, H., Langley, K., Camilleri, R. S., ... Brien, P. O. (2014). Thrombotic thrombocytopenic purpura and pregnancy: Presentation, management, and subsequent pregnancy outcomes. *Blood*. <https://doi.org/10.1182/blood-2014-02-553131>
- Shang, D., Zheng, X. W., Niiya, M., & Zheng, X. L. (2006). Apical sorting of ADAMTS13 in vascular endothelial cells and Madin-Darby canine kidney cells depends on the CUB domains and their association with lipid rafts. *Blood*. <https://doi.org/10.1182/blood-2006->

- Shapiro, S. E., Nowak, A. A., Wooding, C., Birdsey, G., Laffan, M. A., & McKinnon, T. A. J. (2014). The von Willebrand factor predicted unpaired cysteines are essential for secretion. *Journal of Thrombosis and Haemostasis*. <https://doi.org/10.1111/jth.12466>
- Shibagaki, Y., Matsumoto, M., Kokame, K., Ohba, S., Miyata, T., Fujimura, Y., & Fujita, T. (2006). Novel compound heterozygote mutations (H234Q/R1206X) of the ADAMTS13 gene in an adult patient with Upshaw-Schulman syndrome showing predominant episodes of repeated acute renal failure. *Nephrology Dialysis Transplantation*. <https://doi.org/10.1093/ndt/gfk072>
- Shim, K., Anderson, P. J., Tuley, E. A., Wiswall, E., & Sadler, J. E. (2008). Platelet-VWF complexes are preferred substrates of ADAMTS13 under fluid shear stress. *Blood*. <https://doi.org/10.1182/blood-2007-05-093021>
- Skipwith, C. G., Cao, W., & Zheng, X. L. (2010). Factor VIII and platelets synergistically accelerate cleavage of von Willebrand factor by ADAMTS13 under fluid shear stress. *Journal of Biological Chemistry*. <https://doi.org/10.1074/jbc.M110.131227>
- Sorvillo, N., Pos, W., Van Den Berg, L. M., Fijnheer, R., Martinez-Pomares, L., Geijtenbeek, T. B., ... Voorberg, J. (2012). The macrophage mannose receptor promotes uptake of ADAMTS13 by dendritic cells. *Blood*. <https://doi.org/10.1182/blood-2011-09-377754>
- South, K., Freitas, M. O., & Lane, D. A. (2017). A model for the conformational activation of the structurally quiescent metalloprotease ADAMTS13 by von willebrand factor. *Journal of Biological Chemistry*. <https://doi.org/10.1074/jbc.M117.776732>
- South, K., Luken, B. M., Crawley, J. T. B., Phillips, R., Thomas, M., Collins, R. F., ... Lane, D. A. (2014). Conformational activation of ADAMTS13. *Proceedings of the National Academy of Sciences of the United States of America*. <https://doi.org/10.1073/pnas.1411979112>
- Sporn, L. A., Chavin, S. I., Marder, V. J., & Wagner, D. D. (1985). Biosynthesis of von Willebrand protein by human megakaryocytes. *Journal of Clinical Investigation*, 76(3), 1102–1106. <https://doi.org/10.1172/JCI112064>
- Sporn, L. A., Marder, V. J., & Wagner, D. D. (1986). Inducible secretion of large, biologically potent von Willebrand factor multimers. *Cell*, 46(2), 185–190. [https://doi.org/10.1016/0092-8674\(86\)90735-X](https://doi.org/10.1016/0092-8674(86)90735-X)
- Stockschlaeder, M., Schneppenheim, R., & Budde, U. (2014). Update on von Willebrand factor multimers: Focus on high-molecular-weight multimers and their role in hemostasis. *Blood Coagulation and Fibrinolysis*. <https://doi.org/10.1097/MBC.0000000000000065>
- Tan, K., Duquette, M., Liu, J. H., Dong, Y., Zhang, R., Joachimiak, A., ... Wang, J. H. (2002). Crystal structure of the TSP-1 type 1 repeats: A novel layered fold and its biological implication. *Journal of Cell Biology*. <https://doi.org/10.1083/jcb.200206062>
- Tao, Z., Wang, Y., Choi, H., Bernardo, A., Nishio, K., Sadler, J. E., ... Dong, J. F. (2005). Cleavage of ultralarge multimers of von Willebrand factor by C-terminal-truncated mutants of ADAMTS-13 under flow. *Blood*. <https://doi.org/10.1182/blood-2004-11-4188>
- Tersteeg, C., Joly, B. S., Gils, A., Lijnen, R., Deckmyn, H., Declerck, P. J., ... Vanhoorelbeke, K. (2017). Amplified endogenous plasmin activity resolves acute thrombotic thrombocytopenic purpura in mice. *Journal of Thrombosis and Haemostasis*, 15(12), 2432–2442. <https://doi.org/10.1111/jth.13859>

- Tersteeg, Claudia, Schiviz, A., De Meyer, S. F., Plaimauer, B., Scheiflinger, F., Rottensteiner, H., & Vanhoorelbeke, K. (2015). Potential for Recombinant ADAMTS13 as an Effective Therapy for Acquired Thrombotic Thrombocytopenic Purpura. *Arteriosclerosis, Thrombosis, and Vascular Biology*. <https://doi.org/10.1161/ATVBAHA.115.306014>
- Thomas, M. R., de Groot, R., Scully, M. A., & Crawley, J. T. B. (2015). Pathogenicity of Anti-ADAMTS13 Autoantibodies in Acquired Thrombotic Thrombocytopenic Purpura. *EBioMedicine*. <https://doi.org/10.1016/j.ebiom.2015.06.007>
- Tsai, H. M. (1996). Physiologic cleavage of von Willebrand factor by a plasma protease is dependent on its conformation and requires calcium ion. *Blood*.
- Tsai, H. M. (2012). Von Willebrand factor, shear stress, and ADAMTS13 in hemostasis and thrombosis. *ASAIO Journal*. <https://doi.org/10.1097/MAT.0b013e31824363e7>
- Tsai, H. M., & Lian, E. C. Y. (1998). Antibodies to von Willebrand factor-cleaving protease in acute thrombotic thrombocytopenic purpura. *New England Journal of Medicine*. <https://doi.org/10.1056/NEJM199811263392203>
- Uchida, T., Wada, H., Mizutani, M., Iwashita, M., Ishihara, H., Shibano, T., ... Murata, M. (2004). Identification of novel mutations in ADAMTS13 in an adult patient with congenital thrombotic thrombocytopenic purpura. *Blood*. <https://doi.org/10.1182/blood-2004-02-0715>
- Uemura, M., Tatsumi, K., Matsumoto, M., Fujimoto, M., Matsuyama, T., Ishikawa, M., ... Fujimura, Y. (2005). Localization of ADAMTS13 to the stellate cells of human liver. *Blood*. <https://doi.org/10.1182/blood-2005-01-0152>
- Underwood, M., Peyvandi, F., Garagiola, I., Machin, S., & Mackie, I. (2016). Degradation of two novel congenital TTP ADAMTS13 mutants by the cell proteasome prevents ADAMTS13 secretion. *Thrombosis Research*. <https://doi.org/10.1016/j.thromres.2016.09.014>
- Upshaw, J. D. (1978). Congenital Deficiency of a Factor in Normal Plasma That Reverses Microangiopathic Hemolysis and Thrombocytopenia. *New England Journal of Medicine*. <https://doi.org/10.1056/NEJM197806152982407>
- Van Stappen, T., Vande Casteele, N., Van Assche, G., Ferrante, M., Vermeire, S., & Gils, A. (2017). DOP029 Clinical relevance of detecting anti-infliximab antibodies with a drug-tolerant assay: post-hoc analysis of the taxit trial. *Journal of Crohn's and Colitis*. <https://doi.org/10.1093/ecco-jcc/jjx002.066>
- Van Wart, H. E., & Birkedal-Hansen, H. (1990). The cysteine switch: A principle of regulation of metalloproteinase activity with potential applicability to the entire matrix metalloproteinase gene family. *Proceedings of the National Academy of Sciences of the United States of America*. <https://doi.org/10.1073/pnas.87.14.5578>
- Vanhoorelbeke, K., Cauwenberghs, N., Vandecasteele, G., Vauterin, S., & Deckmyn, H. (2002). A reliable von Willebrand factor: Ristocetin cofactor enzyme-linked immunosorbent assay to differentiate between type 1 and type 2 von Willebrand disease. *Seminars in Thrombosis and Hemostasis*. <https://doi.org/10.1055/s-2002-27818>
- Verbij, F. C., Stokhuijzen, E., Kaijen, P. H. P., Van Alphen, F., Meijer, A. B., & Voorberg, J. (2016). Identification of glycans on plasma-derived ADAMTS13. *Blood*. <https://doi.org/10.1182/blood-2016-06-720912>
- Verhenne, S., Vandeputte, N., Pareyn, I., Izsvák, Z., Rottensteiner, H., Deckmyn, H., ...

- Vanhoorelbeke, K. (2017). Long-term prevention of congenital thrombotic thrombocytopenic purpura in ADAMTS13 knockout mice by sleeping beauty transposon-mediated gene therapy. *Arteriosclerosis, Thrombosis, and Vascular Biology*. <https://doi.org/10.1161/ATVBAHA.116.308680>
- Versteeg, H. H., Heemskerk, J. W. M., Levi, M., & Reitsma, P. H. (2013). New Fundamentals in hemostasis. *Physiological Reviews*, *93*(1), 327–358. <https://doi.org/10.1152/physrev.00016.2011>
- Veyradier, A., & Meyer, D. (2005). Thrombotic thrombocytopenic purpura and its diagnosis. *Journal of Thrombosis and Haemostasis*. <https://doi.org/10.1111/j.1538-7836.2005.01350.x>
- Vorchheimer, D. A., & Becker, R. (2006). Platelets in atherothrombosis. *Mayo Clinic Proceedings*. <https://doi.org/10.4065/81.1.59>
- Wagner, D. D. (1990). Cell biology of von Willebrand factor. *Annual Review of Cell Biology*.
- Wagner, Denisa D., Saffaripour, S., Bonfanti, R., Sadler, J. E., Cramer, E. M., Chapman, B., & Mayadas, T. N. (1991). Induction of specific storage organelles by von Willebrand factor propolypeptide. *Cell*. [https://doi.org/10.1016/0092-8674\(91\)90648-I](https://doi.org/10.1016/0092-8674(91)90648-I)
- Watanabe, N., Ikeda, H., Kume, Y., Satoh, Y., Kaneko, M., Takai, D., ... Yatomi, Y. (2009). Increased production of ADAMTS13 in hepatic stellate cells contributes to enhanced plasma ADAMTS13 activity in rat models of cholestasis and steatohepatitis. *Thrombosis and Haemostasis*. <https://doi.org/10.1160/TH08-11-0732>
- Westwood, J. P., Webster, H., Mcguckin, S., Mcdonald, V., Machin, S. J., & Scully, M. (2013). Rituximab for thrombotic thrombocytopenic purpura: Benefit of early administration during acute episodes and use of prophylaxis to prevent relapse. *Journal of Thrombosis and Haemostasis*. <https://doi.org/10.1111/jth.12114>
- Xiang, Y., De Groot, R., Crawley, J. T. B., & Lane, D. A. (2011). Mechanism of von Willebrand factor scissile bond cleavage by a disintegrin and metalloproteinase with a thrombospondin type 1 motif, member 13 (ADAMTS13). *Proceedings of the National Academy of Sciences of the United States of America*. <https://doi.org/10.1073/pnas.1018559108>
- Yamaguchi, Y., Moriki, T., Igari, A., Nakagawa, T., Wada, H., Matsumoto, M., ... Murata, M. (2011). Epitope analysis of autoantibodies to ADAMTS13 in patients with acquired thrombotic thrombocytopenic purpura. *Thrombosis Research*. <https://doi.org/10.1016/j.thromres.2011.03.010>
- Zanardelli, S., Chion, A. C. K., Groot, E., Lenting, P. J., McKinnon, T. A. J., Laffan, M. A., ... Lane, D. A. (2009). A novel binding site for ADAMTS13 constitutively exposed on the surface of globular VWF. *Blood*. <https://doi.org/10.1182/blood-2009-05-224915>
- Zanardelli, S., Crawley, J. T. B., Chan Kwo Chion, C. K. N., Lam, J. K., Preston, R. J. S., & Lane, D. A. (2006). ADAMTS13 substrate recognition of von Willebrand factor A2 domain. *Journal of Biological Chemistry*. <https://doi.org/10.1074/jbc.M508316200>
- Zander, C. B., Cao, W., & Zheng, X. L. (2015). ADAMTS13 and von Willebrand factor interactions. *Current Opinion in Hematology*. <https://doi.org/10.1097/MOH.0000000000000169>
- Zhang, P., Pan, W., Rux, A. H., Sachais, B. S., & Zheng, X. L. (2007). The cooperative activity between the carboxyl-terminal TSP1 repeats and the CUB domains of ADAMTS13 is crucial for recognition of von Willebrand factor under flow. *Blood*. <https://doi.org/10.1182/blood-2007-04-083329>

- Zhang, Q., Zhou, Y. F., Zhang, C. Z., Zhang, X., Lu, C., & Springer, T. A. (2009). Structural specializations of A2, a force-sensing domain in the ultralarge vascular protein von Willebrand factor. *Proceedings of the National Academy of Sciences of the United States of America*. <https://doi.org/10.1073/pnas.0903679106>
- Zheng, X., Chung, D., Takayama, T. K., Majerus, E. M., Sadler, J. E., & Fujikawa, K. (2001). Structure of von Willebrand Factor-cleaving Protease (ADAMTS13), a Metalloprotease Involved in Thrombotic Thrombocytopenic Purpura. *Journal of Biological Chemistry*. <https://doi.org/10.1074/jbc.C100515200>
- Zheng, X. L. (2013). Structure-function and regulation of ADAMTS-13 protease. *Journal of Thrombosis and Haemostasis*. <https://doi.org/10.1111/jth.12221>
- Zheng, X. Long. (2015). ADAMTS13 and von Willebrand Factor in Thrombotic Thrombocytopenic Purpura. *Annual Review of Medicine*. <https://doi.org/10.1146/annurev-med-061813-013241>
- Zheng, X., Nishio, K., Majerus, E. M., & Sadler, J. E. (2003). Cleavage of von Willebrand factor requires the spacer domain of the metalloprotease ADAMTS13. *Journal of Biological Chemistry*. <https://doi.org/10.1074/jbc.M305331200>
- Zhou, W., Inada, M., Lee, T. P., Benten, D., Lyubsky, S., Bouhassira, E. E., ... Tsai, H. M. (2005). ADAMTS13 is expressed in hepatic stellate cells. *Laboratory Investigation*. <https://doi.org/10.1038/labinvest.3700275>
- Zhou, Y. F., Eng, E. T., Zhu, J., Lu, C., Walz, T., & Springer, T. A. (2012). Sequence and structure relationships within von Willebrand factor. *Blood*. <https://doi.org/10.1182/blood-2012-01-405134>
- Zhou, Y. F., & Springer, T. A. (2014). Highly reinforced structure of a C-terminal dimerization domain in von Willebrand factor. *Blood*. <https://doi.org/10.1182/blood-2013-11-523639>
- Zondlo, N. J. (2013). Aromatic-proline interactions: Electronically tunable CH/ $\pi$  interactions. *Accounts of Chemical Research*. <https://doi.org/10.1021/ar300087y>

# Addendum I – Product information

Table AI.1. Product description of all products mentioned in Part III Materials & Methods

Product	Manufacturer	Catalogues number
Bromophenol blue	Acros Organics	403140050
BSA	Carl Roth	2834.2
Dried milk powder	Carl Roth	T145.3
EDC	Thermo Scientific	#22980
EDTA	Acros Organics	11844-0025
Ethanol	VWR	20820296
GAB-AuNPs	BBI Solutions	BA.GAB40
GAH-AuNPs	BBI Solutions	BA.GAH40
Glycerol	Acros	158920010
Hydrogen chloride (HCl)	Acros	124630010
HRP-labelled High sensitivity streptavidin	Thermo Scientific	21130
HRP-labelled monoclonal anti IgG <sub>1,2,3,4</sub> antibodies	Sanquin Division Reagents	M1328 M1329 M1330 M1331
HRP-labelled polyclonal goat anti-human IgG (Fc specific) antibody	Sigma Aldrich	A0170
Mercapto-ethanol	Sigma Aldrich	M3148-250ML
MES	Sigma Aldrich	M-5287
Monosodium phosphate (NaH <sub>2</sub> PO <sub>4</sub> )	Merck	106346.1000
NHS	Thermo Scientific	#24500
Himark prestained protein standard (SDS-PAGE)	Thermo Scientific	LC5699
Streptavidin conjugated to HRP	Roche	11089153001
Sodium acetate (NaAc)	Sigma Aldrich	S8750
Sodium hydroxide (NaOH)	Acros Organics	124260010
Sulfuric acid (H <sub>2</sub> SO <sub>4</sub> )	Acros Organics	124540010
Superblock™ Blocking Buffer	Thermo Scientific	37580
TMB III solution	Biopanda diagnostics	TMB-P-001
Tween20	Acros Organics	233360010
Tween80	Acros Organics	278630010
ZnSO <sub>4</sub> .7H <sub>2</sub> O	Acros Organics	424605000

## AI.2. Plasma samples

---

Citrated plasma samples were available for analysis from 19 acute iTTP patients, provided by the Aix-Marseille Université (Marseille, France), and 80 healthy donors (HD), supplied by the Belgian Red Cross Flanders (Ghent, Belgium). Analysis is approved by the local Ethical Committee (N°#2007/23, Marseille, France and 260220, Leuven, Belgium), whereas informed consent from each patient was obtained in accordance with the Declaration of Helsinki.

## AI.3. In-house developed products

---

All murine, monoclonal anti-human ADAMTS13 antibodies (e.g.: 1C4, etc.), that target diverse epitopes in different ADAMTS13 domains (Figure AI.3.), were in-house developed and purified in the Laboratory for Thrombosis Research. Furthermore, rhADAMTS13 and both truncated ADAMTS13 variants (MDTCS and T2C2) were in-house synthesized and purified from respectively T-REx™- and CHO-derived cell lines.

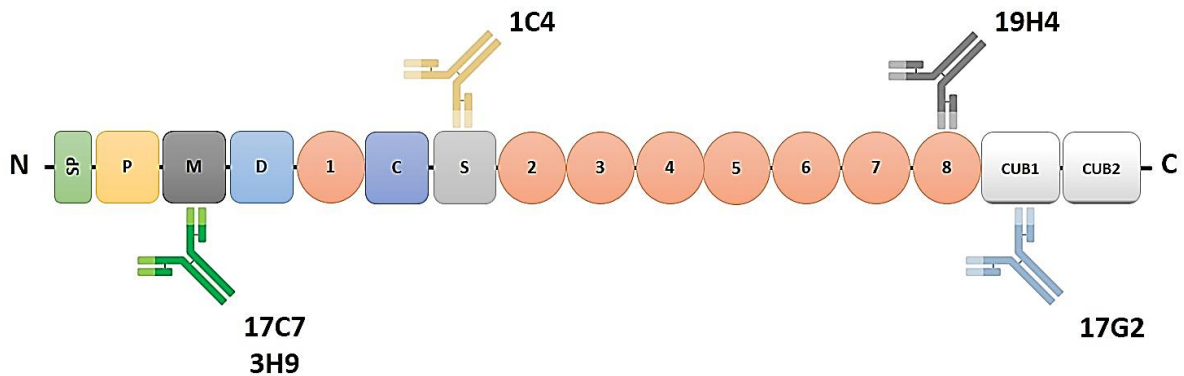


Figure AI.3.: **Epitopes of in-house developed murine anti-human ADAMTS13 antibodies:** In-house developed monoclonal antibodies with epitopes in different domains of ADAMTS13; Metalloprotease domain (17C7, 3H9), Spacer domain (1C4), Thrombospondin type-1 repeat domain (19H4) and CUB1 domain (17G2).

# Addendum II – Buffer composition

Table All.1. 10x PBS\* (pH 6.5)

Product	Manufacturer	Catalogues number
0.137 M NaCl	Carl Roth	9265.2
2.7 mM KCl	Acros Organics	196770010
6.5 mM Na <sub>2</sub> HPO <sub>4</sub> ·2H <sub>2</sub> O	Sigma Aldrich	71643
1.5 mM KH <sub>2</sub> PO <sub>4</sub>	Acros Organics	205920025
* diluted to 1x PBS with demiwater		

Table All.2. (bi)carbonate coating buffer (pH 9.6)

Product	Manufacturer	Catalogues number
50 mM Na <sub>2</sub> CO <sub>3</sub>	Merck	0088537
50 mM NaHCO <sub>3</sub>	Acros Organics	217120025

Table All.3. Colouring solution (per 96-well microtiter plate)

Product	Manufacturer	Catalogues number
10 mL phosphate buffer: 0.2 M Na <sub>2</sub> HPO <sub>4</sub> ·2H <sub>2</sub> O	Sigma Aldrich	71643
10 mL citric acid buffer: 0.1 M citric acid	Sigma Aldrich	124910010
8 µL H <sub>2</sub> O <sub>2</sub>	Acros Organics	202065000
200 µL OPD (50 g/L*)	Sigma Aldrich	P1526
* diluted to 50 g/L in 50% phosphate buffer and 50% citric acid buffer		

Table All.4. HBS buffer (pH 7.4)

Product	Manufacturer	Catalogues number
50 mM HEPES	Carl Roth	6763.3
5 mM CaCl <sub>2</sub> ·2H <sub>2</sub> O	Sigma Aldrich	C3881-500G
1 µM ZnCl <sub>2</sub>	Sigma Aldrich	208086-100G
0.15 M NaCl	Carl Roth	9265.2

Table All.5. 7.5% SDS-PAGE running gel

Product	Manufacturer	Catalogues number
5mL 0.75 M Tris pH 8.8	Sigma Aldrich	252859-500G
2.06 mL Demiwater	/	/
40 $\mu$ L 25% SDS	Acros	226145000
2.44 mL 30% AA/BAA	Bio-Rad	161-0158
0.5 mL 3% APS	Bio-Rad	161-0700
5 $\mu$ L TEMED	Bio-Rad	161-0800

Table All.6. 4% SDS-PAGE stacking gel

Product	Manufacturer	Catalogues number
2.5 mL 0.25 M Tris pH 6.8	Sigma Aldrich	252859-500G
1.6 mL Demiwater	/	/
20 $\mu$ L 25% SDS	Acros	226145000
0.65 mL 30% AA/BAA	Bio-Rad	161-0158
250 $\mu$ L 3% APS	Bio-Rad	161-0700
2.5 $\mu$ L TEMED	Bio-Rad	161-0800

Table All.7. 10x Electrophoresis buffer\* (for 1 L at pH 8.8 – 9)

Product	Manufacturer	Catalogues number
30.3 g Tris	Sigma Aldrich	252859-500G
144 g Glycine	Sigma Aldrich	CAS 56-40-6
10 g SDS	Acros	226145000
* diluted to 1x Electroporation buffer with demiwater		

Table All.8. Western blot transfer buffer

Product	Manufacturer	Catalogues number
1.5 g Tris	Sigma Aldrich	252859-500G
750 mg Glycine	Sigma Aldrich	CAS 56-40-6
25 mL Methanol	Fisher Scientific	10365710
400 $\mu$ L 25% SDS	Acros	226145000

# Addendum III – Laboratory equipment

Table AIII.1. List of laboratory equipment mentioned in Part III Materials & methods

Equipment	Manufacturer	Catalogues number
0.2 mL Thin-walled 8 PCR tubes	Thermo Scientific	AB-0266
96-well microtiter plate	Greiner	655092
ÄKTA device	GE Healthcare	Not Applicable (N/A)
Buffer tank for mini protean tetra cell	Bio-Rad	165-8039
Cell lid with power cables for mini tetra cell	Bio-Rad	165-8041
CHO-derived CHOEBNALT85 cells	Icosagen Cell Factory	N/A
Combs well 1.0 mm	Bio-Rad	165-3359
FLUOstar OPTIMA reader	BMG Labtech	N/A
Mini protean casting frame	Bio-Rad	165-3304
Mini protean casting stand	Bio-Rad	165-3303
Ni <sup>2+</sup> HisTrap™ excel column	GE Healthcare	17-5247-01
Novablot filter paper 8x10 cm	Fisher Scientific	11852210
PowerPac Power supply	Bio-Rad	164-5050
Pre-functionalized, gold-coated FO probes	FOx Biosystems	N/A
Roti PVDF 0.45 µM 8x10 cm	Carl Roth	T830.1
Small plate mini protean	Bio-Rad	165-3308
Spacer plate 1.0 mm integrated spacer	Bio-Rad	165-3311
Trans-Blot <sup>®</sup> SD Semi-Dry Transfer Cell	Bio-Rad	1703940
T-Rex™ system	Invitrogen	K1020-01
Vivaflow® 200, 50 000 MWCO, PES system	Sartorius	VF20P3
White Fox 1.0 device	FOx Biosystems	N/A
Zn <sup>2+</sup> HisTrap™ HP column	GE Healthcare	17-5247-01

# Addendum IV – Additional experiments

Table AIV.1. Overview of extra experiments conducted next to the work for this thesis

<b>ADAMTS13 activity assay</b>	Optimization FRETs-VWF73 ADAMTS13 activity assay
	ADAMTS13 activity in plasma samples (FRETs-VWF71 assay)
<b>ADAMTS13 antigen ELISA</b>	ADAMTS13 antigen in plasma samples from TTP patients
	Quality control ADAMTS13 antigen after ADAMTS13 depletion
<b>ADAMTS13 immune complex ELISA</b>	Optimization ADAMTS13 immune complex ELISA
<b>Anti-ADAMTS13 autoantibody ELISA</b>	Anti-ADAMTS13 autoantibody ELISA on Ni-plates ( <i>Manuscript in preparation: S. Horta, J. Qu, C. Dekimpe, Q. Bonne, et al.</i> )
<b>Mice genotyping</b>	Quick gDNA isolation and genotyping of ADAMTS13 and Rag-1 knock-out mice through PCR
<b>SDS-PAGE</b>	Optimization SDS-PAGE protocol

# Addendum V – Risk analysis

At the KU Leuven Campus Kulak Kortrijk, the Laboratory for Thrombosis Research is a containment level 1 laboratory (L1) that is part of the Interdisciplinary Research Facility (IRF) Life Sciences. During the experiments of this thesis, several risks were concerned. Therefore, an educative Health, Safety and Environment (HSE) session was followed. Preventive measures were implemented concerning the exposure and handling of hazardous materials as well as for the application of biological products (e.g.: patient plasma), which could potentially transmit infectious diseases. When performing experimental work, a lab coat was consistently worn to diminish potential threats. In addition, when handling patient plasma samples, wearing protective gloves was mandatory. Also, gloves were worn when working with irritating and/or carcinogenic components, such as OPD, H<sub>2</sub>O<sub>2</sub>, H<sub>2</sub>SO<sub>4</sub> or EDC/NHS. Furthermore, general safety guidelines were followed to prevent any physical injury, like cuts or punctures. After each experiment, the product wastes were compiled in applicable biological and chemical waste bins. All information on HSE, precautions regarding chemicals and waste disposal originates from the KU Leuven database on dangerous materials and labels or is in line with the safety data sheets provided by the manufacturers.



**LABORATORY FOR THROMBOSIS RESEARCH**

E. Sabbelaan 53  
8500 KORTRIJK BELGIUM  
tel. + 32 56 24 60 61  
karen.vanhoorelbeke@kuleuven.be  
www.kuleuven.be

